Methane Decomposition for Hydrogen Production over Biomass Ash Derived Ceria Promoted Cobalt Catalyst

By

Jehangeer Raza

00000274482

Session 2018-2020

Supervised By

Dr. Asif Hussain Khoja

U.S. –Pakistan Centers for Advanced Studies in Energy (USPCAS-E)

National University of Sciences and Technology (NUST)

H-12, Islamabad 44000, Pakistan

September 2021

Methane Decomposition for Hydrogen Production over Biomass Ash Derived Ceria Promoted Cobalt Catalyst

By

Jehangeer Raza

00000274482

Session 2018-2020

Supervised By

Dr. Asif Hussain Khoja

A Thesis Submitted to U.S. – Pakistan Centers for Advanced Studies in Energy in partial fulfillment of the requirements for the degree of

MASTERS of SCIENCE in

THERMAL ENERGY ENGINEERING

U.S.– Pakistan Centers for Advanced Studies in Energy (USPCAS-E)

National University of Sciences and Technology (NUST)

H-12, Islamabad 44000, Pakistan

September 2021

THESIS ACCEPTANCE CERTIFICATE

Certified that final copy of MS/MPhil thesis written by Mr. Jehangeer Raza, (Registration No. 00000274482), of U.S.-Pakistan Center for Advanced Studies in Energy (USPCAS-E), NUST has been vetted by undersigned, found complete in all respects as per NUST Statues/Regulations, is in the allowable limits of plagiarism, errors, and mistakes and is accepted as partial fulfillment for award of MS/MPhil degree. It is further certified that necessary amendments as pointed out by GEC members of the scholar have also been incorporated in the said thesis.

Signature: _____

Name of Supervisor: Dr. Asif Hussian Khoja

Date: _____

Signature (HoD TEE): _____

Date: _____

Signature (Principal/Dean): _____

Date: _____

Certificate

This is to certify that work in this thesis has been carried out by **Mr. Jehangeer Raza** and completed under my supervision in Fossil Fuels laboratory, USPCAS-E, National University of Sciences and Technology, H-12, Islamabad, Pakistan.

Supervisor:

_____
Dr. Asif Hussain Khoja
U.S.-Pak Centers for Advanced Studies in Energy
NUST, Islamabad

GEC member 1:

_____
Dr. Rabia Liaquat
U.S.-Pak Centers for Advanced Studies in Energy
NUST, Islamabad

GEC member 2:

_____
Dr. Sehar Shakir
U.S.-Pak Centers for Advanced Studies in Energy
NUST, Islamabad

GEC member 3:

_____
Dr. Nadia Shahzad
U.S.-Pak Centers for Advanced Studies in Energy
NUST, Islamabad

HoD-TEE:

_____
Dr. Majid Ali
U.S.-Pak Centers for Advanced Studies in Energy
NUST, Islamabad

Principal/Dean:

_____
Prof Dr. Adeel Waqas
U.S.-Pak Centers for Advanced Studies in Energy
NUST, Islamabad

Acknowledgements

All praise to Allah Almighty who gave me the strength and ability to understand, learn and complete my thesis report.

It is a genuine pleasure to express my deep sense of thanks and heartiest gratitude to my research supervisor Dr. Asif Hussain Khoja for letting me be part of the research group at Fossil Fuels Lab, USPCAS-E, NUST, Islamabad. I feel privileged to have worked under his kind supervision. It's the blend of his patience, persistence, guidance and motivation that made me accomplish my research aims in due time. He has taught me the methodology to carry out the research and to present the research work as clearly as possible.

I am deeply indebted to my respected GEC committee members, Dr. Rabia Liaquat, Dr. Sehar Shakir and Dr. Nadia Shahzad who honored my committee's presence. I would like to sincerely thank my fellows and friends for their unconditional support. Specially, I pay gratitude to Lab Engineer Mr. Ali Abdullah for their unmatchable support during the whole research work.

I am extremely grateful to my parents for their love, prayer, caring and sacrifices for educating and preparing me for my future. I am very much thankful to my sisters and brother for their support and valuable prayers.

Abstract

The biomass fly ash (BFA) was studied as catalyst support material for thermo-catalytic decomposition of methane, in order to produce COx free hydrogen gas and solid carbon nano-materials as by-product. Cobalt based, CeO_2 promoted, BFA supported catalyst were synthesized via impregnation method and was tested in fixed bed reactor for hydrogen production via thermo-catalytic decomposition of methane. The material characterization techniques such as X-ray powder diffraction, scanning electron microscopy, energy-dispersive X-ray spectroscopy, thermal gravimetric analysis, and Fourier transformed infrared were used to evaluate the catalyst's physicochemical properties. The pure crystalline micro-flake BFA was modified with synthesized CeO_2 nanowires, and the resulted nano-composite catalyst were thermally stable up to 900 °C. The catalyst stability makes it ideal catalyst for methane thermal catalytic decomposition. The catalyst, activity was assessed at 850 °C in order to determine H_2 yield and CH_4 conversion. In catalyst screening experiments, the obtained results demonstrated that support and promoter have a significant impact on CH_4 conversion and H_2 yield. Using 5% Co/CeO_2-BFA as the catalyst, a maximum conversion of 71 percent for CH_4 with 44.9 percent H_2 yield was recorded for 34 hours on stream activity. While BFA and Co-BFA as catalysts converted 36% and 47% of CH_4, respectively, indicating that the inclusion of a promoter increases both CH_4 conversion and H_2 yield. Compared to conventional catalyst support, using waste-sourced catalyst support for CH_4 decomposition is a greener and more cost-effective option since it reduces the expenses and time required to prepare it.

Keywords: *Methane decomposition; Biomass fly ash; CeO_2; H_2 production;*

Table of content

List of Figures

List of Tables

List of Abbreviations

Abbreviation:	Description
BFA	Biomass fly Ash
DRM	Dry Reforming of Methane
POM	Partial Oxidation of Methane
SRM	Steam Reforming of Methane
XRD	X-ray Diffraction
SEM	Scanning Electron Microscopy
TGA	Thermo-gravimetric analysis
FTIR	Fourier Transform Infrared Spectroscopy
EDS	Energy Dispersive X-ray
FBR	Fixed Bed Reactor
TOS	Time of Stream
GHG	Greenhouse Gases
TGM	Tip Growth Mechanism
BGM	Base Growth Mechanism

Chapter 1: Introduction

1.1 Background

With the population growth and industrial revolution around the world, energy demand has risen exponentially. The exploration of the fossil fuel resources has been increased to meet the necessary energy demands, which contributing to fossil fuel depletion [1]. The excess use of the fossil fuel overcome the energy demands, but also contribute to the emission of greenhouse gases (GHG) which causes global warming [2]. Efforts around the world has been made to fulfill energy demands and also to minimize GHG emission, which are the broad-based technical and social challenge of transforming the world energy framework currently based on fossil fuels [3].

Across the globe, attempts have been made to shift over energy system from conventional fossil fuel source to renewable, clean, sustainable and low-carbon sources of energy [4, 5]. But sadly the renewable technologies such solar, wind, bio and nuclear are in the stage of development and also have some concern in term of its cost and safety [2]. Hence, it is essential to put our efforts in some other alternatives such as production of syngas [6], methanol [7] and hydrogen [8] from carbon dioxide and methane gas which are the major contributor towards the global warming. Currently, scientific community putting their efforts for the production of syngas to utilize it as liquid fuel and hydrogen production for the application of fuel cell with addition to other uses [9]. H_2 used in fuel cells to generate heat and electrical energy concurrently, which is known to be the safer and more effective use of H_2 [10]. The non-availability of "elemental hydrogen" in the universe is a major issue with using hydrogen for fuel cell technology [11].

1.2 Problem Statement

The environmental and economics concern with the process traditionally used for the hydrogen production via utilizing hydrocarbons and the catalyst stability are among the factors which the industries are facing [12-15]. At the same the other methods used for the hydrogen production have their limitation in term of maturity and efficiency, such as water splitting require very high temperature of about 2200 ℃ and also highly sophisticated separation membrane for oxygen and hydrogen [16]. Therefore, thermo-

catalytic decomposition of methane is a straight forward solution to the issues listed above for hydrogen production [17]. Thermo-catalytic decomposition of methane is an endothermic process which decompose methane to produce hydrogen gas, collected at the exit of reactor and solid carbon nano-materials as by-product which are deposited over the catalyst and is collected, as shown in reaction **R1**. Thermo-catalytic decomposition of methane is an economical method in terms of reducing the process temperature needed in the absence of a catalyst, and no additional process is required for hydrogen gas purification as there is no impurity in the production of hydrogen[17]. Carbon nanomaterials are employed in a variety of applications due to their mechanical robustness, high electron conductivity, and good acid and basic resistance [18].

$$CH_{4(g)} \rightarrow C_{(s)} + 2H_{2(g)} \quad \Delta H^{\circ}_{25^{\circ}C} = 75 \text{ kJ mol}^{-1} \text{ (Methane Decomposition)} \qquad \text{(R1)}$$

The catalyst stability is a major challenge in the way of thermo-catalytic decomposition of methane. Scientific community have used various transition metal (Ni, Fe, Co) [19] and noble metals (Pd, Pt, Ru) [20] catalyst and supported with metal oxide such as Al_2O_3 [21], SiO_2 [22], MgO [23], ZrO_2 [12], La_2O_3 [24], TiO_2 [25] for methane decomposition reaction. In terms of economics and complex methods of preparation, metal oxide as a catalyst support material is of great concern [26]. Therefore, the use of waste materials for catalyst support will mitigate those concerns. Different techniques and treatments have been applied to these materials in order to make them suitable for catalyst support, which is likely to reduce the cost and complexity of catalyst support material preparation [27]. Both bottom ash and fly ash are produced in large quantities by biomass-fired power stations, and their disposal is a big concern. Biomass fly ash (BFA) has some amazing structural features and contains numerous metal oxides, making it appropriate for use as a support material in a heterogeneous catalyst for thermo-catalytic methane decomposition and other reforming applications [26].

1.3 Research hypothesis

The use of various transition metal like nickel, iron and cobalt as catalyst in methane reforming technologies is a well-known fact. The instability of the nickel loaded catalyst, support materials preparation and high temperature management was another

concern with some reforming technologies. Therefore, we used an alternative method for hydrogen production, thermo-catalytic decomposition of methane in the fixed bed reactor system and in the presence of cobalt loaded over biomass fly ash as support and promoted with cerium oxide. BFA has been found to be the mix matric of various metal oxides such as Al_2O_3, $CaSO_4$, $CaCO_3$, Fe_2O_3 and SiO_2, which assist in the reaction of methane decomposition, and cerium oxide has been added as a promoter to aid boost the stability of the catalyst and provide better dispersion of cobalt over BFA.

1.4 Objectives of study

The research study discussed in this thesis primarily deals with the biomass fly ash derived cobalt base catalyst promoted with ceria for thermo-catalytic decomposition of methane. The key theme of this research study is the performance of biomass fly ash supported catalyst in term of catalytic activity, methane conversion, hydrogen selectivity and yield. In this research, the experimental work done is firmly in line with the literature. The focusing objective of this research study are:

- To synthesize and characterize BFA supported Co-based catalyst promoted with CeO_2 for thermo-catalytic decomposition of methane process.
- To investigate the catalytic activity and stability of CeO_2/Co-BFA catalyst in fixed bed reactor.
- To analyze process parameters of thermo-catalytic decomposition of methane such as CeO_2 loading and flow rate.

1.5 Scope of study

The main pillar of reaction and process engineering is the synthesis and testing of the catalyst. Initially, biomass fly ash (BFA) was gathered from a nearby biomass-fired power station and prepared for use as a catalytic support material. The hydrothermal process was used to make cerium oxide nanowire. And final nano-composite catalyst loaded with active metal cobalt and CeO_2 as promoter over BFA support were developed with incipient wetness impregnation method. The developed nano-composite were studied, examine and analysed in different ways. The in-depth study of thermo-catalytic decomposition of methane reveal that the process depend on various factors which are reaction mechanism, type of support material, active metal,

type of promoter, catalyst's preparation method and experimental parameters (temperature, pressure and flow rate etc). The scope of the research is shown in **Figure 1.1**

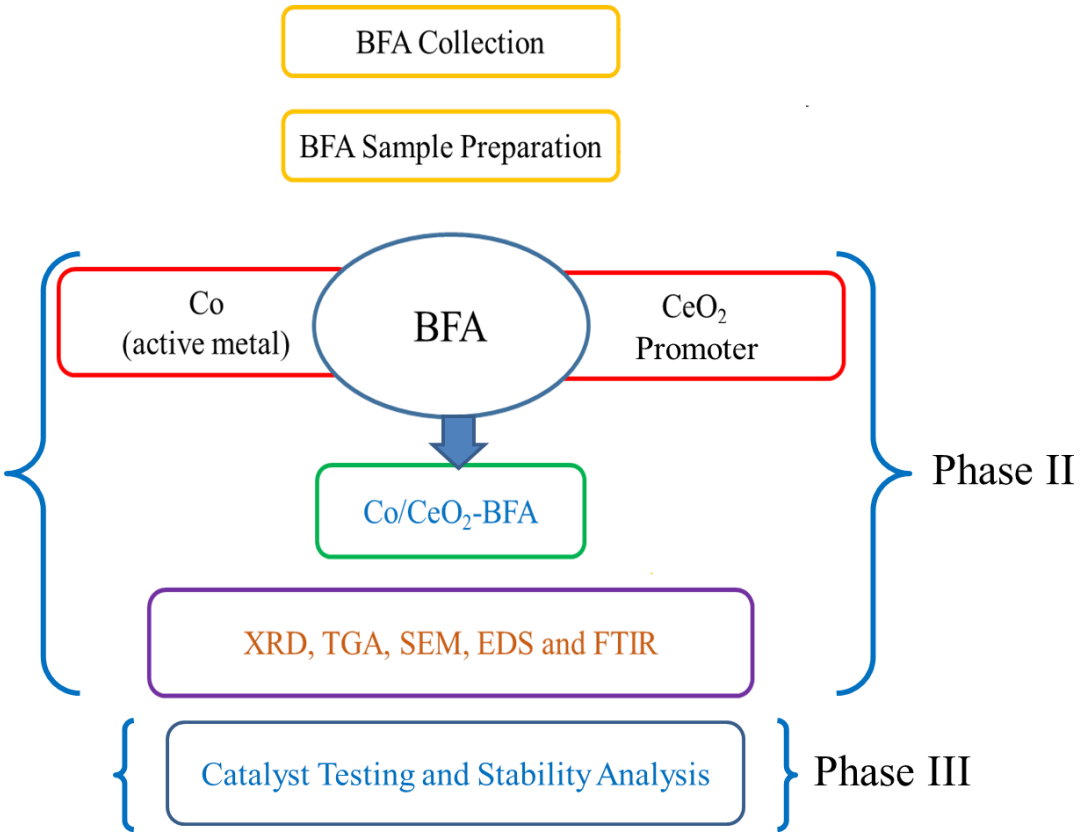

Figure 1.1 Steps involved in research scope.

1.6 Flow chart of thesis

The literature initially carried out to find out sustainable management for BFA, instead of disposing it in landfill sites. In material preparation and characterization section, BFA sample were cleaned and prepared, and finally impregnate with cobalt and CeO_2. The final composite were then characterized by using material characterization technique such as XRD, TGA, SEM, EDS and FTIR.

In the experimentation, the prepared and characterized final nano-composite were tested in FBR while keeping reaction temperature at 850 ℃, and flow rate equal to 20 ml min^{-1}. In results and discussion section, detail discussion of the data related to results were presented. The conclusion section deal with effective utilization of BFA

as catalytic material and adding CeO_2 and Co to BFA enhance the stability and catalytic activity of the final nano-composite

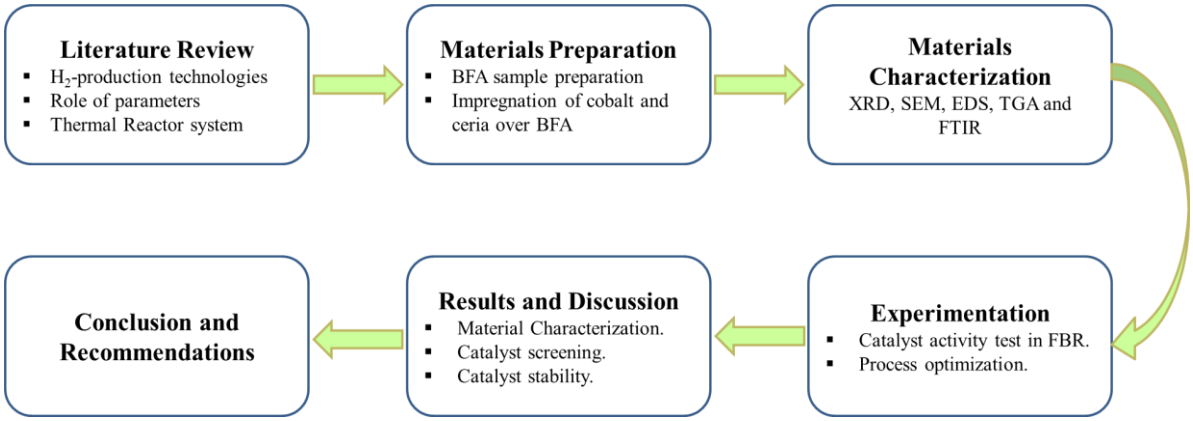

Figure 1.2 Thesis flow diagram

References

[1] F. Dawood, M. Anda, G.M. Shafiullah, Hydrogen production for energy: An overview, International Journal of Hydrogen Energy, 45 (2020) 3847-3869.

[2] U.P.M. Ashik, W.M.A. Wan Daud, H.F. Abbas, Production of greenhouse gas free hydrogen by thermocatalytic decomposition of methane – A review, Renewable and Sustainable Energy Reviews, 44 (2015) 221-256.

[3] L. Weger, A. Abanades, T. Butler, Methane cracking as a bridge technology to the hydrogen economy, International Journal of Hydrogen Energy, 42 (2017) 720-731.

[4] A.S. Al-Fatesh, A.H. Fakeeha, W.U. Khan, A.A. Ibrahim, S.B. He, K. Seshan, Production of hydrogen by catalytic methane decomposition over alumina supported mono-, bi- and tri-metallic catalysts, International Journal of Hydrogen Energy, 41 (2016) 22932-22940.

[5] M. Karaismailoglu, H.E. Figen, S.Z. Baykara, Hydrogen production by catalytic methane decomposition over yttria doped nickel based catalysts, International Journal of Hydrogen Energy, 44 (2019) 9922-9929.

[6] A.H. Khoja, M. Tahir, N.A.S. Amin, Recent developments in non-thermal catalytic DBD plasma reactor for dry reforming of methane, Energy Conversion and Management, 183 (2019) 529-560.

[7] M. Usman, W.M.A.W. Daud, Recent advances in the methanol synthesis via methane reforming processes, RSC Advances, 5 (2015) 21945-21972.

[8] V. Havran, M.P. Dudukovic, C.S. Lo, Conversion of Methane and Carbon Dioxide to Higher Value Products, Industrial & Engineering Chemistry Research, 50 (2011) 7089-7100.

[9] S. Sengodan, R. Lan, J. Humphreys, D. Du, W. Xu, H. Wang, S. Tao, Advances in reforming and partial oxidation of hydrocarbons for hydrogen production and fuel cell applications, Renewable and Sustainable Energy Reviews, 82 (2018) 761-780.

[10] N.P. Brandon, Z. Kurban, Clean energy and the hydrogen economy, Philos Trans A Math Phys Eng Sci, 375 (2017) 20160400.

[11] A. Sartbaeva, V. Kuznetsov, S. Wells, P. Edwards, Hydrogen nexus in a sustainable energy future, Energy & Environmental Science, 1 (2008) 79-85.

[12] A. Wolfbeisser, G. Kovács, S.M. Kozlov, K. Föttinger, J. Bernardi, B. Klötzer, K.M. Neyman, G. Rupprechter, Surface composition changes of CuNi-ZrO_2 during methane decomposition: An operando NAP-XPS and density functional study, Catalysis Today, 283 (2017) 134-143.

[13] H.F. Abbas, W.M.A. Wan Daud, Hydrogen production by methane decomposition: A review, International Journal of Hydrogen Energy, 35 (2010) 1160-1190.

[14] A.H. Fakeeha, A.A. Ibrahim, W.U. Khan, K. Seshan, R.L. Al Otaibi, A.S. Al-Fatesh, Hydrogen production via catalytic methane decomposition over alumina supported iron catalyst, Arabian Journal of Chemistry, 11 (2018) 405-414.

[15] M. Pudukudy, Z. Yaakob, Q.M. Jia, M.S. Takriff, Catalytic decomposition of methane over rare earth metal (Ce and La) oxides supported iron catalysts, Applied Surface Science, 467 (2019) 236-248.

[16] T. Kodama, High-temperature solar chemistry for converting solar heat to chemical fuels, Progress in Energy and Combustion Science, 29 (2003) 567-597.

[17] J.X. Qian, T.W. Chen, L.R. Enakonda, D.B. Liu, J.-M. Basset, L. Zhou, Methane decomposition to pure hydrogen and carbon nano materials: State-of-the-art and future perspectives, International Journal of Hydrogen Energy, 45 (2020) 15721-15743.

[18] L. Zhou, L.R. Enakonda, M. Harb, Y. Saih, A. Aguilar-Tapia, S. Ould-Chikh, J.L. Hazemann, J. Li, N. Wei, D. Gary, P. Del-Gallo, J.M. Basset, Fe catalysts for methane decomposition to produce hydrogen and carbon nano materials, Appl Catal B-Environ, 208 (2017) 44-59.

[19] M. Pudukudy, Z. Yaakob, Z.S. Akmal, Direct decomposition of methane over SBA-15 supported Ni, Co and Fe based bimetallic catalysts, Applied Surface Science, 330 (2015) 418-430.

[20] A. Rategarpanah, F. Meshkani, Y. Wang, H. Arandiyan, M. Rezaei, Thermocatalytic conversion of methane to highly pure hydrogen over Ni–Cu/MgO· Al_2O_3 catalysts: Influence of noble metals (Pt and Pd) on the catalytic activity and stability, Energy Conversion and Management, 166 (2018) 268-280.

[21] M.S. Tian, K.Z. Li, X. Zhu, Y.G. Wei, Y.N. Zheng, L. Zhang, Y.H. Long, H. Wang, Modified Al@Al_2O_3 phase change materials by carbon via in-situ catalytic decomposition of methane, Solar Energy Materials and Solar Cells, 200 (2019) 109924.

[22] M. Pudukudy, Z. Yaakob, Methane decomposition over Ni, Co and Fe based monometallic catalysts supported on sol gel derived SiO2 microflakes, Chemical Engineering Journal, 262 (2015) 1009-1021.

[23] A.E. Awadallah, D.S. El-Desouki, S.M. Abdel-Azim, N.A.K. Aboul-Gheit, S.M. Abdel-Hamid, A.K. Aboul-Gheit, Effect of La, Ce and Nd oxides addition on the activity and stability of Co/MgO catalyst for methane decomposition into COx-free H_2 production and carbon nanotubes, Fullerenes, Nanotubes and Carbon Nanostructures, 26 (2018) 525-534.

[24] J.C. Araújo, L.F. Oton, B. Bessa, A.B. Neto, A.C. Oliveira, R. Lang, L. Otubo, J.M. Bueno, The role of Pt loading on La_2O_3-Al_2O_3 support for methane conversion reactions via partial oxidation and steam reforming, Fuel, 254 (2019) 115681.

[25] A.E. Awadallah, M.S. Mostafa, A.A. Aboul-Enein, S.A. Hanafi, Hydrogen production via methane decomposition over Al_2O_3–TiO_2 binary oxides supported Ni catalysts: Effect of Ti content on the catalytic efficiency, Fuel, 129 (2014) 68-77.

[26] M. Assad Munawar, A. Hussain Khoja, M. Hassan, R. Liaquat, S. Raza Naqvi, M. Taqi Mehran, A. Abdullah, F. Saleem, Biomass ash characterization, fusion analysis and its application in catalytic decomposition of methane, Fuel, 285 (2021) 119107.

[27] F. Goodarzi, Characteristics and composition of fly ash from Canadian coal-fired power plants, Fuel, 85 (2006) 1418-1427.

Chapter 2: Literature Review

2.1 Hydrogen economy

In the universe, hydrogen is simplest, lightest, most abundant element and environmental benign energy source. Hydrogen has both the ability of energy storage and energy and energy source but it should be noted that hydrogen is not the primary energy source [1]. Hydrogen upon burning releases three times more energy as compared to other fuel of same mass [2]. Hydrogen does not exist in the nature in elemental form, as it always appear in chemically bonded form with other elements. External energy sources and technologies are needed for the production of the hydrogen gas, the efficiency of these technologies depend on its economics and maturity [3]. The main sources for hydrogen production are hydrocarbon, coal and biomass [2]. The **Figure 2.1** shows the production sources of hydrogen and its utilization. The process commonly used for the production of the hydrogen are bio-hydrogen production, partial methane oxidation (POM), methane steam reforming (SRM), biomass gasification, coal gasification and water splitting [2, 4-16]. The process like steam reforming and partial oxidation of methane are the well mature and mostly used for the hydrogen production [6-8, 13, 15-18]. All these process have their limitation in term of producing GHG, catalyst deactivation, materials for catalyst, requirement of high temperature and hydrogen purification [10, 15, 17-20].

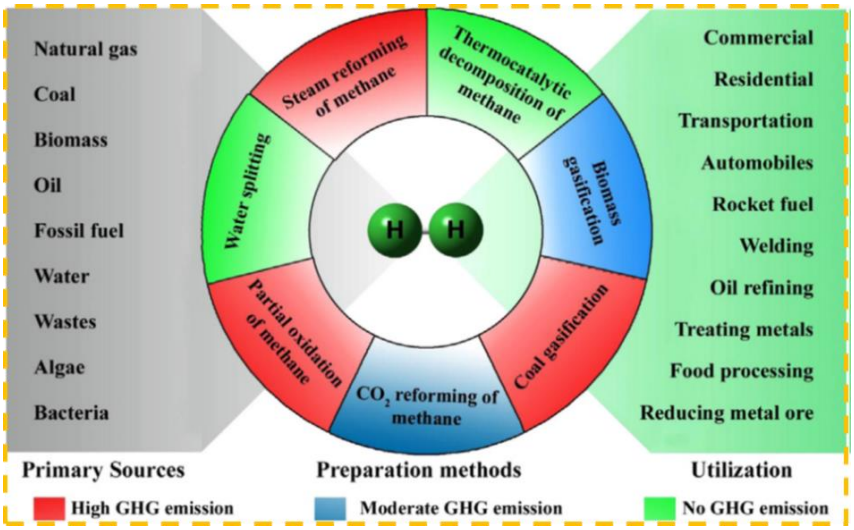

Figure 2.1 Detail representation of hydrogen sources, production methods and its utilization [2].

The relation between hydrocarbons and energy are strong enough that it's looking hard to observe change in situations in the future. The cost and maturity of technologies make it easy choice to use hydrocarbons for the hydrogen production [5]. But with limited hydrocarbon resources and the issue of global warming due to GHG emissions will leads the world to new hydrogen economy [21].

The hydrogen economy means the use of hydrogen gas as commercial fuel which will provides significant portion of energy and service of country [22]. Hydrogen well help in transformation of the world energy model (base on fossil fuel), where hydrogen will be the main energy carrier [23]. Hydrogen is a renewable energy source that has virtually no environmental effects, socially acceptable and will have a positive impact on the global economy [22]. Hydrogen has capability of providing energy to buildings, transport networks, industries, and has ability of storing energy for potential use [24]. **Figure 2.2** represent sector wise hydrogen usage across the globe.

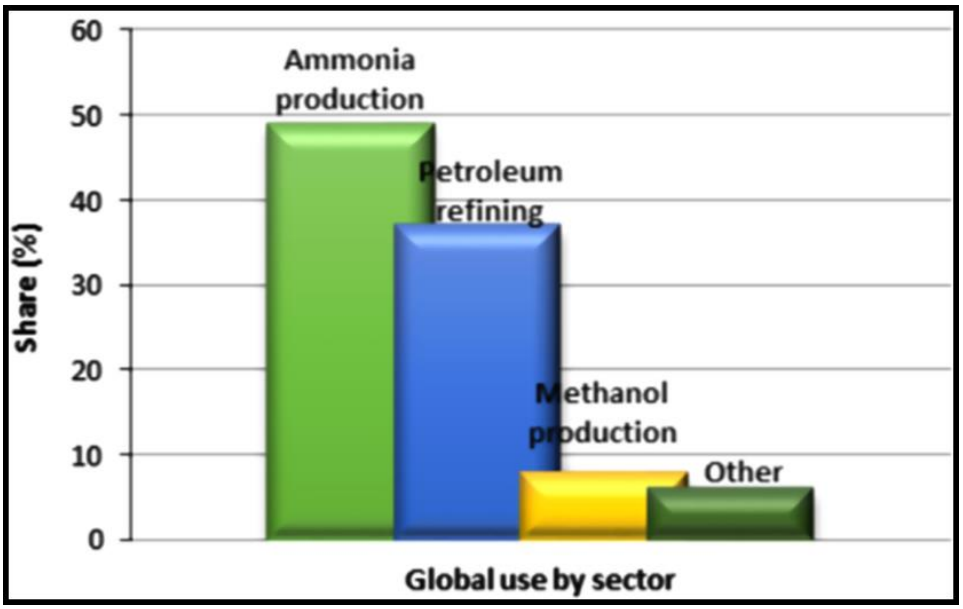

Figure 2.2 Sector wise usage of hydrogen across the globe [2].

The fuel cell, an electrochemical technology use hydrogen effectively as it produce heat and electrical energy simultaneously [25]. Fuel cell technology are maturing, economical and environmentally safe related to GHG emissions. Fuel cell and vehicles based on fuel cell are gaining market share in competition with traditional power

generation sources and transport vehicles [26]. The chemical reaction taking place in the fuel cell is very much opposite to the electrolysis of water, as hydrogen and oxygen reacts to produce electrical energy directly and at the same time generate heat which is utilize for electricity production [25].

2.2 H_2-production technologies

Various reforming technologies were utilizing for hydrogen production from fossil fuel, such as steam reforming of methane, partial oxidation of methane, coal gasification and auto-thermal reforming [5]. Among these technologies Steam reforming and partial oxidation of methane are mature technologies which are used at commercial scale for hydrogen production [2]. These conventional technologies have shorting coming in term of GHG emissions, economics and complex arrangement for separation of hydrogen gas. All the conventional and renewable technologies for hydrogen production are shown in **Figure 2.3.**

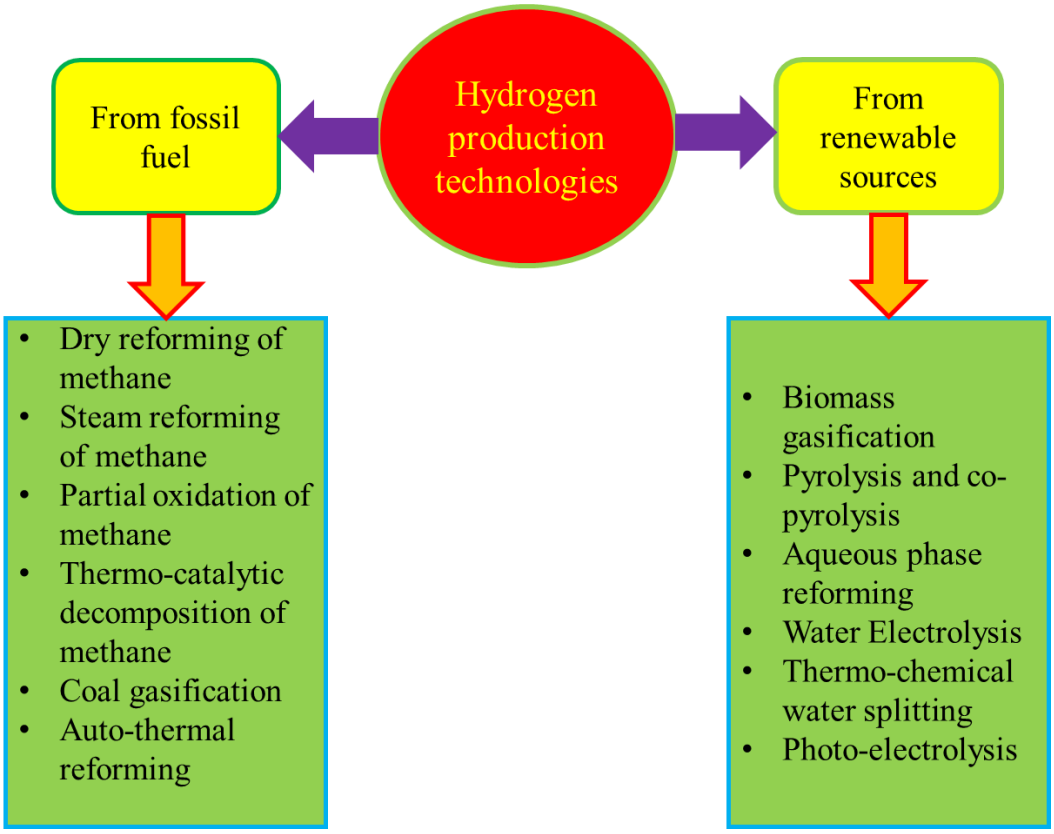

Figure 2.3 Hydrogen production based on its primary source.

Apart from these conventional method renewable technologies are developing such as water splitting, biomass gasification and photo-catalysis. But these technologies are immature and not economical [27]. Water splitting technology consume huge amount electrical energy to decompose highly stable water molecule into H_2 and O_2 without CO_2 emissions and also not economical because of its low efficiency and high cost [28]. In case of photo-catalysis the selection of suitable catalyst is the major concern [27]. To overcome the short coming and concern related to these conventional and renewable method, thermo-catalytic decomposition of methane were utilize.

2.3 Thermo-catalytic decomposition of methane

Thermo-catalytic decomposition of methane is simple and uni-step process which decompose the methane molecule into hydrogen gas and solid carbon nano-materials as by-product [29]. Thermo-catalytic decomposition of methane is an endothermic reaction at moderate temperature as presented in reaction **R2.**

$$CH_4 \rightarrow C + 2H_2 \quad \Delta H^{\circ}_{25^{\circ}C} = 75 \text{ kJ mol}^{-1} \text{ (Methane Decomposition)} \qquad \text{(R2)}$$

The methane molecules are highly stable at low temperature due to which it require high amount of energy to break down [16]. The solution to this problem is to choose the right catalyst that helps to carry out the process at a lower temperature. Therefore this process named as thermo-catalytic of methane. Mainly three steps involved in thermo-catalytic decomposition of methane [30]:

1. Activation of methane molecule: in which the molecule were absorbed over the catalyst surface and active metal part of catalyst causes to break the molecule.
2. The breaking carbon hydrogen bond occurs.
3. As a consequence of elementary carbon dissolution in the active catalyst phase, metastable carbide was formed.
4. Consequently, carbon precipitate in form of nano-materials are deposited over catalyst surface.

2.4 Catalyst used for thermo-catalytic decomposition of methane

The catalyst are usually employed to reduce time and energy required for the reaction [31]. During the last decade focus have been on the development of the efficient and easy methods for preparation of catalyst for the process of thermo-catalytic decomposition of methane.[2, 5, 30]

The catalyst usually composed of three main components 1). Support, 2). Active metal and 3). Promoter. All these components have their own role in the catalytic activity. The support material usually provide surface area for dispersion of active metal over it and help in better dispersion of active metal [32-34]. Active metal causes activation of the reactant molecules and have effect on morphology of the deposited carbon during thermo-catalytic decomposition of methane [35, 36]. The promoter helps in better metal dispersion over the support and improve stability of the catalyst [37].

The economics and preparation methods are the major concern while selecting suitable catalyst for the process of thermo-catalytic decomposition of methane [19]. In literature, various approaches like bi-metallic catalysts, tri-metallic catalysts [30] and co-supported catalyst were prepared and utilize for thermo-catalytic decomposition of methane which results in the promising CH_4 conversion and H_2 yield, but still facing some issues in term of metal sintering and drop in hydrogen yield rapidly after some time of reaction [17, 38].

Recently, across the globe researcher focus has been shifted from conventional preparation of catalyst to more structure catalyst like perovskite and spinal structure like $LaNiO_3$, $LaNiCoO_3$ have shown some fascinating results as compared to Ni loaded over LaO_3 [39]. The **table. 2.1** given below lists some catalyst used for thermo-catalytic decomposition of methane.

Table 2.1 List of catalyst employed for thermo-catalytic decomposition of methane

Catalyst	Temperature (°C)	TOS (min)	CH_4 conversion ($\%X_{CH4}$)	H_2-yield ($\%Y_{H2}$)	Preparation method	Carbon morphology	Ref
NiO unsupported	800	360	NA	66	Facile precipitation	Irregular carbon shape	[1]
Ni/CeO_2	700	360	NA	62	Solid state fusion	CNTs	[2]
Ni/ZrO_2	700	360	NA	61	Solid state fusion	CNTs	[2]
Ni/La_2O_3	700	360	NA	58	Solid state fusion	CNTs	[2]
Ni/Ce_{25}-Al_{75}	700	400	NA	53	Co-precipitation	CNFs + CNTs	[3]
Ni/Fe-Cu-Al_2O_3	750	600	80	NA	Wet impregnation	CNFs	[4]
Ni/Pd-Al_2O_3	750	600	78	NA	Wet impregnation	CNFs	[5]
Ni/Si-Al	700	400	NA	52	Impregnation	MWCNTs	[6]
Ni-Co/Al_2O_3	650	80	67.8	NA	Sol-gel	CNTs	[7]

Fe_2O_3	800	360	NA	50	Facile precipitation	Graphene sheets	[1]
30Fe-15Co/Al_2O_3	700	180	73	72	Wet impregnation	CNFs	[8]
20%Fe/Al_2O_3	800	180	80	NA	Impregnation	CNFs	[9]
60%Fe/Al_2O_3	700		NA	77	Co-precipitation	CNTs	[10]
Fe-Co/MgO	700		NA	85	Co-impregnation	MWCNTs	[11]
Fe-Activated carbon	850		45	NA	Co-impregnation	CNFs	[12]
Co/Si-Al	750		NA	53	Impregnation	MWCNTs	[6]
Co/Al_2O_3	700		NA	90	Impregnation	MWCNTs	[13]
Co/MgO	700		NA	80	Impregnation	MWCNTs	[13]
Fe-Co/$CeZrO_2$	700	125	54	57.7	Wet-impregnation	CNTs	[14]
Fe-Mo/$CeZrO_2$	700	125	45	56.2	Wet-impregnation	CNTs	[14]
Ni/Mn	725	120	58	58	---	CNTs	[15]
Ni/Cu	725	120	56	56	---	CNTs	[16]

Ni/Fe	725	120	47	47	---	CNTs	[16]
Ni/SBA-15	700	420	NA	42	Impregnation	CNTs	[17]
0.4Pd-Ni/SBA-15	700	420	NA	48	Impregnation	CNTs	[17]
Ni/$MgAl_2O_4$	700	420	NA	22	Impregnation	CNTs	[18]
Pd-Ni/$MgAl_2O_4$	700	420	NA	50	Impregnation	CNTs	[18]
Ru-AC (Activated carbon)	800	3600	21	NA	---	CNTs	[19]
Activated biochar (AB)	800	3600	51	NA	---	CNTs	[19]

2.5 Cobalt as catalyst for thermo-catalytic decomposition of methane

In literature various metal base catalyst were used for thermo-catalytic decomposition of methane, among them Ni-based catalyst are most commonly used due its cost, availability and the high methane conversion and hydrogen yield at lower reaction temperature [1]. According to literature, Ni-base catalyst have limitations in term of metal sintering, quick catalyst deactivation due to carbon deposition at higher rate and catalyst instability at higher temperature [2, 3]. Fe-base catalyst also studied and were shown good catalytic activity at higher temperature [4] but Fe-base catalyst have catalytic activity at high temperature (above 700℃) and were basically used for high value carbon nano-materials via methane decomposition [5].

Literature shows that Co-base catalyst is a competitive candidate for the process of thermo-catalytic decomposition of methane, Co-base catalyst have shown better catalytic activity and are more stable at elevated temperature, and also results in deposition of some high quality carbon nano-materials [6, 7]. The Co-based catalyst have shown higher catalytic activity and stability because of the formation of some cobalt oxides such as Co_3O_4 [8] and carbon nano-fibers with larger length and bigger diameter were formed with higher Co concentration [9]. The suitability of these transition metals (Ni, Fe, Co) for thermo-catalytic decomposition of methane is their non-filled 3d orbital, which contribute in the activation and dissociation of methane over the catalyst surface [10].

The catalytic activity of Ni and Co-based catalyst loaded over alumino-silicate as catalyst support were compared and the results reveal that Co-based catalyst have higher hydrogen yield and catalyst stability as compared to the Ni-based catalyst. The physiochemical properties further explore that Co-based catalyst have better metal-support interaction and Co metal have better dispersion over the support material as compared Ni-based. The characterization reveals that the crystallinity and degree of graphitization of deposited carbon for Co-based catalyst are higher. The influence of the operating condition over the Co/Al_2O_3 catalyst were observed [11]. The author studied the effect of Co loading, different reaction temperature (600-800 ℃) and different methane partial pressure over methane conversion. The results reveal that

best condition for hydrogen production are reaction temperature of 800℃, 20% of cobalt loading and N_2:CH_4 molar ratio of 6:1.

2.6 Biomass fly ash as catalyst support

The power plants where solid fuels like coal and biomass were feed as fuel are producing enormous quantity of the both kinds of ashes i.e bottom ash (BA) and fly ash (BFA) and its management and handling are the main concern for the globe environmental problem [12]. As general practice these ashes are dumped to landfill sites. However, several researchers around the world are now interested in the long-term management of waste ashes in order to maximize waste material recovery. In literature coal fly ash were utilized effectively in road construction, cement production, building materials such as concrete and for zeolite preparation [13].

The coal ash consist of various metal oxides such as Al_2O_3, Fe_2O_3, SiO_2, and MgO [14], which make it suitable candidate for catalytic application. In another study, Ni-based catalyst, supported by coal ash were used for hydrogen production via steam reforming of the acetic acid and phenol and the outcomes displayed that hydrogen production and reactant conversion were highly enhanced in the presence of coal ash supported catalyst [15]. The steam gasification of palm shell over coal ash as catalyst were studied for the production of hydrogen and syngas. The presence of coal ash influences the yield of hydrogen and syngas [16].

The biomass ash used for steam reforming process for the production of hydrogen were obtained from the combustion of various solid fuels and waste, such as coal, waste rubber tyres, and refuse-derived carbon, was used as a catalyst's support, with promising results because the metal oxide present in the catalyst's support (ashes) aided in catalytic activity [17]. Biomass fly ash (BFA) is studied extensively, in order to efficiently find out different physiochemical properties of BFA, the author used various characterization techniques [12]. The findings show that, among other applications, BFA may be used for catalysis because it contains various metal oxides such as Al_2O_3, Fe_2O_3, SiO_2, MgO, $CaCO_3$, and K_2O and has a flake-like morphology. Despite of the favourable physiochemical properties, BFA were consistently ignored in literature for catalytic applications.

2.7 Catalyst's deactivation

The major cause for metal catalyst deactivation during thermo-catalytic decomposition of methane is the deposition of the solid carbon nano-materials over the surface of the catalyst surface which leads to blockage of the active metal sites from the reaction. The deposited solid nano-materials effect catalytic activity in several ways such as:

i. Encapsulation of the active metal particles with deposited carbon nano-materials [18].
ii. The surrounding of the active metal sites filled intensively with the deposited carbon nano-materials which made access difficult for methane molecules to the active sites [19].
iii. Disintegration of the catalyst could occur due to excess accumulation of the deposited carbon nano-materials [20].
iv. Reactor jamming can occur in some cases because of too much deposition of the carbon nano-materials [21].

For optimization of the reaction process and catalyst's design, the determination of deactivation and process have more practical importance.

In the steady state process condition, the rate of methane decomposition, elemental carbon diffusion and carbon nano-materials growth should be same [4]. The deposition of the solid carbon materials occur when the rate of methane decomposition are higher than the diffusion rate of elemental carbon [22]. The deposited carbon over the catalyst surface usually form a layer which is known as encapsulating carbon [18]. The encapsulating carbon prevent reactant gases to interact with the active sites present in catalyst. The catalyst deactivation depend on the factors such as (1) Catalyst deactivation have inverse relation with the partial pressure of methane (P_{CH4}) and hydrogen (P_{H2}) [23], (2) Type of active metal used in catalyst [24], (3) Metal loading in the catalyst [1], (4) Metal-support interaction [25], (5) Reaction temperature [26], (6) Methane flow rate [26], (7) Experiment run time [26] (8) Presences of promoter [27].

Other reason for catalyst deactivation during of thermo-catalytic decomposition of methane are fracture of metal particles at higher temperature [23], limited space due

to which mobility of active metal sites are restrained and hence covered by deposited carbon [28], metal loading in given catalyst [29], atomic erosion of bimetallic catalyst [28], and sintering of metal particles also contribute [30].

2.8 Important process parameters

2.8.1 Effect of support

For conventional metallic catalyst, the support presences is important because support material enhance the stability and catalytic performance of the catalyst [22]. The support material effects the dispersion of active metal, crystal size of the catalyst, electronic configuration of the active metal, pore structure and surface area of the catalyst [5]. The materials like Al_2O_3 [31], SiO_2 [32], TiO_2 [33], MgO [34], ZSM-5 [35], La_2O_3 [36], ZrO_2 [37] and zeolite [38] were used in literature as support materials, over which different active metals were loaded and catalyst are developed and designed for thermo-catalytic decomposition of methane.

The surface morphology of support material effects the stability and catalytic performance of the catalyst [25]. Three different support materials named as CeO_2, ZrO_2 and La_2O_3 were used and are loaded with Ni as active metal. The results reveals that higher initial activity was observed for Ni/CeO_2 and Ni/ZrO_2 as compared to the La_2O_3, the reason is high surface area and lower reduction temperature while Ni/La_2O_3 have shown better stability for 360 minutes time on stream (TOS). The porous morphology of the La_2O_3 is the main reason for the higher stability of the Ni/La_2O_3 catalyst, as shown in **Figure 2.4**. As carbon morphology depends on the type of metal used, hence the morphology of the deposited carbon is same because of the Ni loading [25].

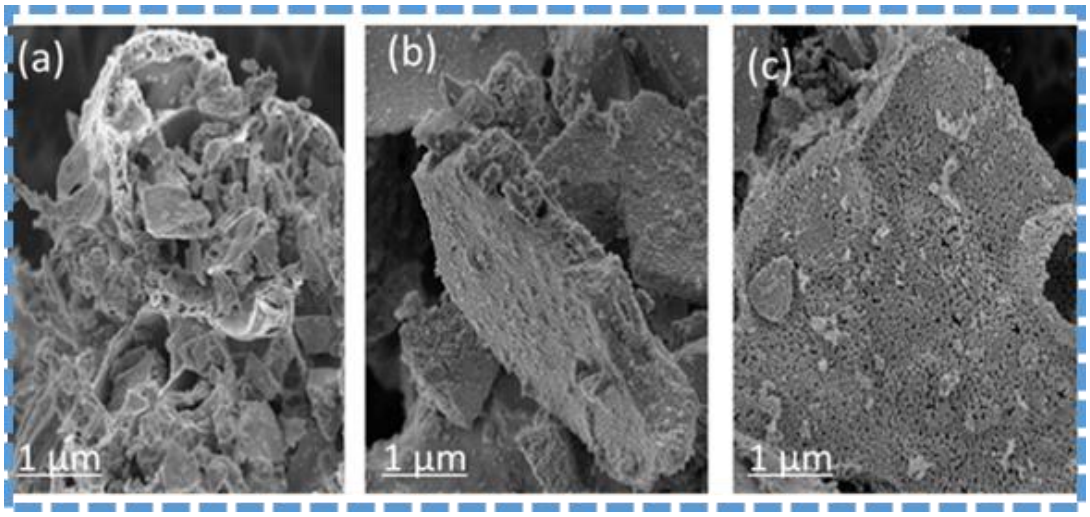

Figure 2.4 FESEM image of (a) Ni/CeO_2 (b) Ni/ZrO_2 (c) Ni/La_2O_3 [11].

2.8.2 Effect of promoter

In design of conventional metal-based catalyst, the promoter is the third important component. The promoter play significant role in active metal dispersion over the support material, effect the morphology of deposited carbon, enhance catalyst stability and catalytic performance [39]. The noble metal like Pd are usually utilize as promoter to catalyst, in order to enhance the catalytic properties of the catalyst, further more noble metal can also utilize as active metal to the catalyst [40].

The Ni/SBA-15 catalyst were promoted with Pd and it was observed that catalytic activity of the Pd-Ni/SBA-15 catalyst were highly improved as compared to Ni/SBA-15. The average hydrogen yield of Pd promoted catalyst was 48% which is higher as compared to unprompted catalyst at 700 ℃ [25]. **Figure 2.5** shows the reaction kinetics for un-promoted catalyst and catalyst promoted with 0.2% Pd and 0.4 Pd. The catalyst promoted with Pd have Pd-Ni alloy which leads towards the better dispersion of the NiO over the catalyst support and also have effect over the NiO crystallinity which enhance the stability and activity of the catalyst [41].

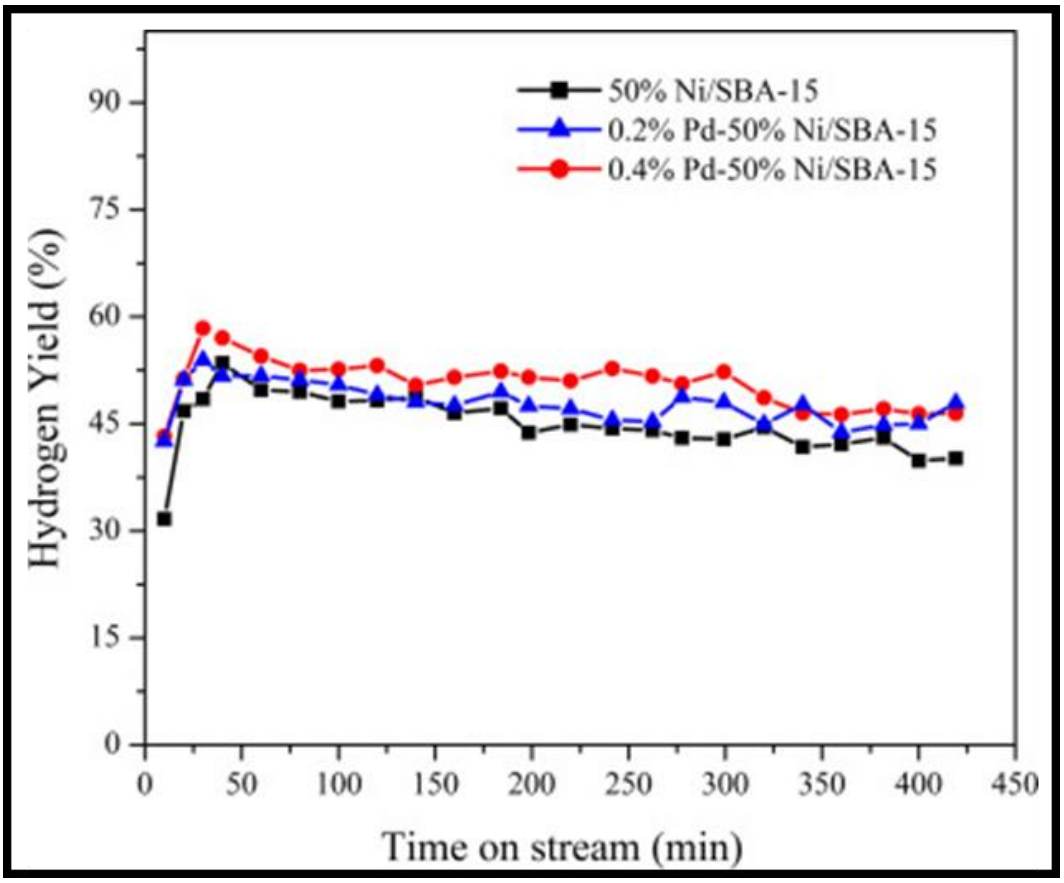

Figure 2.5 Kinetic curve of CH_4 decomposition as function of TOS at 700 ℃ [25].

Another element, copper (Cu) is mostly used as the catalyst promoter for thermo-catalytic decomposition of methane, despite the absence of the d-vacancies in its electronic configuration [42]. But still, Cu is an effective promoter in bimetallic catalyst with other transition metal to improve the stability of the catalyst. In literature, Cu promoted Ni-MgO catalyst and it was observed that Cu-Ni-MgO catalyst have better stability and catalytic activity in the temperature range of 665 ℃ to 725 ℃. The better stability of Cu promoted catalyst are due to the formation of Ni-Cu alloy which reduce the formation of Ni0 sites and hence reduce catalyst deactivation [43].

Furthermore, some metal oxides are also utilize as promoter in the catalyst for thermo-catalytic decomposition of methane [44]. The metal oxide like CeO_2 are used as promoter in Ni/Al_2O_3 catalyst and it was found that the CeO_2 promoted catalyst yield 51% of average hydrogen yield as compared to un-promoted catalyst which results in 42% of hydrogen yield with stability of 390 minutes on TOS. The CeO_2 addition to the

catalyst enhance the physiochemical properties of the catalyst, as $NiAl_2O_4$ spinal structure were observed for CeO_2 promoted catalyst [45].

2.8.3 Effect of flow rate

Flow rate highly effect catalytic activity in case of thermo-catalytic decomposition of methane, as flow rate determines residence time for gas flow in the reactor [46]. Increase in flow rate decrease the contact time between the reactant and catalyst surface [47]. Methane conversion decrease from 62.1%-16.4% with increasing flow rate from 6 L/min to 24 L/min, this is due to decreasing residence time for reactant in reactor [46] Due to reduce residence time with high flow rate the energy density were declined which results in formation of C_2H_2 and C_2H_4 as by-product along with hydrogen and solid carbon, thus decreased value of hydrogen selectivity. Another study [48] also discussed similar results of flow rate over methane conversion and hydrogen production. The relation between methane flow rates into reactor in term of gas hourly space velocity (GHSV) are shown in **Figure 2.6** and **Table 2.2**.

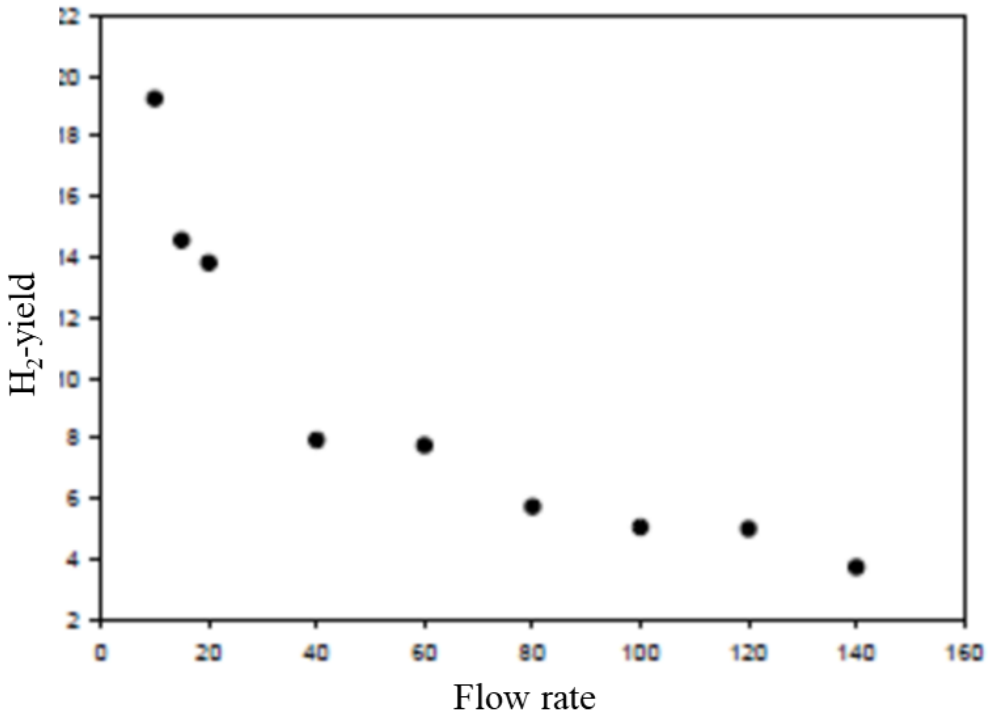

Figure 2.6 Effect of flow rate over hydrogen yield [9].

Table 2.2 Effect of GHSV over initial and final hydrogen yield over Ni/TiO_2 catalyst at 700 ℃ [52].

gas hour space velocities (ml h^{-1} g^{-1})	Initial H_2-yield	Final H_2-yield
6000	56	47
9000	56	42
12000	47	23

The higher flow rate reduce diffusion of methane molecules into catalyst surface which results in decreasing methane conversion and hydrogen yield [47]. Furthermore, high flow rate could also damage active sites as the carbon were depositing over the catalyst surface and not diffusing into catalyst surface [48]. Therefore selection of optimal flow rate should be considered, in order to ensure appropriate contact time between catalyst and methane molecules, to obtained better catalytic activity and stability [27].

2.8.4 Effect of temperature

The methane conversion, hydrogen yield and catalyst stability are highly depended over the reaction temperature due to endothermic nature of the thermo-catalytic decomposition of methane [49]. According to literature with increase in reaction temperature, the initial methane conversion and hydrogen yield were highly enhanced but due to deposition of solid carbon over the catalyst surface the stability and activity of the catalyst were effected significantly [50].

Table 2.3 shows initial and average methane conversion at different temperature while using Ni-based catalyst. The table clearly exhibits that at higher temperature the process shows higher initial methane conversion [51]. The higher formation of solid carbon prevent carbon diffusion into catalyst and deposited over catalyst surface to block active sites of the catalyst and leading to decrease catalyst stability [52].

Table 2.3 Summary of results dependent over reaction temperature while keeping flow rate constant at 120 L $g^{-1}h^{-1}$ [64].

Catalyst	Temp (℃)	Average CH_4 Conversion (%)	Carbon deposition rate ($g_{carbon}/g_{cat}h$)
Ni-Cu-Al	550	10.20	6.56
Ni-Cu-Al	600	13.19	8.51
Ni-Cu-Al	650	16.17	10.40
Ni-Cu-Al	700	31.20	20.06
Ni-Cu-Al	750	22.06	14.18
Ni-Cu-Al	800	19.4	16.22

Additionally, carbon encapsulation over the active sites and losing of catalyst surface morphology due sintering at elevated temperature also participate in lowering catalytic activity [53]. Among the catalyst Ni-based catalyst shown increase in catalytic activity up to 600℃, but noted adverse results at higher temperature [54]. The reaction temperature also effect morphology of deposited carbon, at lower temperature structured CNTs are formed while at higher temperature beside CNTs, carbon nano-capsule were observed [55].

Another study shows that increasing weight percentage of the iron content increasing the life duration of the catalyst during the reaction at 800℃ [54]. The Ni-based and Fe- based catalyst activities at temperature 700℃, 800℃ and 900℃ are compared and found that Ni-based catalyst have shown excellent initial catalytic activity with ample amount of deposited carbon over catalyst at higher temperature but deactivated at higher rate [56]. In case of Fe catalyst, it have shown lower initial activity but higher stability and lower deactivation rate as compared to Ni-based catalyst, as depicted in **Figure 2.7.**

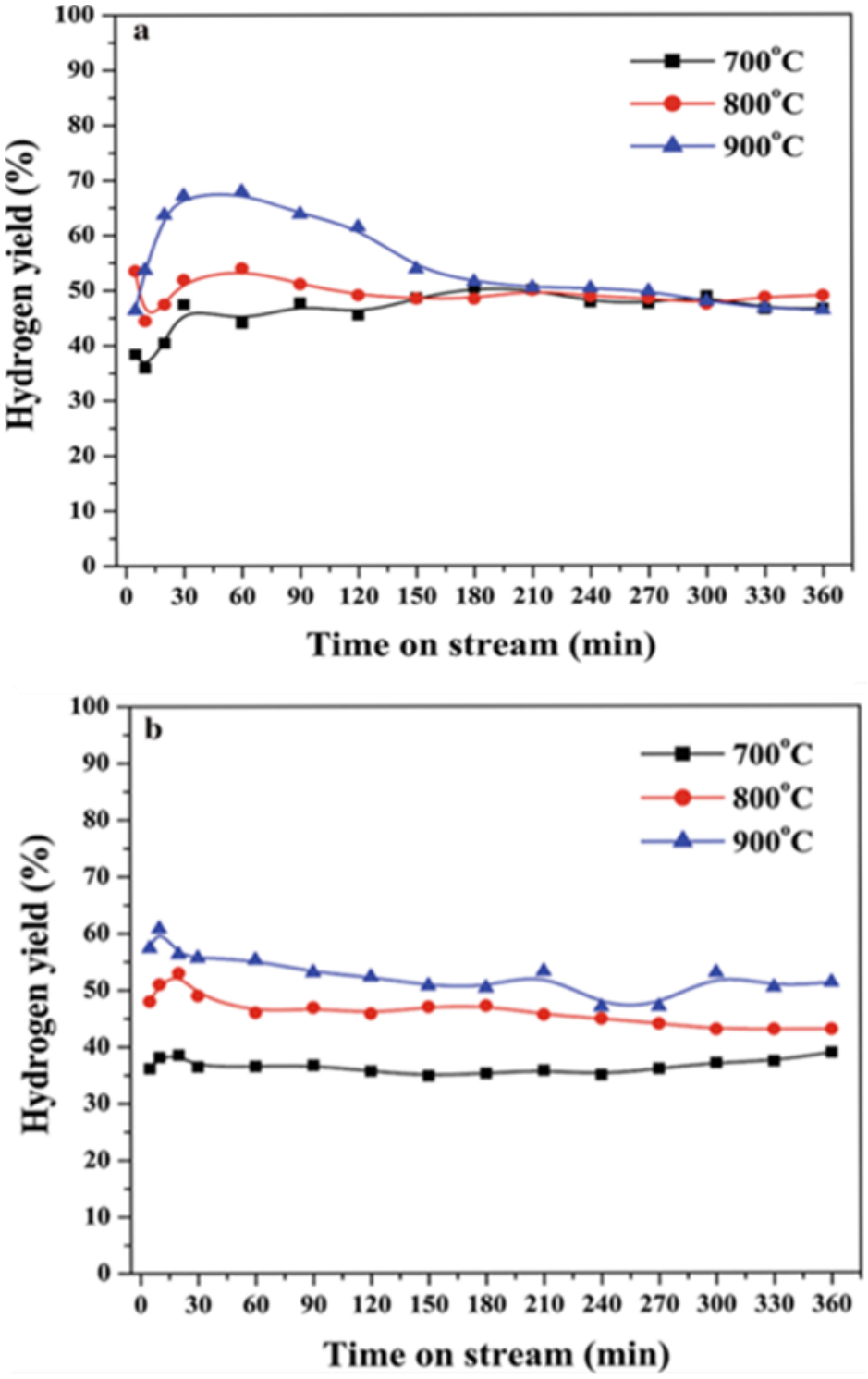

Figure 2.7 Effect of reaction temperature on H_2 yield and stability of (a) Ni catalyst and (b) Fe catalyst. Adopted from [69].

2.8.5 Effect of metal loading

Metal loading on the catalyst support directly effects stability and catalytic activity of the catalyst, this is due to metal-support interaction and dispersion of metal particles over the support [57]. The effect of Fe loading as well as effect of different support (Al_2O_3, MgO, TiO_2) interaction with metal different loading were studied (depicted in **Figure 2.8**) [58]. For Fe/Al_2O_3 catalyst, 15% Fe loading have shown stable catalytic performance throughout TOS. For higher Fe loading, initial methane conversion were increasing consistently which was due to carbon deposition over catalyst surface and the carbon deposition results in increasing pressure and outflow which also effect space velocity [70].

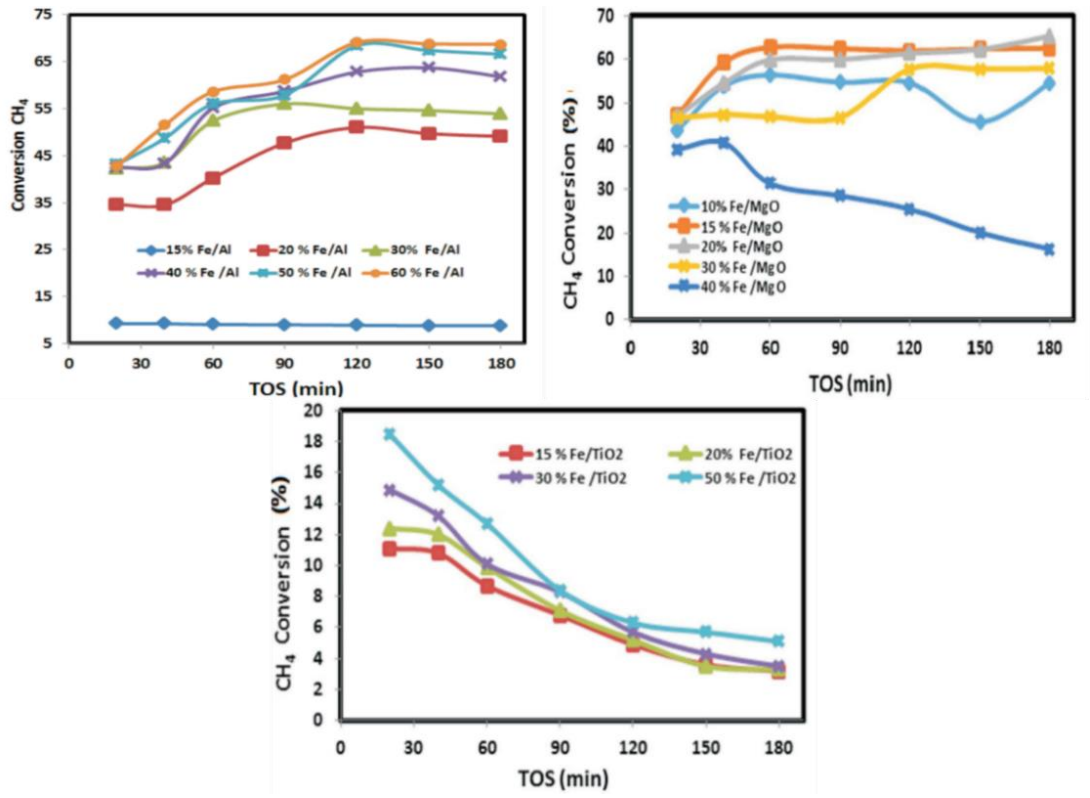

Figure 2.8 Time on stream methane conversion for different Fe loading over Al_2O_3, MgO and TiO_2 support at 700 ℃ [70].

Methane conversion enhance with increasing Fe loading over the support Al_2O_3 in this order $60\%Fe/Al_2O_3 > 50\%Fe/Al_2O_3 > 40\%Fe/Al_2O_3 > 30\%Fe/Al_2O_3 > 20\%Fe/Al_2O_3 > 15\%Fe/Al_2O_3$. While for Fe/MgO catalyst, lower Fe loading have shown excellent catalytic activity and stability as compared to higher Fe content which clearly mean that lower Fe loading has better dispersion over MgO. In case of Fe/TiO_2 catalyst,

different Fe loading were tested but it was found that despite various Fe loading, there is no favourable catalyst with preferable Fe loading [58]. Hence the results shown that for higher Fe loading, Fe/Al_2O_3 catalyst are top choice, with lower Fe loading Fe/MgO are preferred catalyst and Fe/TiO_2 catalyst have shown poor activity despite different Fe loading, which reveals poor Fe interaction with support TiO_2 [69].

Ni-based catalyst shows faster deactivation with higher loading. As increased Ni content in catalyst increase particle size of nickel, decrease metal-support interaction and agglomeration of Ni particles which results in higher methane conversion and CNTs yield, which causes to block active site and deactivate catalyst quickly, [1].

Carbon morphology of the deposited carbon are also highly effect by metal loading. At higher metal loading, larger and broader CNF and CNT are formed due to metal particle agglomeration and tip growth mechanism (TGM). While base growth mechanism (BGM) were observed for low metal loading. These mechanism were developed due to metal-support interaction and are presented in **Figure 2.9** [33].

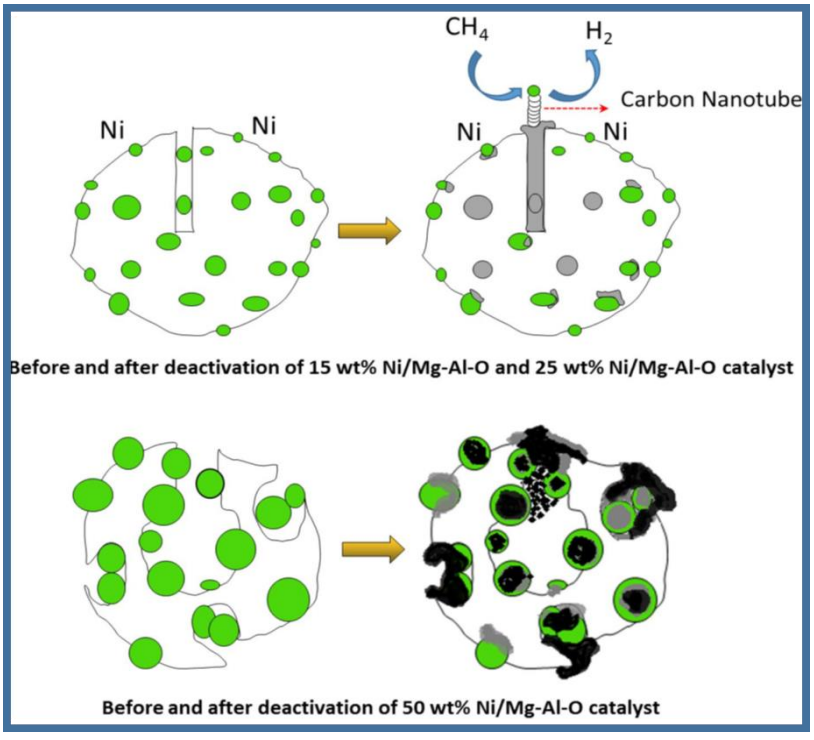

Figure 2.9 Effect of different metal loading over deactivation of catalyst [28].

2.8.6 Effect of catalyst's preparation method

The preparation method of the catalyst alters the physiochemical properties of the catalyst, effects the catalytic performance of the catalyst and change the morphology of deposited carbon [59]. The catalyst preparation method also have obvious effect on metal particles dispersion and support-active metal-promoter interaction [60]. In literature Fe/Al_2O_3 were prepared by incipient wet impregnation and co-precipitating method [59]. The results shows that catalyst prepared with impregnation method shows promising results at 500℃ temperature results in 65% of methane conversion and 62% of hydrogen yield while for catalyst prepared with co-precipitation results in maximum methane conversion of 50% and hydrogen yield of the 45% at same experimental temperature [59]. The XRD of catalyst with co-precipitation method have dominant peaks for alumna while the Fe/Al_2O_3 prepared by impregnation method shows clear peaks for both alumna and Fe oxides due to larger Fe particle size [59].

2.9 Thermal reactor system configuration for thermo-catalytic decomposition of methane

In reaction engineering, reactor systems are very important consideration. The researcher around the world have made their efforts for the development of the reactor system in order to improve its efficiency and material inertness towards reaction [22, 61]. The research is also carried out to use renewable energy such as solar to avoid use of fossil fuel and electricity for the energy which is required for a particular process to carry out in reactor [62]. By the use of the renewable energy, the environmental concern in term of CO_2 emission and economic issues related to the process of thermo-catalytic decomposition of methane for COx-free hydrogen production will be resolved.

Material for the construction of the reactor system is also an important consideration. For the reactors, materials were selected which are stable and inert at high temperature towards the reaction. The most commonly used material for reactor construction is "stainless steel", but as stainless steel is composed of active iron and its alloy, which makes it unfavourable for thermo-catalytic decomposition of methane, as at higher temperature it plays catalytic role in thermo-catalytic decomposition of methane and disturb the original process [63]. Other materials such as ceramics and quartz are now

considered for reactor construction, to increase inertness towards reaction [64]. Thermo-catalytic decomposition of methane is a continuous reaction process at high temperature for hydrogen production, which requires design and construction of proper reactor system to carry out the process.

During the last decade various reactor systems were used for the process of thermo-catalytic decomposition of methane, among them most commonly fixed bed reactor was utilized. Thermo-catalytic decomposition of methane results in gaseous hydrogen and carbon in solid form as by-product. The gaseous hydrogen is collected at the exit of the reactor but the carbon in solid form accumulates over the catalyst surface which cause reduction in catalytic activity of catalyst and as a results drop in hydrogen yield along with catalyst deactivation is observed [65, 66]. The researcher used fluidized bed reactor in order to continually remove the deposited carbon from the reactor periodically and adding fresh catalyst to the reactor for the continuous production of hydrogen. This property of fluidized bed reactor makes it suitable for commercial scale production of hydrogen. The fluidization also results in continues motion of catalyst particle which improve heat and mass transfer rate [67, 68].

2.9.1 Fixed bed reactor

Fixed bed reactors are best for processes that require temperature control, ease of operation, and low reactor body corrosion [38]. The main advantage of this reactor system is that it can be built in a compact size with several orientations (horizontal or vertical) and the experimental parameters are easy to maintain [63]. As a result, fixed bed reactor systems are commonly used in a variety of applications around the world, both on an industrial and laboratory scale [69]. For thermo-catalytic decomposition of methane, fixed bed reactors are most widely used as these reactors are simple to set up and maintain [70]. The typical fixed bed reactor system geometry consists of a long vertical tube usually made of steel or quartz, with the catalyst bed located in the reactor's heating zone. The reactant gases are introduced to reactor and are made to pass through the heating zone where catalyst bed is located [12]. The product gases are passed through a condenser at the end of the tube to eliminate the vapour content before being collected. The in-flow to the reactor is normally controlled with a flow

metre, and temperature of heating zone is controlled with the process controller. Thermocouple was mounted to measure the temperature of heating zone.

The diagram of fixed bed reactor system for thermo-catalytic decomposition of methane with in-flow of methane and nitrogen are shown in **Figure 2.10.**

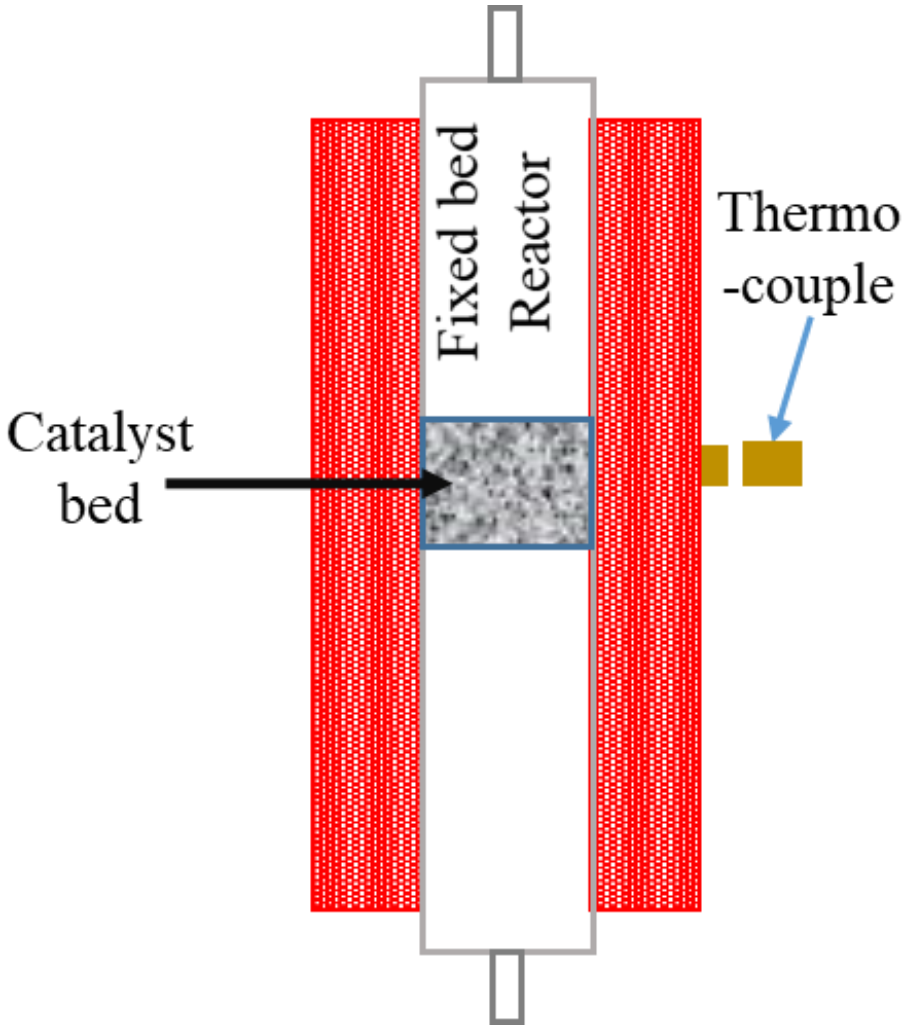

Figure 2.10 Diagram of vertical fixed bed reactor system.

The fixed bed reactors are advantageous because it does not put any restrain over flow rate as in case of fluidize bed reactor. Furthermore, it provide homogenous heating zone to the catalyst to favour the reaction [38]. In design of fixed bed reactor, selection of reactor material have greater importance because the reactor material have serious effect over thermo-catalytic decomposition of methane at higher temperature [71, 72]. The material selected for the construction of fixed bed reactors have the properties to

bear high temperature environment, inert towards the reaction process carried out in reactor, easily available and cost effective. In literature mostly fixed bed reactor of stainless materials have been reported because of its availability and economics [62]. Stainless steel reactor with different diameter and length, and usually powered by electric furnace are used for thermo-catalytic decomposition of methane [73]. The steel reactors are highly recommended for high pressure application and temperature below 800 ℃ [74], and if the thermo-catalytic decomposition of methane were developed commercially, stainless steel material will be utilized for construction of the fixed bed reactors [22, 71].

The major concern associated with steel reactor that iron and its alloy become catalytically active at temperature higher than 800 ℃ [75] and leads towards the formation of some carbon materials which not only cause damage to the reactor material [76], but also the adhere carbon materials to the reactor walls participate in thermo-catalytic decomposition of methane and leading towards the jamming of reactor [22]. To overcome this problem, reactor of quartz or ceramic material has been investigated as these materials are catalytically sable at higher temperature up to 1500 ℃ which not only protect reactor material from damage but also inert towards the reaction carried out in reactor [74].

The conventional fixed bed reactors mostly utilize electric furnace for green and safe fuel (hydrogen) production but still indirectly contribute to the GHG emissions and global warming in terms of electricity usage [62]. Hence to overcome this disadvantage the researchers across the globe are working to utilize renewable energy resources especially solar for heating purpose of the reactor to achieve required temperature [77]. The concentrated solar power were used to achieve the required temperature in heating zone of the reactor system. The solar powered fixed-bed reactor configuration consist of cavity type solar receiver, which are placed vertically in the tubular absorber [78]. The tubular absorber act as blackbody and is separated from ambient atmosphere with transparent insulation. For stability of process, the reaction zone are separated from the irradiation region. The methane conversion reported about 80% at 1050 ℃ in the presence of the Carbon Black as the catalyst [62]. Complete configuration of solar powered fixed bed reactor are shown in **Figure 2.11**.

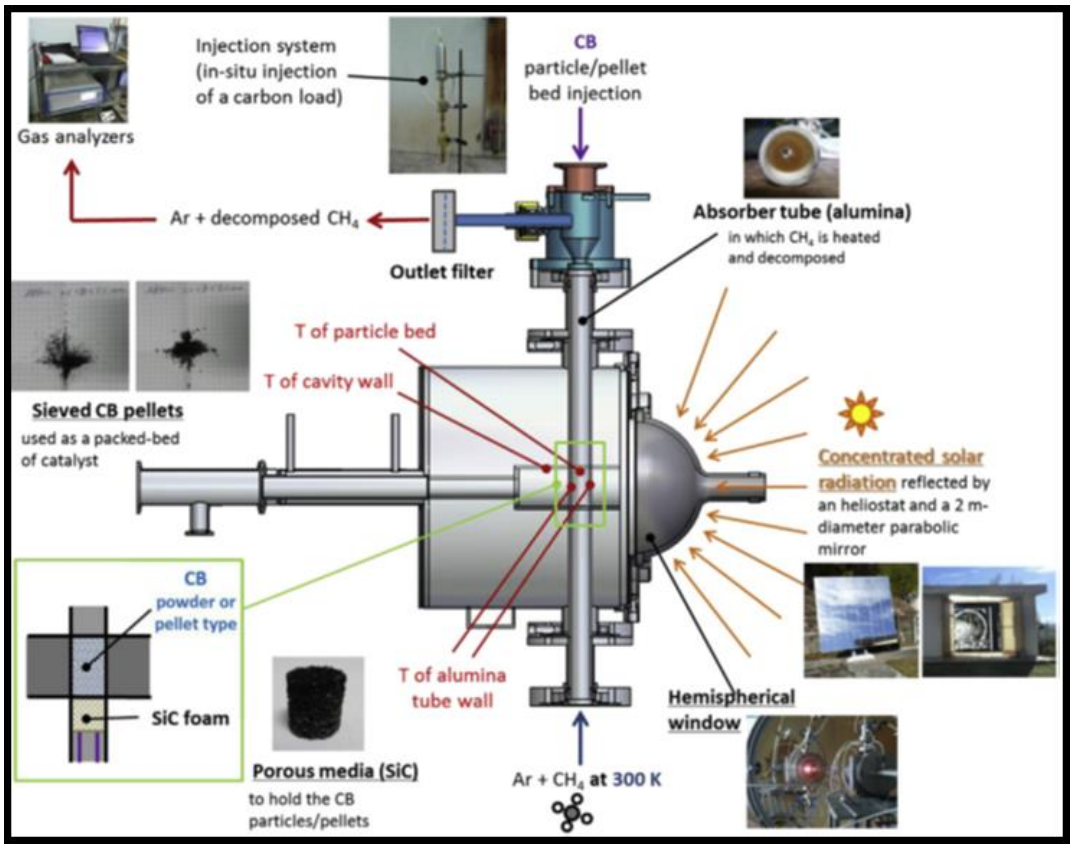

Figure 2.11 Solar powered fixed bed reactor for hydrogen production via thermo-catalytic decomposition of methane [74].

Despite having numerous advantages in term of maintenance and economics, the conventional fixed bed reactors have some drawbacks (1) solid carbon deposition over catalyst surface and covering catalyst's active sites from reaction (2) cause jamming of the reactor which block flow of gases over catalyst (3) carbon deposition contribute to the pressure drop (4) non-uniform temperature distribution in the conventional fixed bed reactor [79-81].

To minimize some of the drawbacks related to conventional fixed bed reactors, Honeycomb Monolith type of reactors were introduced to the application of thermo-catalytic decomposition of methane [82]. Despite being favorable for thermo-catalytic decomposition of methane, very few studies are found over the monolith reactors. The deposited carbon do not cover the catalyst surface and nor drop pressure in the reactor due to structured space in monoliths.

In literature, carbon monolith structure were developed for thermo-catalytic decomposition of methane with CH_4 conversion of 33% at 800 °C [82], monolith and

rector flow diagram are shown in **Figure 2.12**. At same time monolith reactors also face challenges in term of uniform temperature over its structure which leads towards the controlled temperature related issues[83].

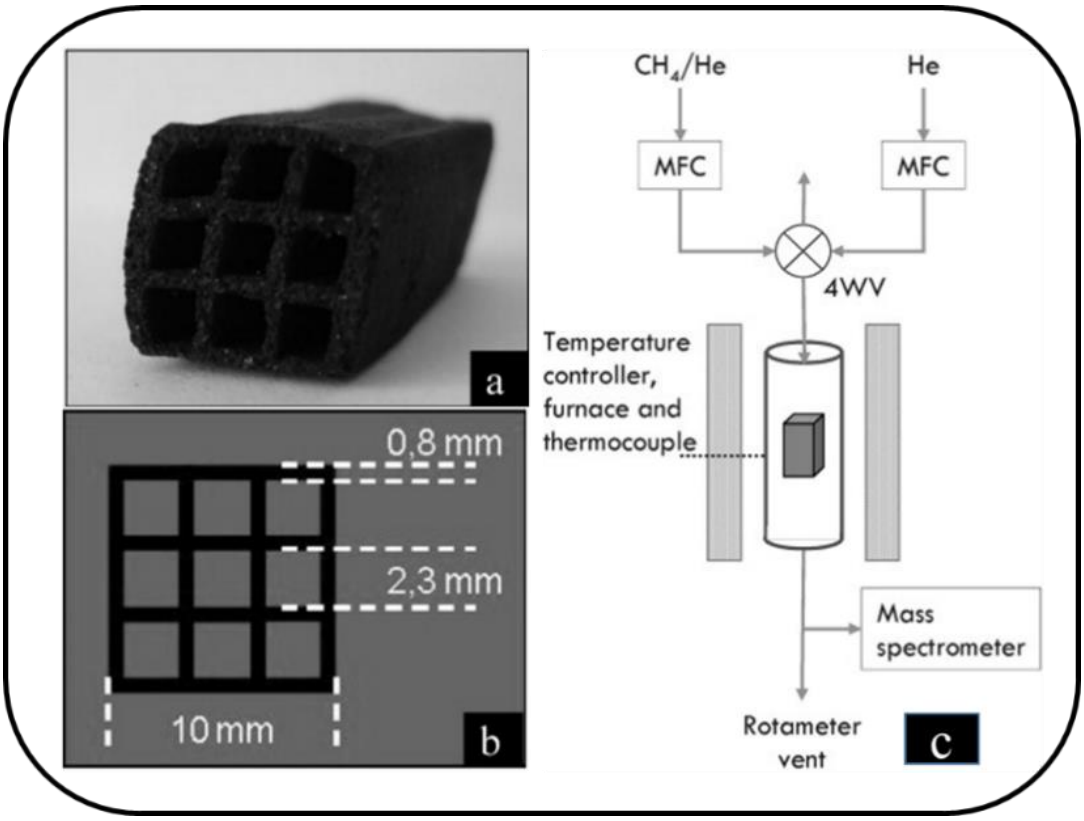

Figure 2.12 (a) Image of carbon used for monolith, (b) Monolith geometry and (c) reactor used for reaction [82].

2.9.2 Fluidized bed reactor

Fluidized bed reactors are widely used for various application such as petroleum, metallurgy, pyrolysis, reforming and chemical industries [84]. To maintain continually reaction of thermo-catalytic decomposition of methane and avoid jamming of the reactor tube due to deposition of solid carbon over the catalyst surface, leads the researcher to development of the fluidized bed reactor system, where the deposited carbon and deactivated catalyst are removed periodically, and fresh catalyst are loaded in the reactor to continue the process without any stoppage of process [19, 70].

Compared to fixed bed reactors, fluidized bed reactors are most suitable for large scale production of hydrogen due to periodic removal and addition of catalyst [70]. Additionally, the temperature in fluidized reactor system were controlled easily as

compared to the fixed bed reactor and also higher temperature at the particular zone in fixed bed reactor create hotspot which damage catalyst and reactor wall with time [85]. Muradov et al. [72] discuss in detail and compare various reactor system such as fluidized bed reactor, fixed bed reactor, free volume reactor and tubular reactor for thermo-catalytic decomposition of methane and come to the conclusion that fluidized bed reactor are most favorable for thermo-catalytic decomposition of methane. The fluidization improve the mass and heat transfer which maximize methane molecules activation and decomposition [19].

The fluidized bed reactor system configuration consist of the fluidized bed of the catalyst in a reactor tube which is usually heated by an electric furnace. A thermocouple has been installed at the reactor to measure the temperature of the heating zone and were controlled by temperature controller. Mass flow controller were used to measure the in-flow gases such as methane and nitrogen to the reactor. A differential pressure transducer were installed to measure the total pressure drop in the distributer and fluidized bed. The schematic flow diagram of fluidized bed reactor system has shown in **Figure 2.13.**

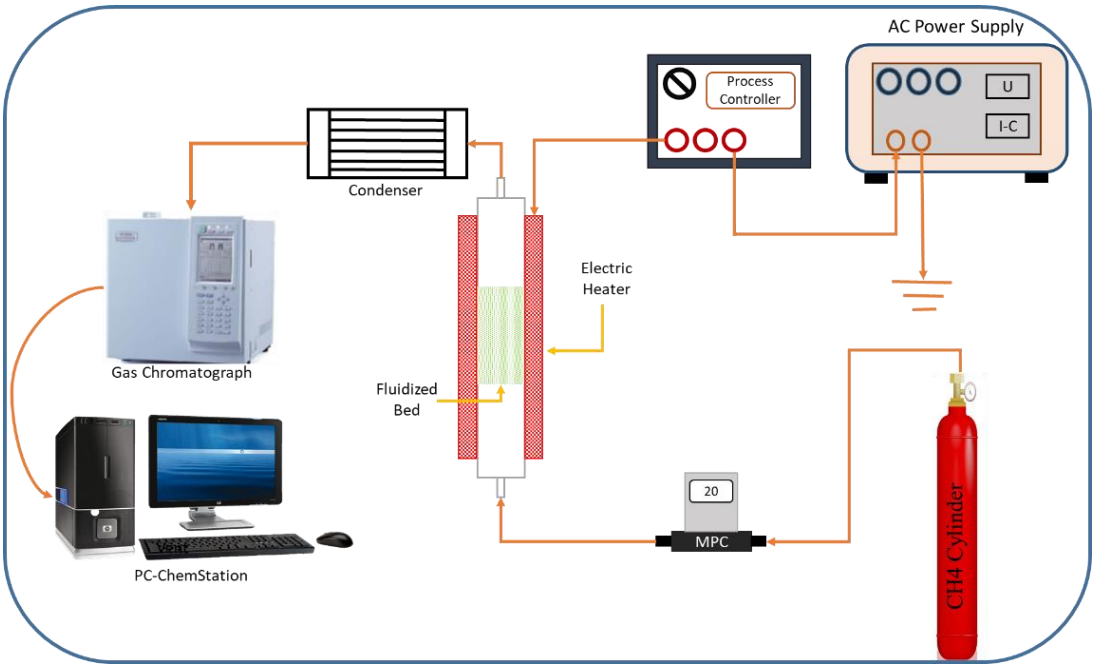

Figure 2.13 Schematic flow diagram of fluidized bed reactor system.

Reaction temperature, gas velocity and particle size are three main factors effecting the fluidization of reactor for methane decomposition [66]. The basic parameter

required for the design and operation of fluidized bed reactor are the minimum fluidization velocity and (V_f) and minimum fluidization flow rate (Q_f). Ergun equation are used for the calculation of theoretical minimum fluidization velocity which are shown in (Eq. (2)), and for calculation of theoretical minimum fluidization flow rate (Qf) (Eq. (3)) were used [86].

Equation for V_f

$$V_{mf} = \frac{d_p{}^2 \left(p_s - p_g \right).g}{1650\mu} \qquad \text{Eq. (2)}$$

Equation of Q_f

$$Q_{mf} = 60\pi\left(\frac{d}{2}\right)^2 . \mathrm{V_{mf}} \qquad \text{Eq. (3)}$$

Whereas, d_p is diameter of particle, ρ_s and ρ_g are solid and gas densities, g is acceleration of gravity, μ is the viscosity of gas and in Q_f equation d represent reactor diameter.

Various configuration of fluidized bed reactor system where used to maximize the efficiency of the reactor. For this purpose a pre-heater was installed before the reactor which heats the in-flow gases up to 450℃, pre-heater basically reduce the activation energy required for the methane molecule to decompose [87].

In another fluidized bed reactor system, two-stage reactor were designed, which not only improved the methane conversion and hydrogen yield but also favored the formation of more structured carbon nano-materials [88]. Two-stage fluidized bed reactor is shown in **Figure 2.14**. In such configuration the reactor were divided into two stage with the help of 10% perforated plate which prevents back mixing of gases but the fluidized solid are allowed to mix easily and a heat exchanger is installed in-between the two stage to accurately control the temperature [88].

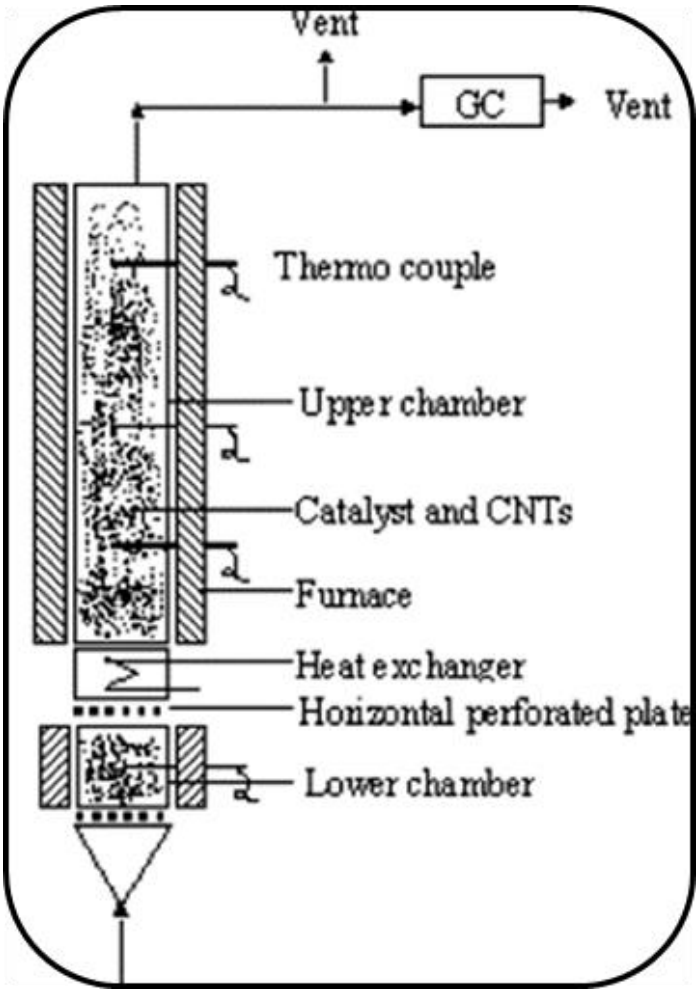

Figure 2.14 Two-stage fluidized bed reactor system [88].

With many advantages and versatile uses, the fluidized bed reactor system still have some limitations which make it critical in some application. For example in methane decomposition during the course of process there is great variation in the density of the reactor bed which some time leads to the disturbing the catalyst's support interaction with active metal and also breaking the carbon nano-tubes [89].

2.9.3 Rotary bed reactor

Rotary bed reactor system basically belongs to the category of fixed bed reactor, but it overcomes the concern related with fluidized fixed bed reactor. It is relatively a new concept as there is no detailed work available in literature about it. Rotary bed reactors applicable at the laboratory scale for the thermo-catalytic decomposition of methane [90]. Rotary bed reactors are advantageous because minimum flow for bed fluidization is not needed and it gives combine advantages of fluidized bed reactor system and

rotary kiln by providing controlled environment. The rotation of bed gives better mixing and avoid agglomeration [89]. Moreover, the freedom of flow rate allows better gas-solid contact [91]. The configuration of the rotary bed reactor system consists of the rotating cylindrical drum about horizontal axis and speed of the cylindrical system were controlled by an electric motor [89]. Electric furnace were used for heating, and thermocouples were installed for measuring temperature controlled by temperature controller. The detail flow diagram of the rotary bed system are shown in **Figure 2.15**.

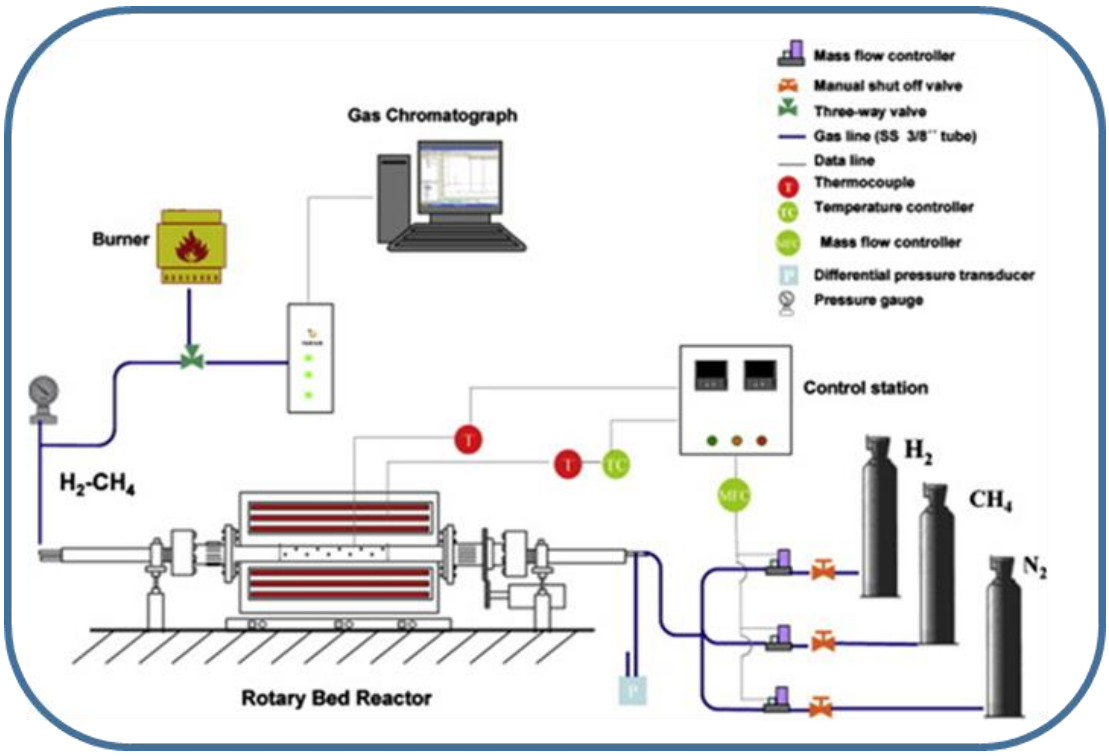

Figure 2.15 Schematic diagram of rotary bed system [89].

2.9.4 Molten metal reactor

To avoid the de-carbonization of the catalyst, recently researchers favor molten metal reactor for thermo-catalytic decomposition of methane [92]. Molten metal reactor avoid jamming of the reactor as the solid deposited carbon removal are possible periodically due to the density difference between the deposited solid carbon and molten metal, where the deposited carbon raised to the top of reactor. Secondly, the molten metal provide an efficient heat transfer. Initially M Steinberg et al. [93] used molten metal reactor system for decarburization of fossil fuel which was followed by M Serban et al. [94], where the molten metal were utilized for the hydrogen production.

With the set up 57% of methane conversion was recorded at 750℃. The reported configuration of molten metal reactor are made of quartz glass to avoid corrosion and stainless steel cladding tube help in providing required mechanical strength to reactor system, shown in **Figure 2.16(a).**

Pure methane gas was introduce through small orifice at the bottom of reactor and pass through "molten tin metal as catalyst" for thermo-catalytic decomposition of methane [95]. In another recent study molten metal bubble column reactor was used for direct conversion of methane to hydrogen and shown in **Figure 2.16(b).** In the proposed setup solid deposited carbon were removed successfully and 95% methane conversion at 1050 ℃ was observed over molten $Ni_{0.27}Bi_{0.73}$ as catalyst [96].

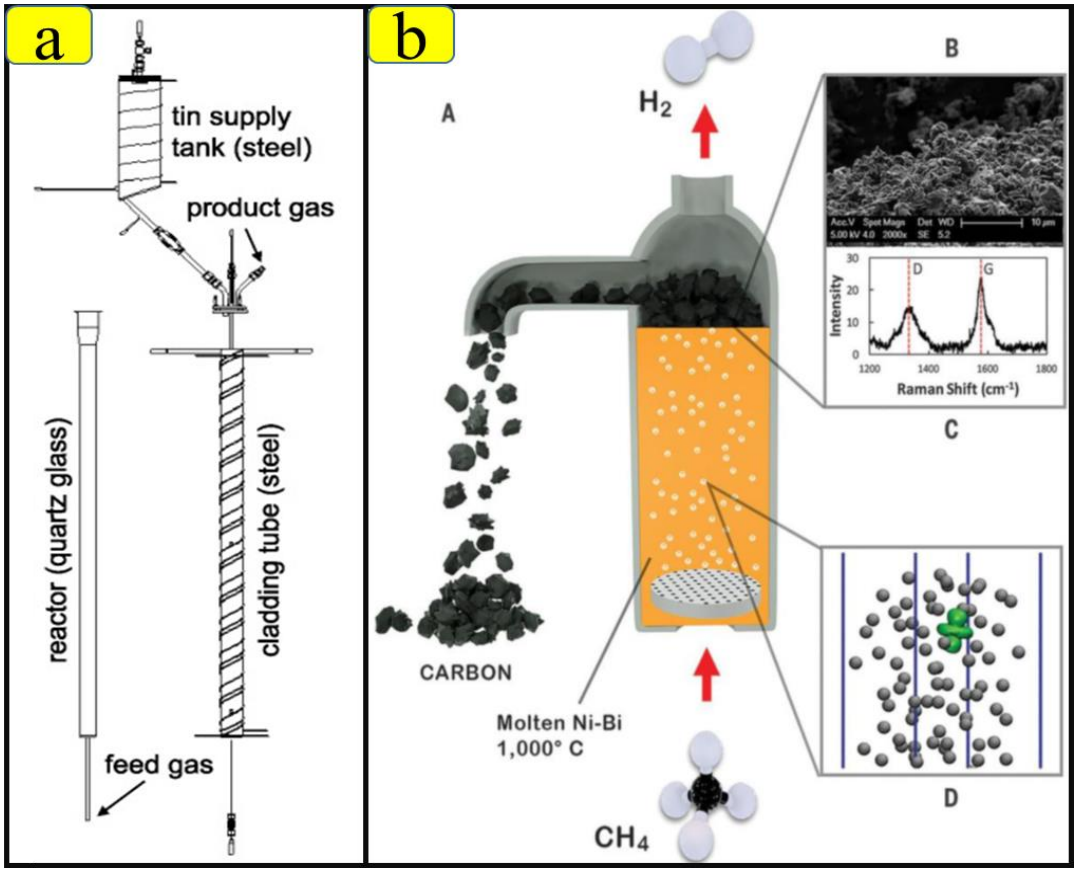

Figure 2.16 (a) Molten metal catalyst filled with tin as catalyst [95] (b) Molten metal bubble column reactor [96].

The concept of molten metal reactor system are very useful as it will solve some critical concern related to the thermo-catalytic decomposition of methane, but still facing major challenges as it require huge amount of energy to keep metal molten at 1000 ℃

or other methods were needed to be identified which keeps metal as molten catalyst at lower temperature [4].

Summary

Excessive usage of fossil fuel resources in order to fulfill the energy demand of the world, which leads to the depletion of the fossil fuel resources and also increase the concentration of GHG in our environment. The researcher across the globe are working concurrently over the both issues. The introduction and development of renewable energies are among the solutions to the given problems, but at the same time these technologies are immature and inefficient. Therefore, effective utilization of fossil fuel are needed in order to handle both depletion of fossil fuel and control GHG emissions. Keeping in mind these related concerns, hydrogen economy were introduced. The main concern with hydrogen economy is the absence of "elemental hydrogen" in the nature which is the main headache. Various hydrogen production technologies based on fossil fuel are used such as dry reforming of methane (DRM), steam reforming of methane (SRM), partial oxidation of methane (POM) and coal gasification. Among them DRM and POM are the commercial process for hydrogen production. Based on renewable energy, hydrogen production technologies are thermo-chemical splitting of water, photo-electrolysis, electrolysis and biomass gasification. These process are very demandable due to usage of renewable energy and sources but still these process are immature and are in developing phase. Apart from these process thermo-catalytic decomposition of methane is also a process use for production of green hydrogen and solid carbon nano-materials. The carbon nano-materials based on its morphology can be utilize for various application which reduce economics of the process.

The various ashes produce from power plants are usually disposed in land fill sites which is the total wastage of this bio-material. For sustainable management of these ashes was taken under study in literature and its physiochemical properties were studied extensively and it was found that the presence of the various oxides made it suitable candidate for catalytic applications.

The main concern with thermo-catalytic decomposition of methane is the quick deactivation of the catalysts due to agglomeration of carbon around the active phase

of the catalyst. To overcome this problem various transition metal based catalyst were used but still no major success were achieved. Therefore, to overcome the economics of the catalyst for thermo-catalytic decomposition of ethane renewable base materials were targeted for usage in thermo-catalytic decomposition of methane. These ash base materials were both use as catalyst and catalyst support.

For thermo-catalytic decomposition of methane process various reactor system were used in order to obtain maximum hydrogen yield and minimize the catalyst deactivation due to carbon deposition. Mostly fixed bed reactors were used because they are easy to maintain and maximum amount of heat transfer to the catalytic bed and in results enhance the methane conversion and hydrogen yield.

References

[1] J.X. Qian, T.W. Chen, L.R. Enakonda, D.B. Liu, J.-M. Basset, L. Zhou, Methane decomposition to pure hydrogen and carbon nano materials: State-of-the-art and future perspectives, International Journal of Hydrogen Energy, 45 (2020) 15721-15743.

[2] U.P.M. Ashik, W.M.A. Wan Daud, H.F. Abbas, Production of greenhouse gas free hydrogen by thermocatalytic decomposition of methane – A review, Renewable and Sustainable Energy Reviews, 44 (2015) 221-256.

[3] F. Dawood, M. Anda, G.M. Shafiullah, Hydrogen production for energy: An overview, International Journal of Hydrogen Energy, 45 (2020) 3847-3869.

[4] R.R.C.M. Silva, H.A. Oliveira, A.C.P.F. Guarino, B.B. Toledo, M.B.T. Moura, B.T.M. Oliveira, F.B. Passos, Effect of support on methane decomposition for hydrogen production over cobalt catalysts, International Journal of Hydrogen Energy, 41 (2016) 6763-6772.

[5] K. Srilatha, D. Bhagawan, S. Shiva Kumar, V. Himabindu, Sustainable fuel production by thermocatalytic decomposition of methane – A review, South African Journal of Chemical Engineering, 24 (2017) 156-167.

[6] C. García-Sancho, R. Guil-López, A. Sebastián-López, R.M. Navarro, J.L.G. Fierro, Hydrogen production by methane decomposition: A comparative study of supported and bulk ex-hydrotalcite mixed oxide catalysts with Ni, Mg and Al, International Journal of Hydrogen Energy, 43 (2018) 9607-9621.

[7] A.A. Ibrahim, A.H. Fakeeha, A.S. Al-Fatesh, A.E. Abasaeed, W.U. Khan, Methane decomposition over iron catalyst for hydrogen production, International Journal of Hydrogen Energy, 40 (2015) 7593-7600.

[8] D. Kang, J.W. Lee, Enhanced methane decomposition over nickel–carbon–B_2O_3 core–shell catalysts derived from carbon dioxide, Applied Catalysis B: Environmental, 186 (2016) 41-55.

[9] M. Karaismailoglu, H.E. Figen, S.Z. Baykara, Hydrogen production by catalytic methane decomposition over yttria doped nickel based catalysts, International Journal of Hydrogen Energy, 44 (2019) 9922-9929.

[10] H. Nishii, D. Miyamoto, Y. Umeda, H. Hamaguchi, M. Suzuki, T. Tanimoto, T. Harigai, H. Takikawa, Y. Suda, Catalytic activity of several carbons with different structures for methane decomposition and by-produced carbons, Applied Surface Science, 473 (2019) 291-297.

[11] M. Pudukudy, Z. Yaakob, Methane decomposition over Ni, Co and Fe based monometallic catalysts supported on sol gel derived SiO_2 microflakes, Chemical Engineering Journal, 262 (2015) 1009-1021.

[12] J.X. Qian, T.W. Chen, L.R. Enakonda, D.B. Liu, G. Mignani, J.-M. Basset, L. Zhou, Methane decomposition to produce CO -free hydrogen and nano-carbon over

metal catalysts: A review, International Journal of Hydrogen Energy, 45 (2020) 7981-8001.

[13] E. Tezel, H.E. Figen, S.Z. Baykara, Hydrogen production by methane decomposition using bimetallic Ni–Fe catalysts, International Journal of Hydrogen Energy, 44 (2019) 9930-9940.

[14] J.B. Zhang, W.T. Xie, X. Li, Q.Q. Hao, H.Y. Chen, X.X. Ma, Methane decomposition over Ni/carbon catalysts prepared by selective gasification of coal char, Energy Conversion and Management, 177 (2018) 330-338.

[15] N. Bayat, F. Meshkani, M. Rezaei, Thermocatalytic decomposition of methane to CO_x-free hydrogen and carbon over Ni–Fe–Cu/Al_2O_3 catalysts, International Journal of Hydrogen Energy, 41 (2016) 13039-13049.

[16] N. Bayat, M. Rezaei, F. Meshkani, Hydrogen and carbon nanofibers synthesis by methane decomposition over Ni–Pd/Al_2O_3 catalyst, International Journal of Hydrogen Energy, 41 (2016) 5494-5503.

[17] A.S. Al-Fatesh, A.H. Fakeeha, W.U. Khan, A.A. Ibrahim, S.B. He, K. Seshan, Production of hydrogen by catalytic methane decomposition over alumina supported mono-, bi- and tri-metallic catalysts, International Journal of Hydrogen Energy, 41 (2016) 22932-22940.

[18] A. Wolfbeisser, G. Kovács, S.M. Kozlov, K. Föttinger, J. Bernardi, B. Klötzer, K.M. Neyman, G. Rupprechter, Surface composition changes of CuNi-ZrO_2 during methane decomposition: An operando NAP-XPS and density functional study, Catalysis Today, 283 (2017) 134-143.

[19] A.H. Fakeeha, A.A. Ibrahim, W.U. Khan, K. Seshan, R.L. Al Otaibi, A.S. Al-Fatesh, Hydrogen production via catalytic methane decomposition over alumina supported iron catalyst, Arabian Journal of Chemistry, 11 (2018) 405-414.

[20] M. Pudukudy, Z. Yaakob, Q.M. Jia, M.S. Takriff, Catalytic decomposition of methane over rare earth metal (Ce and La) oxides supported iron catalysts, Applied Surface Science, 467 (2019) 236-248.

[21] N. Muradov, T. Veziroğlu, From hydrocarbon to hydrogen–carbon to hydrogen economy, International journal of hydrogen energy, 30 (2005) 225-237.

[22] Z. Abdin, A. Zafaranloo, A. Rafiee, W. Merida, W. Lipinski, K.R. Khalilpour, Hydrogen as an energy vector, Renew Sust Energ Rev, 120 (2020) 109620.

[23] L. Weger, A. Abanades, T. Butler, Methane cracking as a bridge technology to the hydrogen economy, International Journal of Hydrogen Energy, 42 (2017) 720-731.

[24] T. Morgan, The hydrogen economy: A non-technical review, UNEP/Earthprint2006.

[25] A. Choudhury, H. Chandra, A. Arora, Application of solid oxide fuel cell technology for power generation—A review, Renewable and Sustainable Energy Reviews, 20 (2013) 430-442.

[26] C.C. Chan, The state of the art of electric, hybrid, and fuel cell vehicles, Proceedings of the Ieee, 95 (2007) 704-718.

[27] H.F. Abbas, W.M.A. Wan Daud, Hydrogen production by methane decomposition: A review, International Journal of Hydrogen Energy, 35 (2010) 1160-1190.

[28] K. Harun, S. Adhikari, H. Jahromi, Hydrogen production via thermocatalytic decomposition of methane using carbon-based catalysts, RSC Advances, 10 (2020) 40882-40893.

[29] M. Pudukudy, Z. Yaakob, M.S. Takriff, Methane decomposition into COx free hydrogen and multiwalled carbon nanotubes over ceria, zirconia and lanthana supported nickel catalysts prepared via a facile solid state citrate fusion method, Energy Conversion and Management, 126 (2016) 302-315.

[30] A.F.a. Syed Muhammad, A. Awad, R. Saidur, N. Masiran, A. Salam, B. Abdullah, Recent advances in cleaner hydrogen productions via thermo-catalytic decomposition of methane: Admixture with hydrocarbon, International Journal of Hydrogen Energy, 43 (2018) 18713-18734.

[31] M. Assad Munawar, A. Hussain Khoja, M. Hassan, R. Liaquat, S. Raza Naqvi, M. Taqi Mehran, A. Abdullah, F. Saleem, Biomass ash characterization, fusion analysis and its application in catalytic decomposition of methane, Fuel, 285 (2021) 119107.

[32] Y. Gao, J. Jiang, Y. Meng, A. Aihemaiti, T. Ju, X. Chen, F. Yan, A novel nickel catalyst supported on activated coal fly ash for syngas production via biogas dry reforming, Renewable Energy, 149 (2020) 786-793.

[33] V. Nichele, M. Signoretto, F. Menegazzo, A. Gallo, V. Dal Santo, G. Cruciani, G. Cerrato, Glycerol steam reforming for hydrogen production: Design of Ni supported catalysts, Applied Catalysis B: Environmental, 111-112 (2012) 225-232.

[34] E. López, J. Kim, A.M. Shanmugharaj, S.H. Ryu, Multiwalled carbon nanotubes-supported Nickel catalysts for the steam reforming of propane, Journal of Materials Science, 47 (2011) 2985-2994.

[35] A. Venugopal, S. Naveen Kumar, J. Ashok, D. Hari Prasad, V. Durga Kumari, K.B.S. Prasad, M. Subrahmanyam, Hydrogen production by catalytic decomposition of methane over Ni/SiO2Ni/SiO2☆, International Journal of Hydrogen Energy, 32 (2007) 1782-1788.

[36] L. Zhou, L.R. Enakonda, M. Harb, Y. Saih, A. Aguilar-Tapia, S. Ould-Chikh, J.-l. Hazemann, J. Li, N. Wei, D. Gary, P. Del-Gallo, J.-M. Basset, Fe catalysts for

methane decomposition to produce hydrogen and carbon nano materials, Applied Catalysis B: Environmental, 208 (2017) 44-59.

[37] A.E. Awadallah, D.S. El-Desouki, S.M. Abdel-Azim, N.A.K. Aboul-Gheit, S.M. Abdel-Hamid, A.K. Aboul-Gheit, Effect of La, Ce and Nd oxides addition on the activity and stability of Co/MgO catalyst for methane decomposition into COx-free H_2 production and carbon nanotubes, Fullerenes, Nanotubes and Carbon Nanostructures, 26 (2018) 525-534.

[38] G. Italiano, A. Delia, C. Espro, G. Bonura, F. Frusteri, Methane decomposition over Co thin layer supported catalysts to produce hydrogen for fuel cell, International Journal of Hydrogen Energy, 35 (2010) 11568-11575.

[39] Z.F. Bian, Z.G. Wang, B. Jiang, P. Hongmanorom, W.Q. Zhong, S. Kawi, A review on perovskite catalysts for reforming of methane to hydrogen production, Renew Sust Energ Rev, 134 (2020) 110291.

[40] M. Pudukudy, A. Kadier, Z. Yaakob, M.S. Takriff, Non-oxidative thermocatalytic decomposition of methane into COx free hydrogen and nanocarbon over unsupported porous NiO and Fe_2O_3 catalysts, International Journal of Hydrogen Energy, 41 (2016) 18509-18521.

[41] W. Ahmed, A.E. Awadallah, A.A. Aboul-Enein, Ni/CeO2–Al2O3 catalysts for methane thermo-catalytic decomposition to CO -free H2 production, International Journal of Hydrogen Energy, 41 (2016) 18484-18493.

[42] A.E. Awadallah, W. Ahmed, M.R.N. El-Din, A.A. Aboul-Enein, Novel aluminosilicate hollow sphere as a catalyst support for methane decomposition to COx-free hydrogen production, Applied Surface Science, 287 (2013) 415-422.

[43] B. Gao, I.W. Wang, L. Ren, J. Hu, Catalytic Methane Decomposition over Bimetallic Transition Metals Supported on Composite Aerogel, Energy & Fuels, 33 (2019) 9099-9106.

[44] A.E. Awadallah, A.A. Aboul-Enein, D.S. El-Desouki, A.K. Aboul-Gheit, Catalytic thermal decomposition of methane to COx-free hydrogen and carbon nanotubes over MgO supported bimetallic group VIII catalysts, Applied Surface Science, 296 (2014) 100-107.

[45] J. Wang, L. Jin, Y. Li, H. Hu, Preparation of Fe-Doped Carbon Catalyst for Methane Decomposition to Hydrogen, Industrial & Engineering Chemistry Research, 56 (2017) 11021-11027.

[46] A.E. Awadallah, A.A. Aboul-Enein, M.M. Yonis, A.K. Aboul-Gheit, Effect of structural promoters on the catalytic performance of cobalt-based catalysts during natural gas decomposition to hydrogen and carbon nanotubes, Fullerenes, Nanotubes and Carbon Nanostructures, 24 (2015) 181-189.

[47] V. Ramasubramanian, H. Ramsurn, G.L. Price, Hydrogen production by catalytic decomposition of methane over Fe based bi-metallic catalysts supported on CeO_2–ZrO_2, International Journal of Hydrogen Energy, 45 (2020) 12026-12036.

[48] M.H. Kim, E.K. Lee, J.H. Jun, S.J. Kong, G.Y. Han, B.K. Lee, T.J. Lee, K.J. Yoon, Hydrogen production by catalytic decomposition of methane over activated carbons: kinetic study, International Journal of Hydrogen Energy, 29 (2004) 187-193.

[49] N.A.M. Zabidi, S. Zein, A.R. Mohamed, Hydrogen production by catalytic decomposition of methane, ME THREE NUMBER T, (2003) 3.

[50] M. Pudukudy, Z. Yaakob, Z.S. Akmal, Direct decomposition of methane over Pd promoted Ni/SBA-15 catalysts, Applied Surface Science, 353 (2015) 127-136.

[51] M. Pudukudy, Z. Yaakob, M.S. Takriff, Methane decomposition over Pd promoted Ni/$MgAl_2O_4$ catalysts for the production of COx free hydrogen and multiwalled carbon nanotubes, Applied Surface Science, 356 (2015) 1320-1326.

[52] N.S.N. Hasnan, S.N. Timmiati, K.L. Lim, Z. Yaakob, N.H.N. Kamaruddin, L.P. Teh, Recent developments in methane decomposition over heterogeneous catalysts: an overview, Materials for Renewable and Sustainable Energy, 9 (2020) 8.

[53] W.O. Alabi, K.O. Sulaiman, H. Wang, Sensitivity of the properties and performance of Co catalyst to the nature of support for CO_2 reforming of CH_4, Chemical Engineering Journal, 390 (2020) 124486.

[54] S. Chen, J. Zaffran, B. Yang, Dry reforming of methane over the cobalt catalyst: Theoretical insights into the reaction kinetics and mechanism for catalyst deactivation, Applied Catalysis B: Environmental, 270 (2020) 118859.

[55] Y. Li, D. Li, G. Wang, Methane decomposition to COx-free hydrogen and nano-carbon material on group 8–10 base metal catalysts: A review, Catalysis Today, 162 (2011) 1-48.

[56] A.E. Awadallah, A.A. Aboul-Enein, A.H. Mahmoud, S.S. Abd El Rehim, A.K. El-Ziaty, A.K. Aboul-Gheit, ZrxMg1-xO supported cobalt catalysts for methane decomposition into COx-free hydrogen and carbon nanotubes, International Journal of Green Energy, 15 (2018) 568-576.

[57] A.E. Awadallah, A.A. Aboul-Enein, Catalytic decomposition of methane to COx-free hydrogen and carbon nanotubes over Co–W/MgO catalysts, Egyptian Journal of Petroleum, 24 (2015) 299-306.

[58] A.E. Awadallah, A.A. Aboul-Enein, A.K. Aboul-Gheit, Effect of progressive Co loading on commercial Co–Mo/Al_2O_3 catalyst for natural gas decomposition to COx-free hydrogen production and carbon nanotubes, Energy conversion and management, 77 (2014) 143-151.

[59] M.A. Ermakova, D.Y. Ermakov, G.G. Kuvshinov, Effective catalysts for direct cracking of methane to produce hydrogen and filamentous carbon, Applied Catalysis A: General, 201 (2000) 61-70.

[60] G.B. Nuernberg, H.V. Fajardo, D.Z. Mezalira, T.J. Casarin, L.F.D. Probst, N.L.V. Carreño, Preparation and evaluation of Co/Al_2O_3 catalysts in the production of

hydrogen from thermo-catalytic decomposition of methane: Influence of operating conditions on catalyst performance, Fuel, 87 (2008) 1698-1704.

[61] A.R.K. Gollakota, V. Volli, C.M. Shu, Progressive utilisation prospects of coal fly ash: A review, Sci Total Environ, 672 (2019) 951-989.

[62] F. Goodarzi, Characteristics and composition of fly ash from Canadian coal-fired power plants, Fuel, 85 (2006) 1418-1427.

[63] S.R. Wang, F. Zhang, Q.J. Cai, X.B. Li, L.J. Zhu, Q. Wang, Z.Y. Luo, Catalytic steam reforming of bio-oil model compounds for hydrogen production over coal ash supported Ni catalyst, International Journal of Hydrogen Energy, 39 (2014) 2018-2025.

[64] M. Shahbaz, S. Yusup, A. Inayat, D.O. Patrick, A. Pratama, M. Ammar, Optimization of hydrogen and syngas production from PKS gasification by using coal bottom ash, Bioresour Technol, 241 (2017) 284-295.

[65] A.S. Al-Rahbi, P.T. Williams, Waste ashes as catalysts for the pyrolysis–catalytic steam reforming of biomass for hydrogen-rich gas production, Journal of Material Cycles and Waste Management, 21 (2019) 1224-1231.

[66] S.L. Geng, Z.N. Han, Y. Hu, Y.B. Cui, J.R. Yue, J. Yu, G.W. Xu, Methane Decomposition Kinetics over Fe_2O_3 Catalyst in Micro Fluidized Bed Reaction Analyzer, Industrial & Engineering Chemistry Research, 57 (2018) 8413-8423.

[67] E. Mahmoodzade, F. Meshkani, M. Rezaei, A. Rastegarpanah, Preparation and improvement of nickel catalyst supported ordered mesoporous spherical silica for thermocatalytic decomposition of methane, Journal of the Energy Institute, 93 (2020) 2488-2496.

[68] B.J. Leal Pérez, J.A. Medrano Jiménez, R. Bhardwaj, E. Goetheer, M. van Sint Annaland, F. Gallucci, Methane pyrolysis in a molten gallium bubble column reactor for sustainable hydrogen production: Proof of concept & techno-economic assessment, International Journal of Hydrogen Energy, 46 (2021) 4917-4935.

[69] J. Zhang, X. Li, H. Chen, M. Qi, G. Zhang, H. Hu, X. Ma, Hydrogen production by catalytic methane decomposition: Carbon materials as catalysts or catalyst supports, International Journal of Hydrogen Energy, 42 (2017) 19755-19775.

[70] M. Ermakova, D.Y. Ermakov, G. Kuvshinov, Effective catalysts for direct cracking of methane to produce hydrogen and filamentous carbon: Part I. Nickel catalysts, Applied Catalysis A: General, 201 (2000) 61-70.

[71] S.K. Saraswat, K.K. Pant, Ni–Cu–Zn/MCM-22 catalysts for simultaneous production of hydrogen and multiwall carbon nanotubes via thermo-catalytic decomposition of methane, International Journal of Hydrogen Energy, 36 (2011) 13352-13360.

[72] S.K. Saraswat, K.K. Pant, Synthesis of hydrogen and carbon nanotubes over copper promoted Ni/SiO_2 catalyst by thermocatalytic decomposition of methane, Journal of Natural Gas Science and Engineering, 13 (2013) 52-59.

[73] L. Avdeeva, O. Goncharova, D. Kochubey, V. Zaikovskii, L. Plyasova, B. Novgorodov, S.K. Shaikhutdinov, Coprecipitated Ni-alumina and Ni□ Cu-alumina catalysts of methane decomposition and carbon deposition. II. Evolution of the catalysts in reaction, Applied Catalysis A: General, 141 (1996) 117-129.

[74] J. Salmones, J. Wang, M. Valenzuela, E. Sánchez, A. Garcia, Pore geometry influence on the deactivation behavior of Ni-based catalysts for simultaneous production of hydrogen and nanocarbon, Catalysis Today, 148 (2009) 134-139.

[75] A.M. Amin, E. Croiset, Z. Malaibari, W. Epling, Hydrogen production by methane cracking using Ni-supported catalysts in a fluidized bed, International Journal of Hydrogen Energy, 37 (2012) 10690-10701.

[76] W. Ahmed, M.R. Noor El-Din, A.A. Aboul-Enein, A.E. Awadallah, Effect of textural properties of alumina support on the catalytic performance of Ni/Al_2O_3 catalysts for hydrogen production via methane decomposition, Journal of Natural Gas Science and Engineering, 25 (2015) 359-366.

[77] W. Wang, H. Wang, Y. Yang, S. Jiang, Ni–SiO2 and Ni–Fe–SiO_2 catalysts for methane decomposition to prepare hydrogen and carbon filaments, International Journal of Hydrogen Energy, 37 (2012) 9058-9066.

[78] M. Pudukudy, Z. Yaakob, A. Kadier, M.S. Takriff, N.S.M. Hassan, One-pot sol–gel synthesis of Ni/TiO_2 catalysts for methane decomposition into COx free hydrogen and multiwalled carbon nanotubes, International Journal of Hydrogen Energy, 42 (2017) 16495-16513.

[79] M. Borghei, R. Karimzadeh, A. Rashidi, N. Izadi, Kinetics of methane decomposition to COx-free hydrogen and carbon nanofiber over Ni–Cu/MgO catalyst, International Journal of Hydrogen Energy, 35 (2010) 9479-9488.

[80] J. Majewska, B. Michalkiewicz, Carbon nanomaterials produced by the catalytic decomposition of methane over Ni/ZSM-5: Significance of Ni content and temperature, New Carbon Materials, 29 (2014) 102-108.

[81] W.U. Khan, A.H. Fakeeha, A.S. Al-Fatesh, A.A. Ibrahim, A.E. Abasaeed, La_2O_3 supported bimetallic catalysts for the production of hydrogen and carbon nanomaterials from methane, International Journal of Hydrogen Energy, 41 (2016) 976-983.

[82] X. Zhang, M. Zhang, J. Zhang, Q. Zhang, N. Tsubaki, Y. Tan, Y. Han, Methane decomposition and carbon deposition over Ni/ZrO_2 catalysts: Comparison of amorphous, tetragonal, and monoclinic zirconia phase, International Journal of Hydrogen Energy, 44 (2019) 17887-17899.

[83] M. Nasir Uddin, W.M.A. Wan Daud, H.F. Abbas, Co-production of hydrogen and carbon nanofibers from methane decomposition over zeolite Y supported Ni catalysts, Energy Conversion and Management, 90 (2015) 218-229.

[84] I.L.S. Mei, S.S.M. Lock, D.V.N. Vo, B. Abdullah, Thermo-Catalytic Methane Decomposition for Hydrogen Production: Effect of Palladium Promoter on Ni-based Catalysts, Bull Chem React Eng, 11 (2016) 191-199.

[85] A. Awad, N. Masiran, M.A. Salam, D.V.N. Vo, B. Abdullah, Non-oxidative decomposition of methane/methanol mixture over mesoporous Ni-Cu/Al2O3 Co-doped catalysts, International Journal of Hydrogen Energy, 44 (2019) 20889-20899.

[86] H. Wang, R.T.K. Baker, Decomposition of methane over a Ni− Cu− MgO catalyst to produce hydrogen and carbon nanofibers, The Journal of Physical Chemistry B, 108 (2004) 20273-20277.

[87] A. Rastegarpanah, F. Meshkani, M. Rezaei, Thermocatalytic decomposition of methane over mesoporous nanocrystalline promoted Ni/MgO· Al_2O_3 catalysts, international journal of hydrogen energy, 42 (2017) 16476-16488.

[88] H. Zhang, C. Du, A. Wu, Z. Bo, J. Yan, X. Li, Rotating gliding arc assisted methane decomposition in nitrogen for hydrogen production, International Journal of Hydrogen Energy, 39 (2014) 12620-12635.

[89] F.-J. Spiess, S.L. Suib, K. Irie, Y. Hayashi, H. Matsumoto, Metal effect and flow rate effect in the hydrogen production from methane, Catalysis Today, 89 (2004) 35-45.

[90] S. Krzyzynski, M. Kozlowski, Activated carbons as catalysts for hydrogen production via methane decomposition, International Journal of Hydrogen Energy, 33 (2008) 6172-6177.

[91] M. Pudukudy, Z. Yaakob, M.S. Takriff, Methane decomposition over unsupported mesoporous nickel ferrites: effect of reaction temperature on the catalytic activity and properties of the produced nanocarbon, RSC Advances, 6 (2016) 68081-68091.

[92] I. Suelves, J.L. Pinilla, M.J. Lázaro, R. Moliner, J.M. Palacios, Effects of reaction conditions on hydrogen production and carbon nanofiber properties generated by methane decomposition in a fixed bed reactor using a NiCuAl catalyst, Journal of Power Sources, 192 (2009) 35-42.

[93] F.M. Berndt, O.W. Perez-Lopez, Catalytic decomposition of methane over Ni/SiO_2: influence of Cu addition, Reaction Kinetics, Mechanisms and Catalysis, 120 (2016) 181-193.

[94] J. Majewska, B. Michalkiewicz, Production of hydrogen and carbon nanomaterials from methane using Co/ZSM-5 catalyst, International Journal of Hydrogen Energy, 41 (2016) 8668-8678.

[95] M. Pudukudy, Z. Yaakob, M.S. Takriff, N.S.M. Hassan, Production of COx free hydrogen and nanocarbon via methane decomposition over unsupported porous nickel and iron catalysts, Journal of Cluster Science, 28 (2017) 1579-1594.

[96] D. Wang, J. Zhang, J.B. Sun, W.M. Gao, Y.B. Cui, Effect of metal additives on the catalytic performance of Ni/Al2O3 catalyst in thermocatalytic decomposition of methane, International Journal of Hydrogen Energy, 44 (2019) 7205-7215.

[97] A.A. Ibrahim, A.S. Al-Fatesh, W.U. Khan, M.A. Soliman, R.L. Al Otaibi, A.H. Fakeeha, Influence of support type and metal loading in methane decomposition over iron catalyst for hydrogen production, Journal of the Chinese Chemical Society, 62 (2015) 592-599.

[98] M. Lazaro, Y. Echegoyen, C. Alegre, I. Suelves, R. Moliner, J. Palacios, TiO_2 as textural promoter on high loaded Ni catalysts for methane decomposition, International Journal of Hydrogen Energy, 33 (2008) 3320-3329.

[100] S. Abanades, H. Kimura, H. Otsuka, Hydrogen production from thermo-catalytic decomposition of methane using carbon black catalysts in an indirectly-irradiated tubular packed-bed solar reactor, International Journal of Hydrogen Energy, 39 (2014) 18770-18783.

[101] M.D. Phillips, A.D. Eastman, Effect of Li/MgO methane coupling catalyst on alonized steel reactors, Catalysis Letters, 13 (1992) 157-174.

[102] I. Ermanoski, N.P. Siegel, E.B. Stechel, A New Reactor Concept for Efficient Solar-Thermochemical Fuel Production, J Sol Energ-T Asme, 135 (2013).

[103] R. Koç, E. Alper, E. Croiset, A. Elkamel, Partial Regeneration of Ni-Based Catalysts for Hydrogen Production via Methane Cracking, Turkish Journal of Chemistry, 32 (2008) 157-168.

[104] A.M. Amin, E. Croiset, W. Epling, Review of methane catalytic cracking for hydrogen production, International Journal of Hydrogen Energy, 36 (2011) 2904-2935.

[105] J.L. Pinilla, M.J. Lázaro, I. Suelves, R. Moliner, J.M. Palacios, Characterization of nanofibrous carbon produced at pilot-scale in a fluidized bed reactor by methane decomposition, Chemical Engineering Journal, 156 (2010) 170-176.

[106] C. Vahlas, B. Caussat, P. Serp, G.N. Angelopoulos, Principles and applications of CVD powder technology, Materials Science and Engineering: R: Reports, 53 (2006) 1-72.

[107] N. Jurtz, M. Kraume, G.D. Wehinger, Advances in fixed-bed reactor modeling using particle-resolved computational fluid dynamics (CFD), Reviews in Chemical Engineering, 35 (2019) 139-190.

[108] A. Rashidi, R. Lotfi, E. Fakhrmosavi, M. Zare, Production of single-walled carbon nanotubes from methane over Co-Mo/MgO nanocatalyst: A comparative study

of fixed and fluidized bed reactors, Journal of Natural Gas Chemistry, 20 (2011) 372-376.

[109] H.F. Abbas, W.M.A.W. Daud, Influence of reactor material and activated carbon on the thermocatalytic decomposition of methane for hydrogen production, Appl Catal a-Gen, 388 (2010) 232-239.

[110] N. Muradov, Hydrogen via methane decomposition: an application for decarbonization of fossil fuels, International Journal of Hydrogen Energy, 26 (2001) 1165-1175.

[111] M. Albrecht, U. Rodemerck, D. Linke, E.V. Kondratenko, Oxidative coupling of methane at elevated pressures: reactor concept and its validation, Reaction Chemistry & Engineering, 3 (2018) 151-154.

[112] X.q. Qiu, Q.m. Zhu, N.b. Wong, K.c. Tin, Catalytic contribution of reactor wall materials on oxidative coupling of methane, Journal of Chemical Technology & Biotechnology: International Research in Process, Environmental AND Clean Technology, 65 (1996) 380-384.

[113] S. Sadjadi, U. Simon, H.R. Godini, O. Gorke, R. Schomacker, G. Wozny, Reactor material and gas dilution effects on the performance of miniplant-scale fluidized-bed reactors for oxidative coupling of methane, Chemical Engineering Journal, 281 (2015) 678-687.

[114] S. Abanades, H. Kimura, H. Otsuka, Kinetic investigation of carbon-catalyzed methane decomposition in a thermogravimetric solar reactor, International Journal of Hydrogen Energy, 40 (2015) 10744-10755.

[115] J.L. Pinilla, D. Torres, M.J. Lázaro, I. Suelves, R. Moliner, I. Cañadas, J. Rodríguez, A. Vidal, D. Martínez, Metallic and carbonaceous –based catalysts performance in the solar catalytic decomposition of methane for hydrogen and carbon production, International Journal of Hydrogen Energy, 37 (2012) 9645-9655.

[116] N. Muradov, F. Smith, C. Huang, A. T-Raissi, Autothermal catalytic pyrolysis of methane as a new route to hydrogen production with reduced CO_2 emissions, Catalysis Today, 116 (2006) 281-288.

[117] P. Ammendola, R. Chirone, G. Ruoppolo, G. Russo, Production of hydrogen from thermo-catalytic decomposition of methane in a fluidized bed reactor, Chemical Engineering Journal, 154 (2009) 287-294.

[118] J.M. Gatica, D.M. Gomez, S. Harti, H. Vidal, Monolithic honeycomb design applied to carbon materials for catalytic methane decomposition, Appl Catal a-Gen, 458 (2013) 21-27.

[119] R.M. Heck, S. Gulati, R.J. Farrauto, The application of monoliths for gas phase catalytic reactions, Chemical Engineering Journal, 82 (2001) 149-156.

[120] J. Werther, Fluidized-bed reactors, Ullmann's encyclopedia of industrial chemistry, (2000).

[121] A. Dunker, S. Kumar, P. Mulawa, Production of hydrogen by thermal decomposition of methane in a fluidized-bed reactor—Effects of catalyst, temperature, and residence time, International Journal of Hydrogen Energy, 31 (2006) 473-484.

[122] J.X. Qian, L.R. Enakonda, W.J. Wang, D. Gary, P. Del-Gallo, J.-M. Basset, D.B. Liu, L. Zhou, Optimization of a fluidized bed reactor for methane decomposition over Fe/Al_2O_3 catalysts: Activity and regeneration studies, International Journal of Hydrogen Energy, 44 (2019) 31700-31711.

[123] D. Torres, S. De Llobet, J. Pinilla, M. Lázaro, I. Suelves, R. Moliner, Hydrogen production by catalytic decomposition of methane using a Fe-based catalyst in a fluidized bed reactor, Journal of natural gas chemistry, 21 (2012) 367-373.

[124] Q. Weizhong, L. Tang, W. Zhanwen, W. Fei, L. Zhifei, L. Guohua, L. Yongdan, Production of hydrogen and carbon nanotubes from methane decomposition in a two-stage fluidized bed reactor, Applied Catalysis A: General, 260 (2004) 223-228.

[125] J.L. Pinilla, R. Utrilla, M.J. Lázaro, I. Suelves, R. Moliner, J.M. Palacios, A novel rotary reactor configuration for simultaneous production of hydrogen and carbon nanofibers, International Journal of Hydrogen Energy, 34 (2009) 8016-8022.

[126] J.L. Pinilla, R. Utrilla, M.J. Lazaro, R. Moliner, I. Suelves, A.B. Garcia, Ni- and Fe-based catalysts for hydrogen and carbon nanofilament production by catalytic decomposition of methane in a rotary bed reactor, Fuel Processing Technology, 92 (2011) 1480-1488.

[127] S. Pirard, G. Lumay, N. Vandewalle, J. Pirard, Motion of carbon nanotubes in a rotating drum: The dynamic angle of repose and a bed behavior diagram, Chemical Engineering Journal, 146 (2009) 143-147.

[128] D. Kang, N. Rahimi, M.J. Gordon, H. Metiu, E.W. McFarland, Catalytic methane pyrolysis in molten $MnCl_2$-KCl, Applied Catalysis B: Environmental, 254 (2019) 659-666.

[129] M. Steinberg, Fossil fuel decarbonization technology for mitigating global warming, International Journal of Hydrogen Energy, 24 (1999) 771-777.

[130] M. Serban, M.A. Lewis, C.L. Marshall, R.D. Doctor, Hydrogen production by direct contact pyrolysis of natural gas, Energy & fuels, 17 (2003) 705-713.

[131] T. Geißler, M. Plevan, A. Abánades, A. Heinzel, K. Mehravaran, R.K. Rathnam, C. Rubbia, D. Salmieri, L. Stoppel, S. Stückrad, A. Weisenburger, H. Wenninger, T. Wetzel, Experimental investigation and thermo-chemical modeling of methane pyrolysis in a liquid metal bubble column reactor with a packed bed, International Journal of Hydrogen Energy, 40 (2015) 14134-14146.

[132] D.C. Upham, V. Agarwal, A. Khechfe, Z.R. Snodgrass, M.J. Gordon, H. Metiu, E.W. McFarland, Catalytic molten metals for the direct conversion of methane to hydrogen and separable carbon, Science, 358 (2017) 917-921.

Chapter 3: Methodology

3.1 Preparation of Ash samples for ash fusion analysis

The biomass fly ash (BFA) was collected from locally fired biomass power, named as Bulleh Shah Packaging Limited mix biomass power plant Kasur, Punjab. This biomass used were consist of wheat straw, black liquor from paper industry, rice straw and wood pieces. **Figure 3.1** reveals the preparation method of the BFA samples. To prepare BFA sample, it was first dried in an oven for 12 hours at temperature of 120℃ in order remove moisture content from BFA. Then the dried BFA were grinded with Hard grove Grindability Index Tester (USA, ASTM D 409-08) and sieved in a Sieving WS Tyler RX-29-10 (USA) to obtain require fine particle size of BFA powder. BFA powder was calcined at 700℃ for time of 3 hours to remove unburnt carbon, alkaline materials and improve the stability of the BFA.

The conventional hydrothermal method was used for the preparation of the cerium oxide and is shown in **Figure 3.1**. For the preparation of 0.1 molar solution and maintaining value of pH at 10, the Cerium (III) nitrate hexa-hydrate (Sigma Aldrich, 99.99%, USA) ($Ce(NO_3)_3.6H_2O$) were added to the deionised water (DI) as per requirement. The prepared homogenous solution, it were stirred for 15 minutes at 60℃. For hydrothermal process, the uniform nitrate solution were transferred to a 200 ml Teflon lined stainless steel autoclave (China). The autoclave containing a homogeneous nitrate solution was placed in an electric furnace at 160°C for 24 hours before being allowed to cool to room temperature. The collected sample were washed many times with DI water and then finally with absolute ethanol (ACS reagent 99.5 %) to make it free of impurities and with pH value of 7.0. The sampled was dried in an oven at 120 ℃ temperature for 10 hours and finally calcined for 3 hours at 700℃.

Conventional incipient wetness impregnation method were used for the preparation of Co/CeO_2-BFA nano-composite [1]. The solution of DI water with BFA and cerium oxide powder were prepared by stirring it for 15 minutes at temperature of 60℃. The solution of 0.1 molarity was prepared by adding Cobalt (II) nitrate hex-hydrate ($Co(NO_3)_2.6H_2O$) (Merck, 99.99%, USA) to DI water and continually stirred the solution for 10 minutes at 60℃. Then both the prepared solution were mixed with each

other and the final solution were stirred for 3 hours at 110℃. After the stirring the sample was dry up in the oven at 110℃ of temperature. The sample were collected and grinded to fine powder. Finally the sample were calcined at 700℃ for 3 hours.

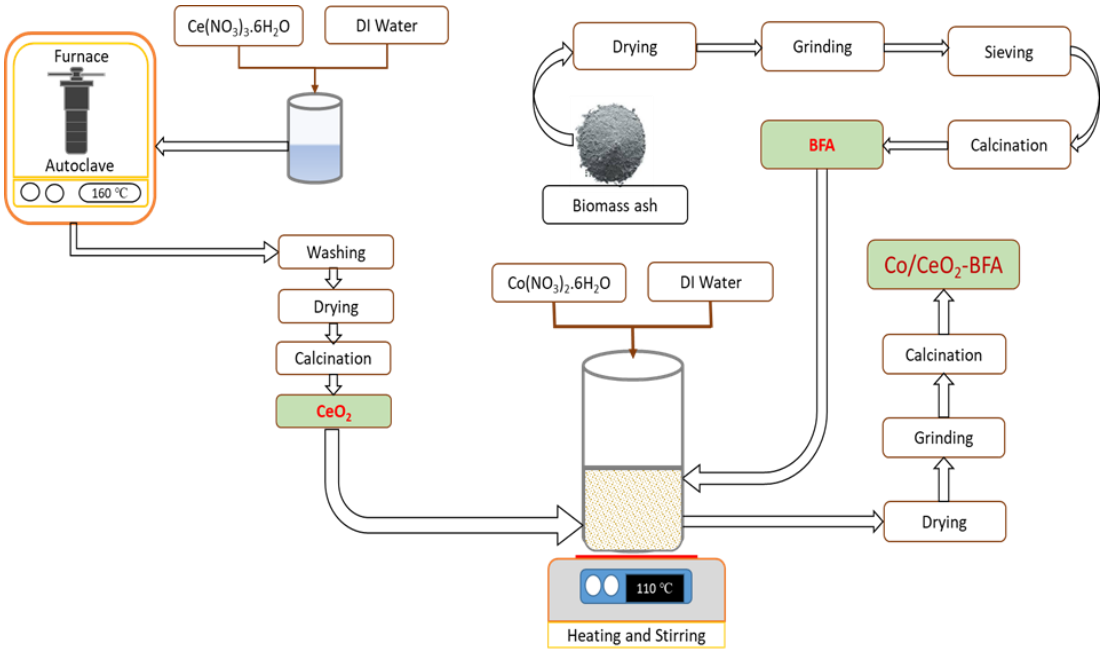

Figure 3.1 Schematic of material synthesis

3.2 Catalyst characterisation

The following characterization equipment were used for the characterization of the fresh and spent catalyst.

3.2.1 X-Ray Diffraction

To determine the crystalline structure, XRD analysis were performed using D8 Advance (Bruker Advanced, Germany) with configuration of Bragg-Brentano along with the scintillation detector and radiation wavelength equal to 1.5418 Å used for examination of crystalline structure shown in **Figure 3.2**.

Figure 3.2 X-Ray Diffraction

The equipment has the step of 0.05°/ 5sec and sample scanning ability of 2θ=5° to 80°. Characterized with software DIFFRAC Plus EVA Version 5.0 to perform XRD analysis

3.2.3 Scanning electron Microscopy

The morphological behavior of the fresh nano-composite and spent catalyst has been studied with SEM analyzer using JEOL JSM-6490A (Japan), shown in **Figure 3.3**.

Figure 3.3 Scanning electron Microscopy

At 30kV the equipment have the resolution power of 3 nm and extension of 10-200,000X, in order to get our desired micrographs. For the elemental analysis of the fresh nano-composite catalyst and spent catalyst were carried out with energy EDX detector (Oxford Instruments, model: 51-AD0007).

3.2.4 Thermogravimetric analysis

Thermal analysis were performed with thermal-gravimetric analyzer TGA 5500 TA Instruments, shown in **Figure 3.4**.

Figure 3.4 Thermogravimetric Analyzer

At the start, the equipment was purged with N_2 flowing at the flow rate of 35 mL min^{-1} for 30 minutes. The sample of weigh of 10 mg were used for analysis. The sample were heated to 900℃ with heating rate of 10℃ min^{-1} in the nitrogen and then in air environment at flow rate of 25 mL min^{-1}.

3.2.5 Fourier Transform Infrared Spectroscopy

For the determination of functional group FTIR spectroscopy was carried out with Cary 630 FTIR (Agilent Technologies, USA), shown **Figure 3.5**. FTIR spectrum recorded in the range of 400 to 650 cm^{-1} wavenumber with the resolution of 2 cm^{-1} was scanned.

Figure 3.5 Fourier Transform Infrared Spectroscopy.

3.3 Methane decomposition experimental setup and calculations

Thermo-catalytic decomposition reaction of methane has been performed in the fixed bed thermal reactor (Parr Instrument, 5401, USA) with continuous flow of gases, as shown in **Figure 3.6.** The fixed bed stainless steel (SS 316) reactor having the inner diameter (ID=12 mm) and length equal to 300 mm, consist of single heating zone. The prepared nano-composite catalyst were sandwich in the quartz wool and was placed in the mid-section of the reactor. The mass flow controller (Brooke instruments, USA) were used for controlling the flow rate of methane gas. The temperature of reactor was controlled by process controller (4871, Parr Instrument). An online SCADA system monitored the temperature and flow rate of the reactor. The supply of the gases to the reactor should be dry and for this purpose condenser were utilized to dry up fed gases.

The gas chromatograph (GC-TCD) (GC-2010 Plus, Shimadzu Japan) equipped with thermal conductivity detector (TCD) were used to measure CH_4 fed and H_2 yield. The thermo-catalytic decomposition of methane is furnished with capillary column (RT-MS5A, 30 m x 0.32 mm ID, 30 µm) used to detect CH_4, and H_2.

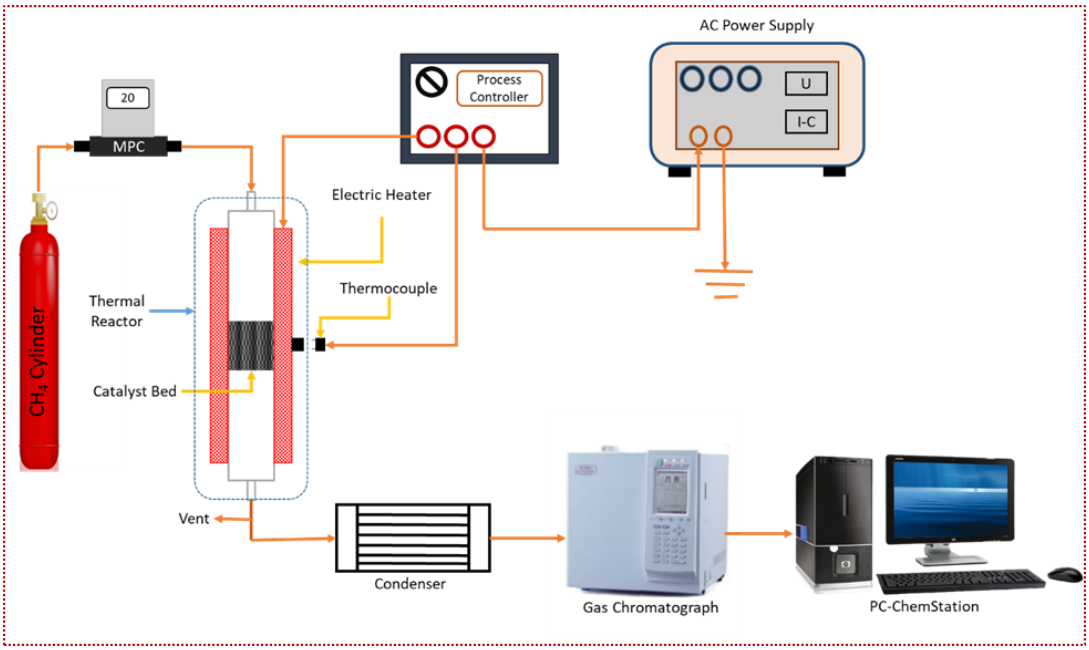

Figure 3.6 Schematic of experimental setup for catalytic methane decomposition.

3.4 Catalytic activity

The performance methane decomposition in fix bed was studied in term of CH_4 conversion (Eq. 2) and H_2 selectivity (Eq. 3) and H_2 yield (Eq. 4).

$$CH_4\,\text{conversion}\left(X_{CH_4}\right)\% = \left[\frac{(nCH_4)_{\text{converted}}}{(nCH_4)_{\text{in}}} \times 100\right] \tag{2}$$

Whereas, X_{CH4} denotes conversion rate of methane, $n(CH_4)_{converted}$ is the number of moles of methane converted and $(CH_4)_{feed}$ is the number moles of methane at inlet of reactor.

$$H_2\ \text{selectivity}\left(S_{H_2}\right)\% = \left[\frac{(nH_2)_{\text{produced}}}{(2\times nCH_4)_{\text{converted}}} \times 100\right] \tag{3}$$

$$H_2\ \text{Yield}\left(Y_{H_2}\right)\% = \left[\frac{(nH_2)_{\text{produced}}}{(2\times nCH_4)_{\text{in}}}\times 100\right] \quad (4)$$

S_{H2} and Y_{H2} represent selectivity and yield of H_2 respectively and $n(H_2)_{produced}$ is the number of moles of hydrogen produced.

References

[1] A.H. Khoja, M. Tahir, N.A. Saidina Amin, Evaluating the performance of a Ni catalyst supported on La_2O_3-$MgAl_2O_4$ for dry reforming of methane in a packed bed dielectric barrier discharge plasma reactor, Energy & Fuels, 33 (2019) 11630-11647.

Chapter 4: Results and Discussion

4.1 Materials Characterization

Figure 4.1 illustrate XRD analysis carried for biomass fly ash (BFA), cerium oxide (CeO_2) and Co/CeO_2-BFA. **Table. 4.1** showed all crystalline phases identified with XRD analysis. The BFA have different metal oxide which is confirm by XRD pattern. The major XRD peak for orthorhombic shaped $CaSO_4$ (PDF# 37-1496) having phase (020) was noticed at 2θ=25.40° [1]. The XRD peak at angle 29.40° indexed directly to $CaCO_3$ (PDF# 47-1743) with phase (104) [2]. The SiO_2 crystalline phase (101) with PDF# 46-1045 was observed at 2θ=26.50° [3]. The cubic structure Fe_2O_3 (PDF# 16-0653) have been identified at an angle 32.80° with phase (220) [4]. The phase (020) of Al_2O_3 with (PDF#46-1131) was observed at 2θ confirms at 30.30° [5]. The cubical structure of MgO (PDF# 45-0946) with phase (211) was found at 2θ= 44°.

The CeO_2 XRD study reveals the presence of face-centered cubic crystalline phase (111) with (PDF# 43-1002) at 2θ equal to 28.50° [6].

The Co loaded final nano-composite catalyst have one ore major peak at an angle 2θ of 44.20°, which indexed explicitly to face-centered-cubic phase (111) of cobalt with (PDF# 15-0806) [7]. By cobalt loading the crystallinity of final nano-composite was dropped which is mainly due to the loading of cobalt and CeO_2 nanowires. XRD study clearly shows that synthesized nano-composite have the required crystalline phases of the CeO_2 nanowires, Cobalt and other metal oxides [8].

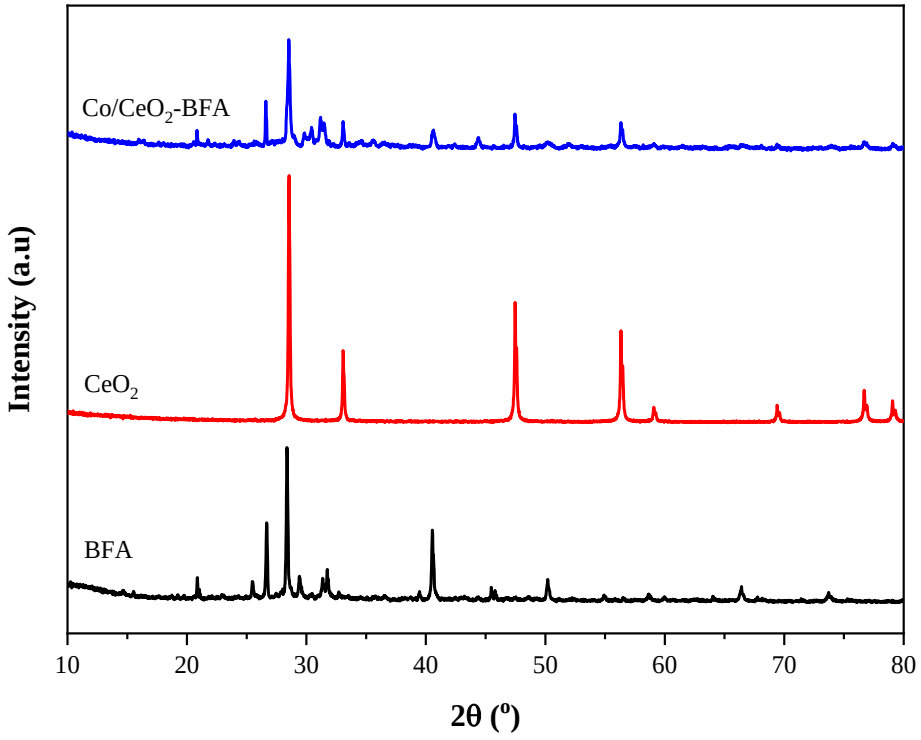

Figure 4.1 XRD analysis of biomass fly ash (BFA), CeO_2, and Co/CeO_2-BFA.

Table 4.1 XRD analysis

Samples	Compound	PDF #	2θ (°)	Phase *(hkl)*
BFA	$CaSO_4$	37-1496	25.40	*(020)*
	$CaCO_3$	47-1743	29.40	*(104)*
	SiO_2	46-1045	26.50	*(101)*
	Fe_2O_3	16-0653	32.80	*(420)*
	Al_2O_3	46-1131	30.30	*(020)*
CeO_2	CeO_2	43-1002	28.50	*(111)*
Co/CeO_2-BFA	Co	15-0806	44.20	*(111)*

Figure 4.2 reveals the morphology of the biomass fly ash (BFA), cerium oxide (CeO_2) and Co/CeO_2-BFA, which was studied using SEM analyzer.

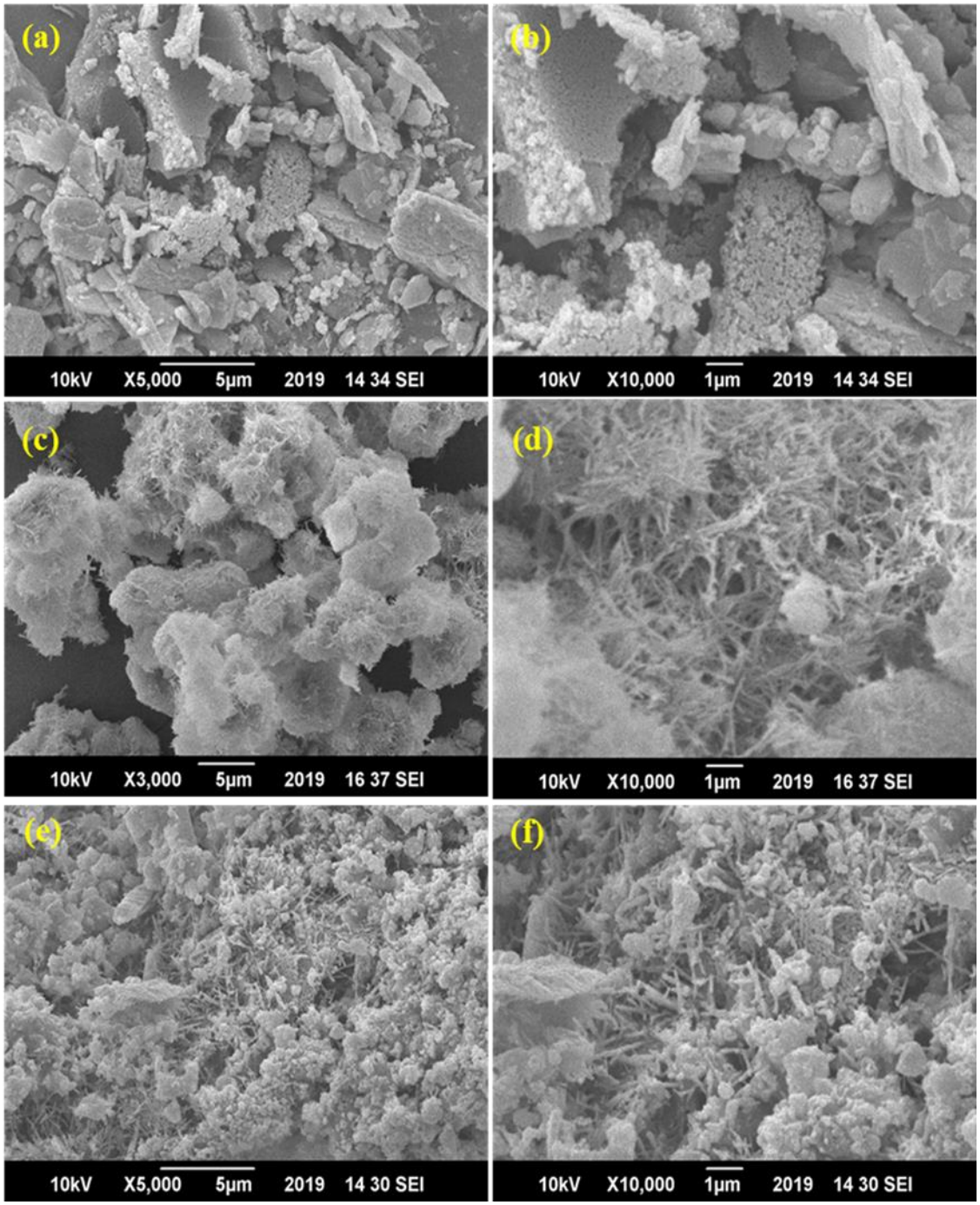

Figure 4.2 SEM micrographs of synthesized catalyst with 5.0 μm and 1.0 μm (a-b) biomass fly ash (BFA) (c-d) cerium oxide (CeO_2) nanowires (e-f) Co/CeO2-BFA.

The BFA micrograph presented in **Figure 4.2(a-b)** shows it has flakes like structure with porosity, which make it suitable material for catalyst support [9]. Such structure of material make it favorable for catalytic use as it gives better dispersion to the metal oxides and as well active metal [6]. The CeO_2 surface morphology shows nanowire structure which is demonstrated in **Figure 4.2(c-d).** Further magnification of CeO_2 illustrates web like structure that is due to the interconnection of these nanowires. The morphological structure of final composite material loaded with active metal cobalt, CeO_2 as promoter and supported over BFA has presented **Figure 4.2(d-e).** The final nano-composite explicitly reveals the incorporation of the CeO_2 with BFA and in turn CeO_2 also give helps in improved dispersion of the Co over support, BFA [10].

The elemental analysis of the nano-composite Co/CeO_2-BFA was carried out with EDX analyzer and is presented in **Figure 4.3**. The EDX analysis clearly reveals the peaks for Co, Ce and also for Si, Ca, Fe and Al which are the main constituents of BFA and which is established from XRD peak.

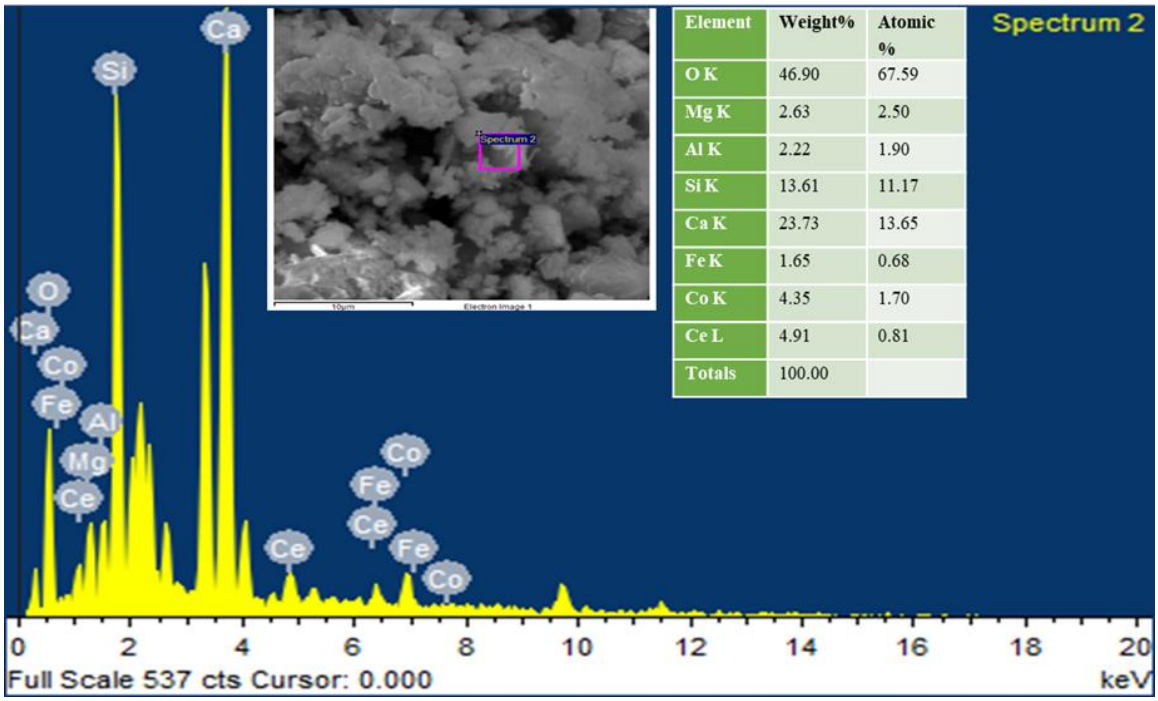

Figure 4.3 EDX study of fresh nano-composite Co/CeO_2-BFA.

The thermal stability of BFA, synthesized nanowire of CeO_2 and final nano-composite Co/CeO_2-BFA is depicted in **Figure 4.4**. The thermal analysis of BFA presented in **Figure 4.4(a)** has shown a total weight loss of 15%. The weight loss for BFA occur in three stages. In the first stage at less than 150℃ of temperature, the small amount of weight loss observed which attributes to the evaporation of moisture content. In the second stage (150℃-550℃) significant amount of weight loss occur due to the evaporation of the volatile matter present in BFA. The major weight loss occur during third stage (550℃-900℃) which is due to the oxidation of the organic matter and the transformation of phase like Si, Fe, Ca [11]. The thermal stability of the synthesized nanowire of CeO_2 is exhibited in **Figure 4.4(b).**

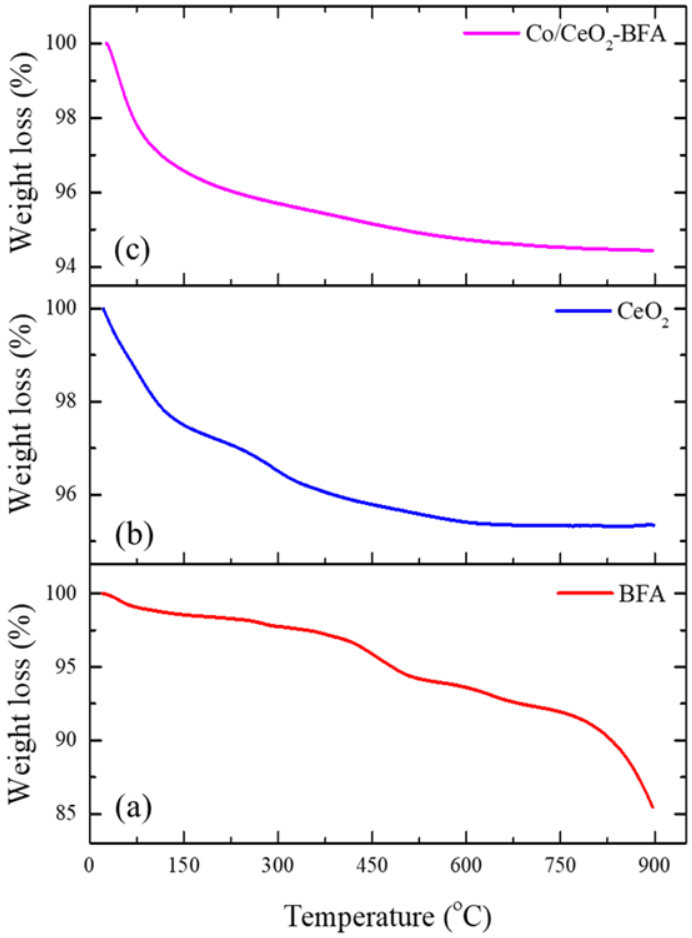

Figure 4.4 TGA analysis of fresh (a) Biomass fly ash (BFA) (b) cerium oxide (CeO_2) nanowires (c) Co/CeO_2-BFA.

The TGA profile reveals that only major weight loss occur due to the loss of moisture content present in the CeO_2 and no further weight loss was observed [12]. **Figure 4.4(c)** portray the thermal stability of nano-composite Co/CeO_2-BFA. At temperature below 750°C, TGA profile shows 5.5% of weight loss which is mainly due to release of the vapor and volatile content [13]. The final nano-composite have lower weight loss as compared to BFA which indicate that the structure and surface morphology of BFA has changed confirmed form XRD and SEM analysis which is due the loading of cobalt and cerium oxide.

Figure 4.5 presents the FTIR examination of BFA, synthesized CeO_2 nanowires and Co/CeO_2-BFA nano-composite which determine the functional groups (qualitative analysis) with in the range of 4000-650 cm^{-1} wavenumber. The CeO_2 FTIR shows weak spectral band from 2500-2000 cm^{-1} which confirms existence of the OH band because of moisture content in CeO_2 [14].

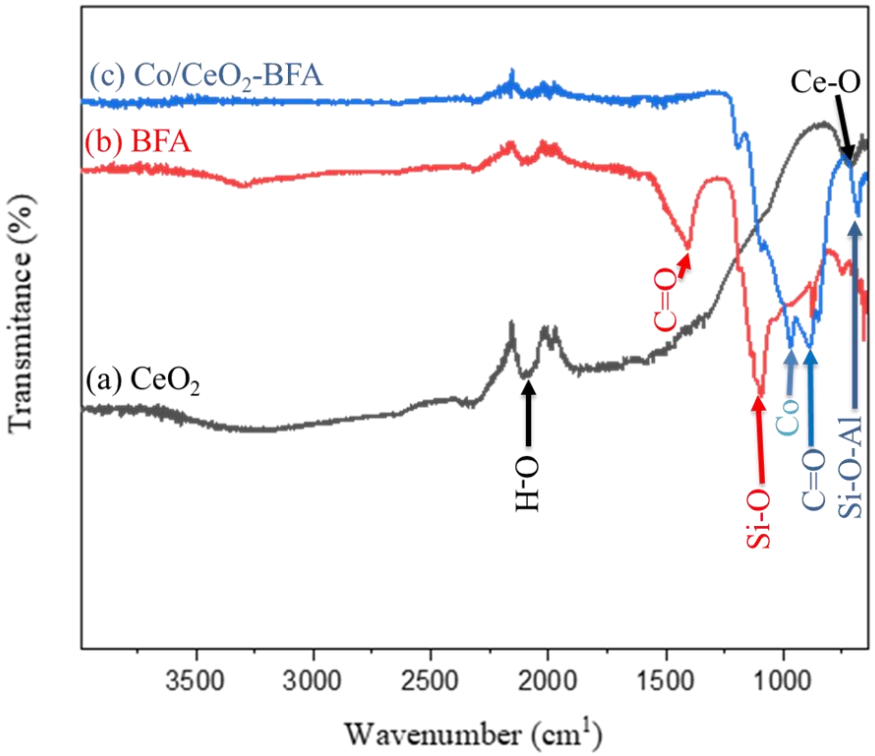

Figure 4.5 FTIR spectroscopy of fresh (a) cerium oxide (CeO_2) (b) biomass fly ash (BFA) (c) CeO_2/ Co-BFA.

The Ce-O band transmittance peak was detected at band below 700 cm^{-1} for both synthesized nanowire CeO_2 and Co/CeO_2-BFA nano-composite [15-17]. The Ce-O band transmittance peak was detected at band below 700 cm^{-1} for both synthesized nanowire CeO_2 and Co/CeO_2-BFA nano-composite [15-17]. The FTIR spectrum of BFA reveals that band at the 1418 cm^{-1} and 882.36 cm^{-1} confirms the stretching vibration for asymmetric C=O, and band at 1110 cm^{-1} indicates the Si-O stretching vibrations [9, 18, 19]. The relatively lower band peak at 743.9 cm^{-1} was observed for symmetric stretching vibration of Si-O-Al [19]. The Co/CeO_2-BFA nano-composite have stretching vibration at 955.6 cm^{-1} for C-O functional group [20] and at 1075 cm^{-1} wave number exhibit stretching mode for presence of Cobalt [21, 22].

4.2 Screening tests of the catalyst

4.2.1 Effect of Co and CeO_2 loading over BFA

Catalytic performance in term of CH_4 conversion (X_{CH4}), H_2 selectivity (S_{H2}) and H_2 yield (Y_{H2}) as function of time on stream (TOS) for BFA, Co/BFA, and Co/CeO_2-BFA has been analyzed, as depicted in **Figure 4.6** while keeping the keeping the experimental parameter constant such as catalyst loading equal to 0.5 g, temperature 850 ℃ and CH_4 flow rate + 20 ml min^{-1}. The mean values are recorded for the X_{CH4}, S_{H2} and Y_{H2} after the catalyst gaining stability. CH_4 conversion values of 28%, 46% and 71% was reported for only BFA, 5%Co/BFA and 5%Co/CeO_2-BFA respectively which is shown in **Figure 4.6(a). Figure 4.6(b)** indicates H_2 selectivity of BFA, 5%Co/BFA and 5%Co/CeO_2-BFA with values equal to 33.5%, 44% and 62% respectively. **Figure 4.6(c)** shows H_2 yield of BFA, 5%Co/BFA and 5%Co/CeO_2-BFA have values 20%, 31% and 44% respectively. This clearly shows that the loading of cobalt as an active metal enhance the catalytic performance BFA. The cobalt as an active metal causes activation of the methane molecules to decompose into hydrogen gas and solid carbon nano-materials. Further addition of the cerium oxide as promoter improve the dispersion of the active metal over the base material and enhance catalyst stability [23, 24]. The yield of hydrogen were

improved due to impregnation of Co and CeO_2 over BFA. The higher conversion of methane were recorded due to addition of CeO_2 which is because of redox properties of the CeO_2 and high mobility of lattice oxygen. Small amount of CO and CO_2 traces were observed in the product gases. In the reduction environment, CeO_2 help in metal support interaction. The cobalt metal have partially filled 4*f*-suborbital which increase electron density during the methane decomposition reaction. The presence of the various metal oxide in BFA such as Al, Fe and Mg which help in the Co exulution process rather covering the active sites of the final nano-composite catalyst.

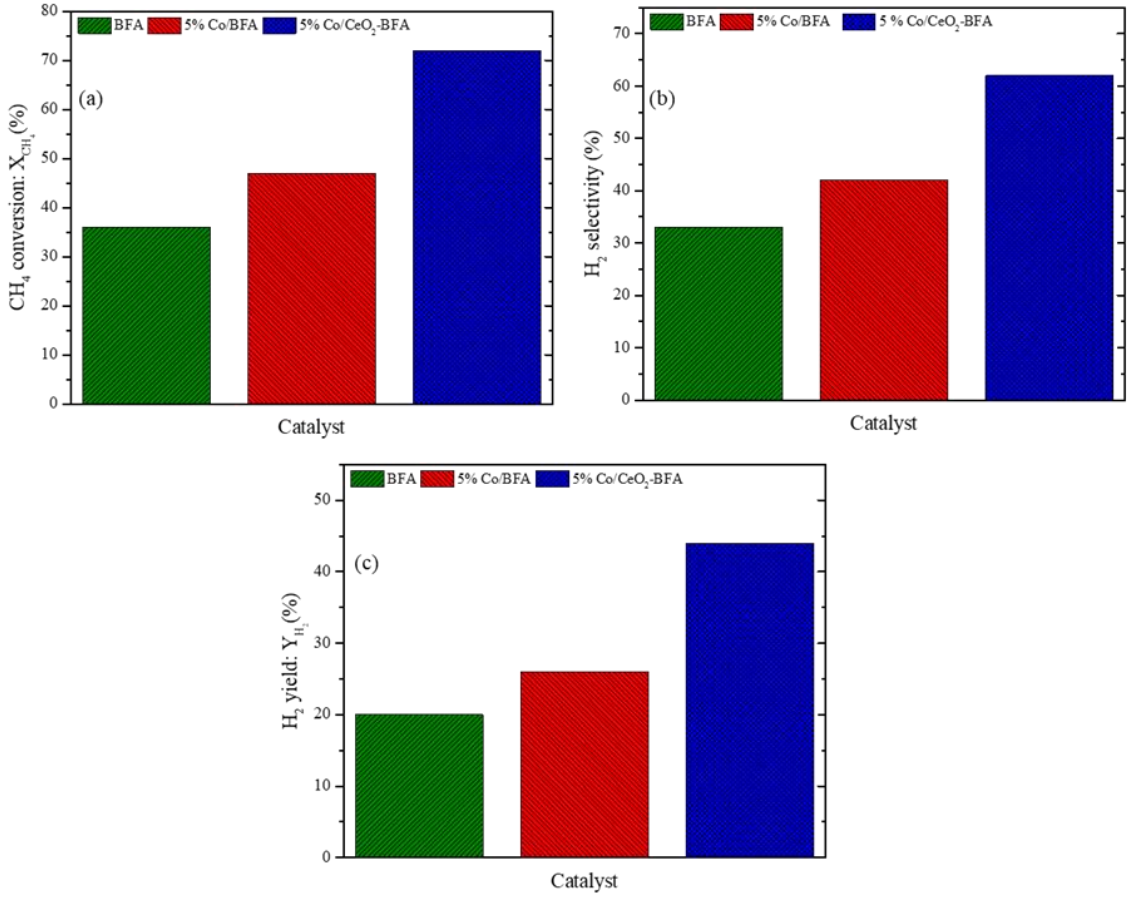

Figure 4.6 Screening test for (a) CH_4 conversion, (b) H_2 selectivity and (c) H_2 yield at temperature = 850 °C, catalyst loading = 0.5 g, CH_4 flow rate= 20 mL min^{-1}.

4.2.2 Effect of CeO_2 loading over 5%Co-BFA

The catalytic performance of the nano-composite were studied with different loading of synthesized CeO_2 nanowire over Co/BFA at the given experimental parameters which are reaction temperature of 850 ℃, CH_4 flow rate = 20 ml min^{-1} and catalyst loading = 0.5 g. The catalytic activity were recorded in term of CH_4-conversion, H_2 -selectivity and H_2-yield, whose values are the mean values which are recorded when the catalyst gained the stability. With increasing by weight percentage of loading of as synthesized CeO_2 nanowire over BFA enhance CH_4-conversion, H_2-selectivity and H_2-yield which were demonstrated in **Figure 4.7**.

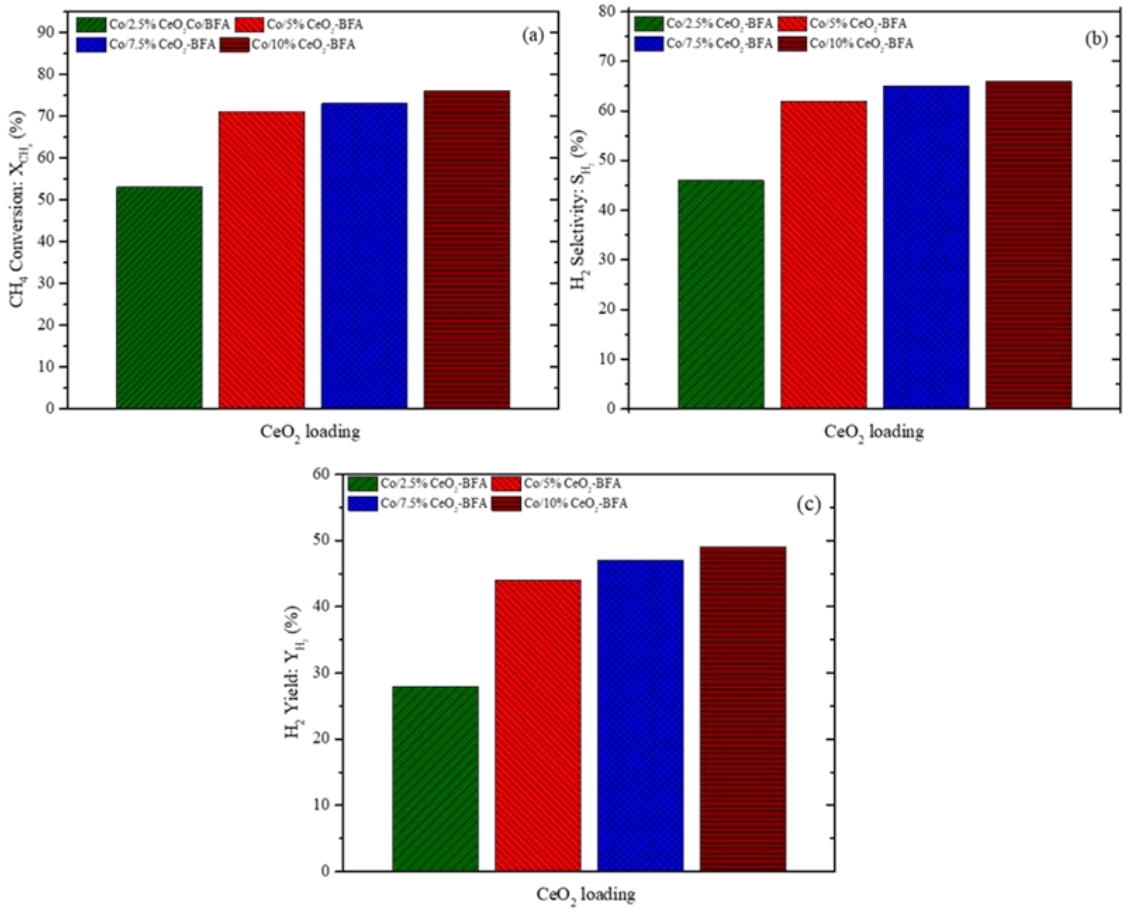

Figure 4.7 Effect of CeO_2 loading on the (a) conversion of CH_4 (b) selectivity of H_2 (c) H_2 yield at temperature = 850 °C, catalyst loading = 0.5 g, CH4 flow rate= 20 mL min^{-1}

For 2.5%, 5%, 7.5% and10% loading of CeO_2 over Co/BFA results in 53%, 71%, 73%, and 76% of CH_4 conversion respectively, as depicted in **Figure 4.7(a).** The hydrogen selectivity values are equal to 46%, 62%, 65% and 66.5% for 2.5%, 5%, 7.5% and 10% of CeO_2 loading over Co/BFA respectively, as shown in **Figure 4.7(b).** Similarly **Figure 4.7(c)** shows the hydrogen yield of 28%, 44%, 47% and 49% respectively for 2.5%, 5%, 7.5% and 10% loading of CeO_2 over Co/BFA. The promoter addition to the catalyst helps in better dispersion of the active metal over the support, avoid the sintering of metal and improve stability at elevated temperature, the as synthesized CeO_2 nanowire act as a promoter and enhance catalyst properties [23, 24]. Up to 5% by weight addition of CeO_2 improves the catalytic performance but beyond that loading leads to the degradation the properties of the catalyst, which is mainly due to the reason that further addition causes to block the porosity of BFA and leads towards the agglomeration of CeO_2 which results in blockage of active sites.

4.2.3 Effect of feed flow rate

The flow rate highly effect the catalyst catalytic activity, increasing the flow rate reduce the CH_4-conversion, H_2-selectivity and H_2-yield because the high flow rate reduce the time of contact for CH_4 with the catalyst [25-27]. The time of interaction for the gas molecules with the catalyst reduces which is due to the high concentration of CH_4. To justify this statement CH_4-conversion, H_2-selectivity and H_2-yield were check at variable flow rates over 5%Co/CeO_2-BFA catalyst and keeping the other experimental parameters constant which are catalyst loading = 0.5 g, temperature equal to 850℃. At flow rate of 10 mL min^{-1}, 20 mL min^{-1}, 30 mL min^{-1} and 40 mL min^{-1}, the CH_4 conversion values were of 74%, 71%, 65% and 60% respectively, which are shown in **Figure 4.8(a)**.

The hydrogen selectivity shown in **Figure 4.8(b)** having values equal to 63% 62% 57% and 50% for the flow rate of 10 mL min^{-1}, 20 mL min^{-1}, 30 mL min^{-1} and 40 mL min^{-1} respectively. **Figure 4.8(c)** shows the values of the hydrogen yield which are equal to 46%, 44%, 38% and 30% for the flow rate of 10 mL min^{-1}, 20 mL min^{-1}, 30 mL min^{-1} and 40 mL min^{-1} respectively.

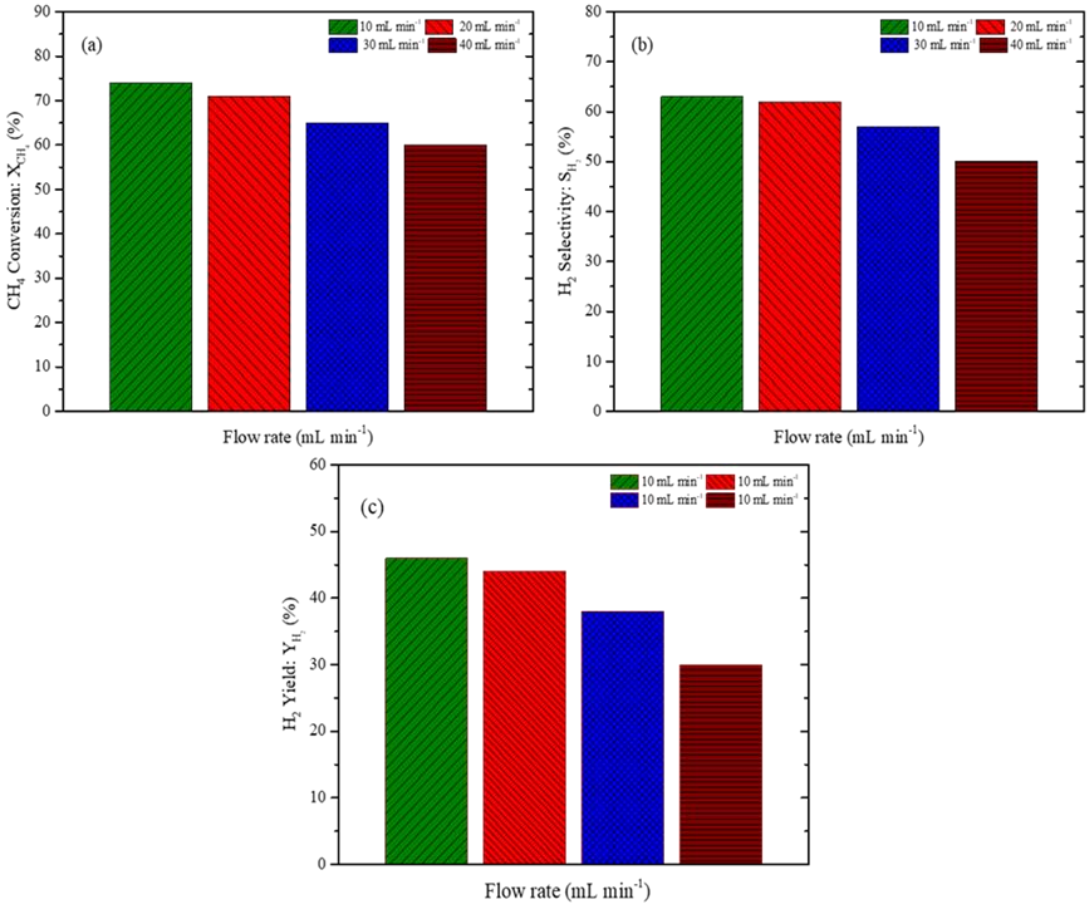

Figure 4.8 CH_4 flow rate effect on (a) conversion of CH_4 (b) H_2 selectivity (c) H_2 yield at reaction temperature = 850 °C , catalyst loading = 0.5 g

4.2.4 Stability analysis of 5%Co/CeO_2-BFA

The nano-composite 5%Co/5%CeO_2-BFA were used as catalyst for analyzing the stability performance. The stability analysis has been carried out at experimental parameters which are CH_4 flow rate equal to 20 mL min^{-1}, reaction temperature of 850℃. For total of 34 hours the stability analysis were carried out and in every 15 minutes the values for CH_4-conversion, H_2-selectivity and H_2-yield were determined. Initially lower catalytic activity were observed which is because of the reason that the produced H_2 was used for the reduction of some of the unreduced active metal species in the catalyst at 850℃ [10, 27]. For the first 12 hours, gradual increase in catalytic activity occur and after which for next 19 hours the catalytic activity remain stable as shown in **Figure 4.9.** After gaining the

stability, the maximum CH_4 conversion was recorded 71.4%, H_2 selectivity and yield values were equal to 64.3% and 44.9%. The excellent catalyst stability was due the better metal dispersion, metal support interaction, morphological structure of catalyst and presence of various metal oxide attribute to catalytic performance [28-30]. The TGA profile clearly exhibit thermal stability of 5%Co/5%CeO_2-BFA nano-composite. The SEM analysis confirm the better dispersion of the cobalt over the BFA, which is one of the main reason for the efficient CH_4 decomposition. The BFA is the mix matrix of various metal oxide i.e Ca, Si, Al and Fe which is confirmed from XRD analysis, that's why the solid carbon deposited over catalyst behave as catalyst support and assist in the methane decomposition reaction [31].

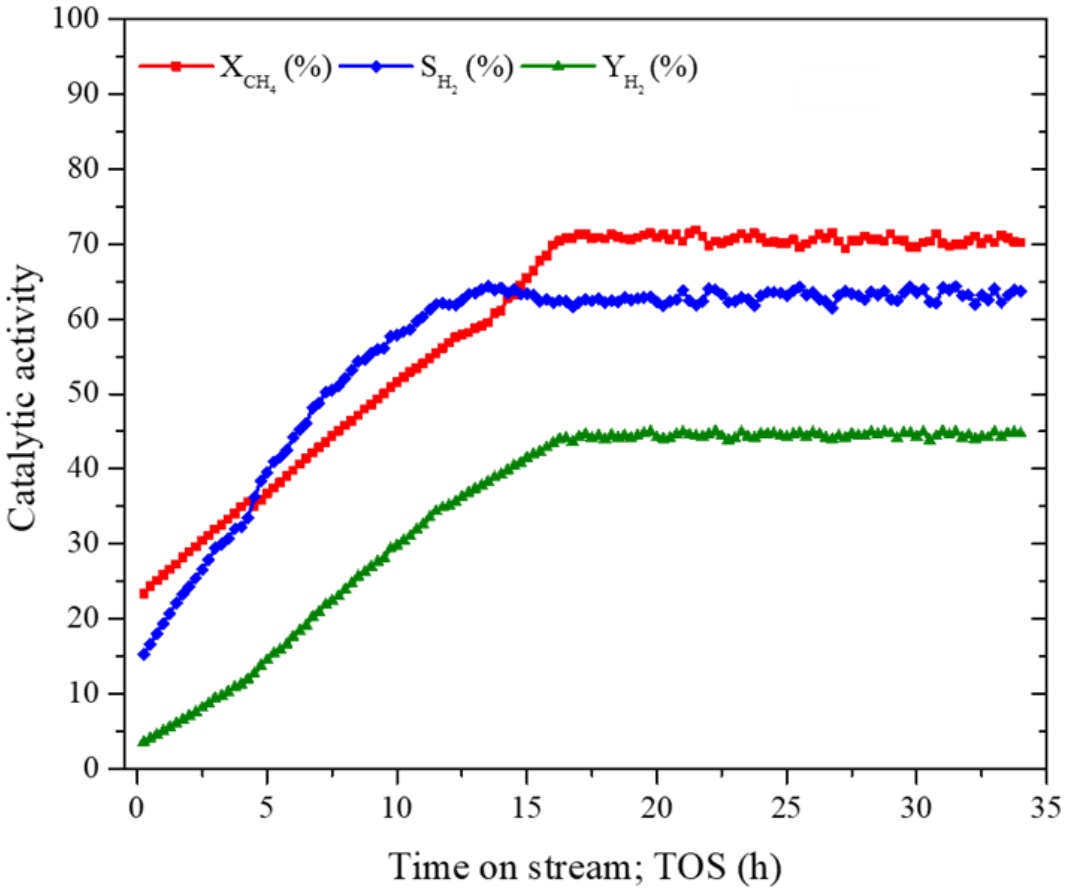

Figure 4.9 Stability analysis; TOS effect on CH_4 conversion, selectivity of H_2 and yield; reaction temperature = 850 °C, catalyst loading = 0.5 g, CH4 flow rate = 20 mL min^{-1}.

4.3 Physicochemical properties of spent catalyst

Catalyst used for 34 hours in the reactor has been collected and its physiochemical properties has been studied. SEM-E, XRD and TGA analyzer were used to study the change in catalyst occur after the deposition of the solid carbon. **Figure 4.10(a-b)** portray the SEM morphology of the spent catalyst. As compared to fresh catalyst, the morphology of the spent is obviously changed due to the deposition of the solid carbon over the catalyst [32].

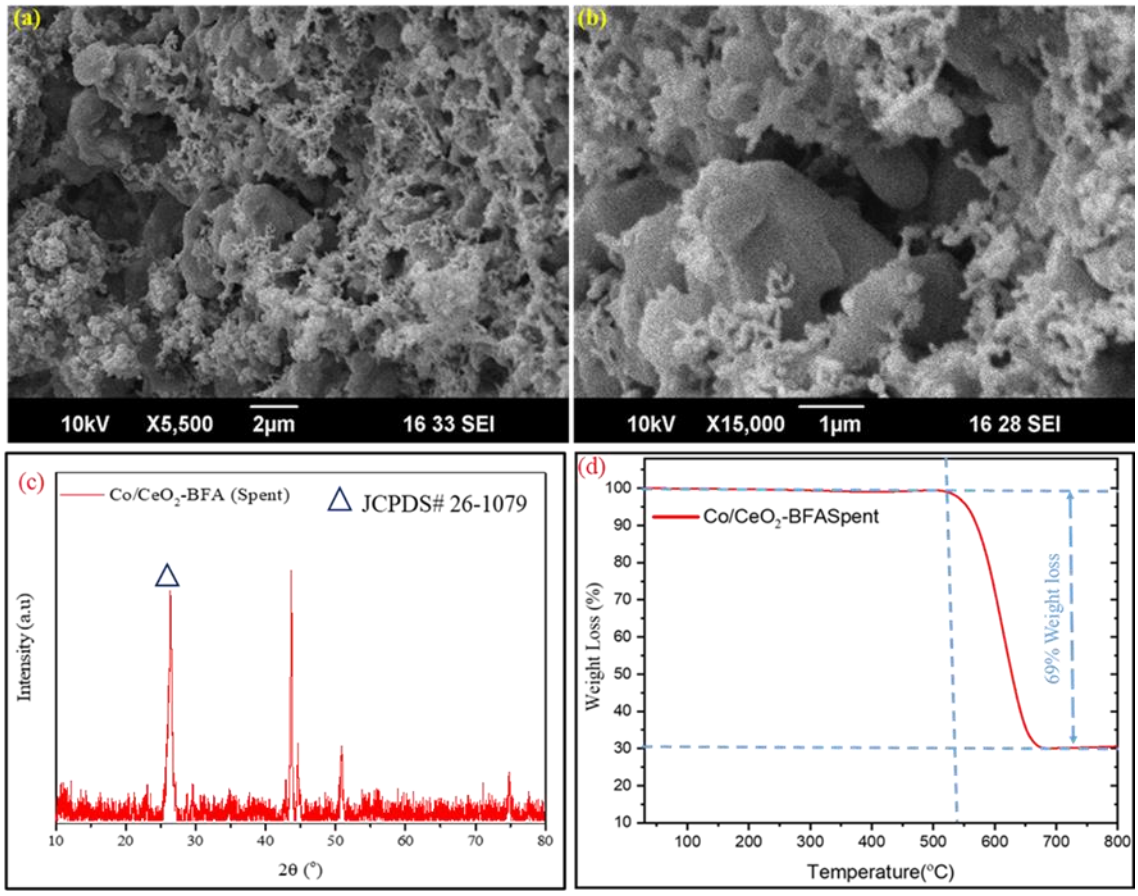

Figure 4.10 SEM micrograph of spent Co/CeO_2-BFA (a) 2.0 μm (b) 1.0 μ (c) XRD of Co/CeO_2-BFA-spent (d) TGA of Co/CeO_2-BFA-spent.

The XRD analysis of spent catalyst is show in **Figure 4.10(c).** The formation of hexagonal graphite carbon (JCPDF# 26-1079) is detected at $2\theta = 26.6^{o}$ with phase (003) has been confirmed with XRD analyzer. The XRD study further confirm the presence of Calcium

carbide, $CaCO_3$ with JCPDF# 47-1743 and phase number (104) is detected at an angle 29.4°. The BFA and CeO_2 structure has been altered because of heating for 34 hours at temperature of 850 ℃ and exultation of solid carbon with support to enhance catalytic activity. The cubic structured CeO_2 (JCPDF# 49-1415) is observed at $2\theta = 43.94^{o}$ with phase (012). At an angle equal to 26.18^{o}, SiO_2 (JCPDF# 11-0252) with phase (101) was detected.

Figure 4.10(d) represent the thermal analysis and weight loss behavior of spent catalyst. The TGA profile of spent catalyst shows 69% of weight loss at temperature range 530 ℃ to 800 ℃ in air environment. The weight loss of the spent catalyst are mainly due to the combustion of the graphite carbon formed over the catalyst surface.

EDX spectrum of the spent catalyst is shown in **Figure 4.11**, which clearly exhibit the peaks for the presence of C, Si, Fe and Ca. the elements like Si, Fe and Ca are the major constituent of BFA and the deposited carbon over the catalyst surface dominate the concentration of cobalt and cerium oxide.

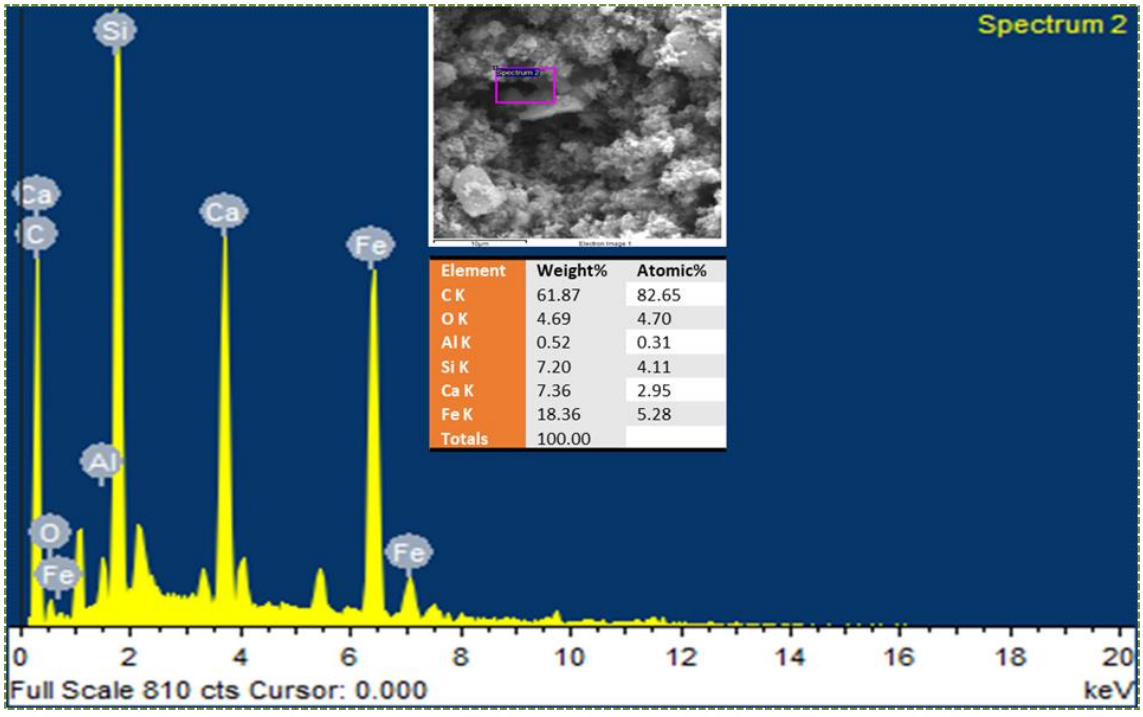

Figure 4.11 EDS analysis of spent Co/CeO_2-BFA after 34 h TOS.

Summary

The BFA sample, synthesized CeO_2 nano-wire and Co loaded nano-composite were characterized by XRD, TGA, SEM, EDS and FTIR. The XRD of the BFA exhibits various diffraction peaks for Fe_2O_3, Al_2O_3, MgO and SiO_2. The SEM shows the morphology of the BFA and reveals that BFA have micro-flakes like structure, which make it suitable materials as catalyst's support for catalytic applications. Furthermore, SEM analysis of final nano-composite shows that the Co and CeO_2 are distributed over the BFA micro-flakes. The material was found to stable up to 900 ℃ which was revealed by TGA and make it suitable for high temperature application. The materials was tested for hydrogen production in FBR via thermo-catalytic decomposition of methane. The material gain stability after 15 hours and were stable till the end of the test. The tests were performed only for BFA, Co-BFA and final nano-composite (Co/CeO_2-BFA) and the results shows that cobalt loaded and CeO_2 promoted catalyst have shown better catalytic activity. The stability of the catalyst was improved with loading of CeO_2 but increasing loading of CeO_2 beyond 5%, decrease the catalytic activity. The higher loading leads to the agglomeration of the structure which reduce the activity.

References

[1] H. Wang, W. Cui, X.a. Dong, J. Li, Q. Chen, Z. Wang, Y. Sun, J. Sheng, Y. Zhou, Y. Zhang, F. Dong, Interfacial activation of reactants and intermediates on $CaSO_4$ insulator-based heterostructure for efficient photocatalytic NO removal, Chemical Engineering Journal, 390 (2020) 124609.

[2] X. Zhang, J. Huang, Z. Kang, D.-P. Yang, R. Luque, Eggshell-templated synthesis of $PbS/CaCO_3$ nanocomposites for CO_3− mediated efficient degradation of tetracycline under solar light irradiation, Molecular Catalysis, 484 (2020) 110786.

[3] A. Kumar, M.K. Naskar, Single-step process without organic template for the formation of zeolite A from RHA, International Journal of Applied Ceramic Technology, 16 (2019) 1525-1532.

[4] Y. Wang, J. Ma, S. Zuo-Jiang, K. Chen, Tailorable magnetic properties of ε-Fe_2O_3/SiO_2 hybrid via alkaline etching, Ceramics International, 43 (2017) 16482-16487.

[5] W. Nabgan, T.A. Tuan Abdullah, R. Mat, B. Nabgan, Y. Gambo, K. Moghadamian, Acetic acid-phenol steam reforming for hydrogen production: Effect of different composition of La_2O_3-Al_2O_3 support for bimetallic Ni-Co catalyst, Journal of Environmental Chemical Engineering, 4 (2016) 2765-2773.

[6] M. Pudukudy, Z. Yaakob, M.S. Takriff, Methane decomposition into COx free hydrogen and multiwalled carbon nanotubes over ceria, zirconia and lanthana supported nickel catalysts prepared via a facile solid state citrate fusion method, Energy Conversion and Management, 126 (2016) 302-315.

[7] A.I. Paksoy, B.S. Caglayan, E. Ozensoy, A.N. Ökte, A.E. Aksoylu, The effects of Co/Ce loading ratio and reaction conditions on CDRM performance of Co Ce/ZrO_2 catalysts, International Journal of Hydrogen Energy, 43 (2018) 4321-4334.

[8] A.Y. Khodakov, Fischer-Tropsch synthesis: Relations between structure of cobalt catalysts and their catalytic performance, Catalysis Today, 144 (2009) 251-257.

[9] M. Assad Munawar, A. Hussain Khoja, M. Hassan, R. Liaquat, S. Raza Naqvi, M. Taqi Mehran, A. Abdullah, F. Saleem, Biomass ash characterization, fusion analysis and its application in catalytic decomposition of methane, Fuel, 285 (2021) 119107.

[10] M. Pudukudy, Z. Yaakob, Methane decomposition over Ni, Co and Fe based monometallic catalysts supported on sol gel derived SiO_2 microflakes, Chemical Engineering Journal, 262 (2015) 1009-1021.

[11] J. Valencia, N. Arias-Duque, O. Giraldo, A. Rosales-Rivera, Synthesis and characterization of magnesium-doped layered manganese oxides, Revista Mexicana de Física, 58 (2012) 151-154.

[12] M. El-Hagary, E.R. Shaaban, S.H. Moustafa, G.M.A. Gad, The particle size-dependent optical band gap and magnetic properties of Fe-doped CeO_2 nanoparticles, Solid State Sciences, 91 (2019) 15-22.

[13] J. Temuujin, U. Bayarzula, E. Surenjav, K.D. Sung, C.Y. Sik, Influence of cerium oxide (CeO_2) addition on the mechanical properties of glass ceramics precursor prepared from fly ash, Journal of Ceramic Processing Research, 18 (2017) 112-115.

[14] S. Khajeh Talkhoncheh, M. Haghighi, Syngas production via dry reforming of methane over Ni-based nanocatalyst over various supports of clinoptilolite, ceria and alumina, Journal of Natural Gas Science and Engineering, 23 (2015) 16-25.

[15] J. Kalembkiewicz, D. Galas, E. Sitarz-Palczak, The Physicochemical Properties and Composition of Biomass Ash and Evaluating Directions of its Applications, Polish Journal of Environmental Studies, 27 (2018) 2593-2603.

[16] W. Mozgawa, M. Krol, J. Dyczek, J. Deja, Investigation of the coal fly ashes using IR spectroscopy, Spectrochim Acta A Mol Biomol Spectrosc, 132 (2014) 889-894.

[17] Y.A. Syed Khadar, A. Balamurugan, V.P. Devarajan, R. Subramanian, S. Dinesh Kumar, Synthesis, characterization and antibacterial activity of cobalt doped cerium oxide (CeO_2:Co) nanoparticles by using hydrothermal method, Journal of Materials Research and Technology, 8 (2019) 267-274.

[18] M.T. Farid, I. Ahmad, S. Aman, M. Kanwal, G. Murtaza, I., Ali., M. Ishfaq, SEM , FTIR AND DIELECTRIC PROPERTIES OF COBALT SUBSTITUTED SPINEL FERRITES, 2015.

[19] W. Girma, I. Diaz, Encapsulation of Co (II) Complex with A Schiff Base Ligands Derived from 1, 10- Phenantroline-5, 6-Dione and O-Phenylene Diamine in Zeolite Y, 2016.

[20] M. Pudukudy, Z. Yaakob, Q.M. Jia, M.S. Takriff, Catalytic decomposition of methane over rare earth metal (Ce and La) oxides supported iron catalysts, Applied Surface Science, 467 (2019) 236-248.

[21] W. Ahmed, A.E. Awadallah, A.A. Aboul-Enein, $Ni/CeO_2–Al_2O_3$ catalysts for methane thermo-catalytic decomposition to CO -free H2 production, International Journal of Hydrogen Energy, 41 (2016) 18484-18493.

[22] F.-J. Spiess, S.L. Suib, K. Irie, Y. Hayashi, H. Matsumoto, Metal effect and flow rate effect in the hydrogen production from methane, Catalysis Today, 89 (2004) 35-45.

[23] E. Tezel, H.E. Figen, S.Z. Baykara, Hydrogen production by methane decomposition using bimetallic Ni–Fe catalysts, International Journal of Hydrogen Energy, 44 (2019) 9930-9940.

[24] H. Zhang, C. Du, A. Wu, Z. Bo, J. Yan, X. Li, Rotating gliding arc assisted methane decomposition in nitrogen for hydrogen production, International Journal of Hydrogen Energy, 39 (2014) 12620-12635.

[25] H.D. Setiabudi, C.C. Chong, S.M. Abed, L.P. Teh, S.Y. Chin, Comparative study of Ni-Ce loading method: Beneficial effect of ultrasonic-assisted impregnation method in CO_2 reforming of CH_4 over Ni-Ce/SBA-15, Journal of Environmental Chemical Engineering, 6 (2018) 745-753.

[26] A. Leba, R. Yıldırım, Determining most effective structural form of nickel-cobalt catalysts for dry reforming of methane, International Journal of Hydrogen Energy, 45 (2020) 4268-4283.

[27] A.S. Al-Fatesh, A.H. Fakeeha, A.A. Ibrahim, W.U. Khan, H. Atia, R. Eckelt, K. Seshan, B. Chowdhury, Decomposition of methane over alumina supported Fe and Ni–Fe bimetallic catalyst: Effect of preparation procedure and calcination temperature, Journal of Saudi Chemical Society, 22 (2018) 239-247.

[28] L. Wei, M. Zhu, Y. Ma, Z. Zhang, D. Zhang, Hydrogen production by methane cracking over Xiaolongtan lignite chars: The role of mineral matter, Fuel, 183 (2016) 345-350.

[29] T.J. Siang, S. Singh, O. Omoregbe, L.G. Bach, N.H.H. Phuc, D.-V.N. Vo, Hydrogen production from CH_4 dry reforming over bimetallic Ni–Co/Al_2O_3 catalyst, Journal of the Energy Institute, 91 (2018) 683-694.

Chapter 5: Conclusion and Recommendations

5.1 Conclusions

The efficient use of BFA collected from biomass power plant was a matter of serious concern. To solve out this issue, the physiochemical properties of the BFA have been studied and it was concluded that BFA is best suited as catalyst support in various technologies. The presence of various metal oxides in BFA have been confirmed with XRD study and the SEM morphology reveals that BFA has porosity in its flake like structure which make it likely contender for catalyst support material. For thermo-catalytic decomposition of methane only BFA as catalyst was tested and it have shown some promising results. But with addition of active metal like cobalt and promoted with synthesized nanowire of cerium oxide enhance the efficiency and performance of catalyst. The promoter help in better dispersion of active metal and enhance the stability of catalyst and this role has been played by cerium oxide. 5% Co/CeO_2-BFA nan-composite as catalyst give maximum CH_4 conversion was 71%, H_2 selectivity and yield were 62% and 44% respectively. The 5% Co/CeO_2-BFA nan-composite has been test for 34 hours to check the stability of and the nano-composite did not show any decline in the activity at the end. Hence concluded that the catalyst derived from biomass ash is an economical because the use of the BFA could reduce the cost of heterogeneous catalyst.

5.2 Recommendations

Thermo-catalytic decomposition of methane is the most effective method and a greener route for hydrogen gas production and solid carbon nano-materials as by-product. But the major challenge associated with the given process is the catalyst deactivation due to deposition of the carbon over the catalyst surface, which block the active sites of the catalyst. Furthermore, the better physiochemical properties of BFA reveals that BFA in future should be utilize for catalytic application. The reactor design should be kept in consideration along with the experimental parameters for maximum conversion of methane and hydrogen yield.

APPENDIX-PUBLICATIONS

A-1 Jehangeer Raza, Asif Hussain Khoja, Salman Raza Naqvi, Muhammad Taqi Mehran, Sehar Shakir, Rabia Liaquat, Muhammad Tahir and Ghulam Ali "*Methane decomposition for hydrogen production over biomass fly ash-based CeO_2 nanowires promoted cobalt catalyst*". Journal of Environmental Chemical Engineering (2021) (IF=4.3, under review)

Contents lists available at ScienceDirect

Journal of Environmental Chemical Engineering

journal homepage: www.elsevier.com/locate/jece

Methane decomposition for hydrogen production over biomass fly ash-based CeO_2 nanowires promoted cobalt catalyst

Jehangeer Raza [a], Asif Hussain Khoja [a,*], Salman Raza Naqvi [b], Muhammad Taqi Mehran [b], Sehar Shakir [c], Rabia Liaquat [c], Muhammad Tahir [d], Ghulam Ali [c]

[a] Fossil Fuels Laboratory, Department of Thermal Energy Engineering, US-Pakistan Centre for Advanced Studies in Energy (USPCAS-E), National University of Sciences and Technology (NUST), Sector H-12, Islamabad 44000, Pakistan
[b] School of Chemical and Materials Engineering (SCME), US-Pakistan Centre for Advanced Studies in Energy (USPCAS-E), National University of Sciences and Technology (NUST), Sector H-12, Islamabad 44000, Pakistan
[c] Department of Energy Systems Engineering, US-Pakistan Centre for Advanced Studies in Energy (USPCAS-E), National University of Sciences and Technology (NUST), Sector H-12, Islamabad 44000, Pakistan
[d] Chemical Reaction Engineering Group (CREG), School of Chemical and Energy Engineering, Faculty of Engineering, Universiti Teknologi Malaysia (UTM), 81310 Skudai, Johor Bahru, Malaysia

ARTICLE INFO

Editor: V. Victor

Keywords:
Methane decomposition
Biomass fly ash
CeO_2
H_2 production

ABSTRACT

In this work, the biomass fly ash (BFA) was investigated as a potential catalyst for the thermo-catalytic decomposition of methane and attractive approach for hydrogen (H_2) production. The BFA based CeO_2 nanowires promoted cobalt catalyst was synthesized for catalytic methane (CH_4) decomposition and was tested in a fixed bed reactor. The physicochemical properties of the catalyst were investigated using various techniques such as X-ray powder diffraction, scanning electron microscopy, energy-dispersive X-ray spectroscopy, thermal gravimetric analysis, and Fourier transformed infrared. The pure crystalline micro-flake BFA was modified using synthesized CeO_2 nanowires and the resulted micro flakes cross-linked with nanowires shown thermal stability up to 900 °C. The high stability of the catalyst makes it suitable for the thermal catalytic decomposition of methane. The activity of the catalyst was tested at 850 °C to analyze the H_2 production and CH_4 conversion. The obtained results revealed that support and promoter exhibit a strong impact on the CH_4 conversion and H_2 yield in catalyst screening tests. A maximum conversion of 71% for CH_4 with 44.9% H_2 yield was recorded for 34 h on stream activity while using 5% Co/CeO_2-BFA as the catalyst. While BFA and Co-BFA as catalyst showed 36% and 47% conversion of CH_4, respectively which indicates that the addition of promoter shows an increase in values of both conversion of CH_4 and H_2 yield. Compared to traditional catalyst support, the use of waste-sourced catalyst support for CH_4 decomposition provides a greener and more economical route for H_2 production.